Electromechanics, optics and measurement

Follow the field into an instrument. Predict which mechanical displacement, temperature change or optical signal can be observed and determine what can be learned from it.

Contents

1. **When a suspended capacitor loses its stable equilibrium**
   An electrode suspended on a spring can remain motionless at a bias that makes the calculated electrostatic force grow as it moves. Static force balance alone misses the voltage at which that equilibrium disappears. Deriving the small-signal frequency gives an independent measurement of the same instability.
2. **Which part of a sample changes a four-electrode impedance measurement?**
   Driving one electrode pair and measuring another yields a transfer impedance whose spatial sensitivity can be positive, negative or nearly zero. A second field solution supplies the sensitivity without perturbing every element of a numerical mesh.
3. **Measuring the force on a sliding dielectric**
   A suspended strip slides between two electrodes without touching them. Predict the pull, infer the air clearance from a capacitance trace and find where an electrical measurement can detect a change in mechanical stiffness.
4. **Designing a displacement bridge at its noise limit**
   A moving electrode changes two capacitances in opposite directions. Derive the displacement signal, reconstruct its noise in metres and select a carrier voltage consistent with measured mechanical stiffness and electrical losses.
5. **A moving-coil galvanometer as an electrical and mechanical system**
   A scale division records an angle, yet the quantity marked on the dial is electric current. A spring, a magnetic field and the resistance of the external measuring circuit connect the two. Derive the calibration, predict how a pointer approaches its reading, and find which experiment measures the charge of a short pulse.
6. **Eddy-current braking, magnetic penetration and the heat left behind**

A conducting loop moves above a row of magnetic poles. The drag first increases with speed, but a rapid crossing need not generate proportionally greater braking. Trace the work done against the Lorentz force into circuit energy, heat and a measurable temperature change. Then decide which features of a solid plate the single-loop model can capture.

7. Measuring magnetic core loss by a hysteresis loop and by calorimetry

A closed loop on a graph of magnetic induction against field encloses an area with units of energy per unit volume. A thermometer measures kelvins. Bring these two observations onto the same scale, account for the winding heat, and determine when the two experiments actually test the same material loss.

8. A diamagnetic specimen in a gravitational and magnetic trap

A suspended specimen can have exactly the right vertical magnetic force and still slide sideways out of its apparent equilibrium. Derive the force on induced magnetisation, impose gravity, and use the curvature of a measured field to decide whether small disturbances return the specimen to its starting point.

9. Optical trapping and Brownian calibration of a dielectric bead

An image of a bead remaining near a focus does not establish the strength of its trap. Derive the force pulling a small dielectric sphere into a bright region, compare it with the forward force from scattering and learn what a motion record can tell you about stiffness, drag and temperature. The model here uses an inert dielectric sphere in a homogeneous Newtonian liquid.

10. Coupled optical and mechanical resonances

A vibrating mirror can imprint its position on an optical field, while the stored light pushes back on the mirror. An apparent pair of peaks can indicate two hybrid modes, interference at a readout port or two unrelated resonances. Starting from energy in a moving cavity, derive the coupled response and learn which measurements establish a coupling strength and its uncertainty.

11. Thermal radiance, étendue and detector calibration

A square millimetre of a heated object emits thermal radiation into an entire hemisphere. A detector sees only the rays accepted by its optics and only wavelengths to which it responds. Derive the equilibrium spectrum, follow it through an optical collection system and infer what temperature or emissivity a calibrated reading can actually determine.

12. Moving-mirror Doppler metrology

A moving mirror changes optical phase, shifts the reflected frequency and exchanges energy and momentum with the light. In many displacement measurements the classical phase rule is extraordinarily accurate. Derive its exact inertial-frame counterpart, identify which time a detector samples and find the practical uncertainties that usually matter well before a relativistic correction does.

13. Weighing a small deposit with a piezoelectric resonator

Two nearby frequencies appear in the electrical response of one mechanical mode. Derive the series and parallel resonances, then use their different sensitivities to recognise added mass and stray capacitance.

Electromechanics, optics and measurement · 1. When a suspended capacitor loses its stable equilibrium

An electrode suspended on a spring can remain motionless at a bias that makes the calculated electrostatic force grow as it moves. Static force balance alone misses the voltage at which that equilibrium disappears. Deriving the small-signal frequency gives an independent measurement of the same instability.

Start with the electrical and mechanical control variables

A movable conducting plate of area A faces a fixed electrode. Its unstressed gap is g. Define positive displacement x toward the fixed plate, with spring force $-kx$, mass m and viscous damping coefficient b. For $0 \le x < g$ assume ideal parallel plates, negligible tilt and fringing, constant ϵ, and a linear elastic spring. The capacitance is $C(x) = \epsilon A/(g - x)$. The model ends when the plates approach contact or when the suspending structure departs from its specified elastic law. It cannot by itself calculate adhesion, contact resistance or post-contact motion.

Before differentiating electrical energy specify whether the source holds voltage or charge. At fixed charge Q, electrical energy is $Q^2/[2C(x)]$, and its negative displacement derivative gives the force toward increasing x. At fixed voltage V, a source supplies $V\,dQ$ as the plates move. The appropriate potential for mechanical equilibrium is the spring energy plus the field energy minus QV, which here is $\mathcal{U}_V = kx^2/2 - C(x)V^2/2$. Differentiating gives the outward spring reaction and the attractive electrical force $F_e = V^2 C'(x)/2 = \epsilon A V^2/[2(g - x)^2]$. An independent derivation multiplies the conductor pressure $\epsilon E^2/2$ by area with $E = V/(g - x)$. Both give a positive force. Replacing the source potential with the stored energy at fixed voltage would reverse its sign.

Locate all equilibria before choosing a branch

Define $s = x/g$ and $\Lambda = \epsilon A V^2/(2kg^3)$. The static force equation reduces to

$$\Lambda = s(1 - s)^2.$$

At a specified voltage one can find s by scanning the curve $s \mapsto s(1 - s)^2$ over the physically admissible interval $0 \le s < 1$. Its derivative is $(1 - s)(1 - 3s)$, giving an interior maximum $4/27$ at $s = 1/3$. For $0 < \Lambda < 4/27$ there are two physical roots. The smaller is a local minimum of $\mathcal{U}_V$ while the larger is a local maximum. Their merger is a fold of the static equilibrium branch:

$$x_{\mathrm{pi}} = g/3,$$

$$V_{\mathrm{pi}} = \sqrt{\frac{8kg^3}{27\epsilon A}}.$$

The often-quoted one-third displacement is the result for a linear spring, ideal voltage drive and this capacitance geometry. It is not a universal travel limit determined by the gap alone. Additional mechanical restoring forces or a different electrical boundary condition change the fold. Neither positive net electrical force nor the mere existence of a real solution is evidence of stable operation. A

root finder started near the almost closed gap can converge to the unstable large-displacement root with an extremely small static residual.

The two branches can be distinguished experimentally without deliberately reaching contact. At static equilibrium $kx = F_e$. Linearise the total force about x_0 while maintaining voltage at its prescribed value. The incremental restoring stiffness and corresponding weak-damping natural frequency are

$$k_{\text{eff}} = k - \frac{\epsilon A V^2}{(g - x_0)^3} = k\,\frac{1 - 3s_0}{1 - s_0},$$

$$f_{\text{small}} = \frac{1}{2\pi}\sqrt{\frac{k_{\text{eff}}}{m}}.$$

A small push toward the fixed electrode is restored only when $k_{\text{eff}} > 0$. The familiar electrostatic softening is the reason the smaller equilibrium is stable. The small-signal frequency tends to zero as the fold is approached. With appreciable damping the observed amplitude resonance and ringdown oscillation have slightly different frequencies; fit the full mechanical response rather than identifying an arbitrary peak with the undamped f_{small}.

Background · Can a sudden step pull in a statically stable actuator?

An ideal voltage step applied to a plate initially at rest can push it past the unstable equilibrium. During the motion at fixed voltage the effective potential per kg^2 is $u(s) = s^2/2 - b/[2(1 - s)]$, where $s = x/g$ and $b = \epsilon A V^2/(kg^3)$. Neglect damping and begin at $s = 0$. At the dynamical threshold the initial energy equals the saddle energy and the slope vanishes at that saddle.

$$u(s) = u(0) \implies b = s(1 - s),$$

$$u'(s) = 0 \implies b = 2s(1 - s)^2.$$

The two equations meet at $s = 1/2$, $b = 1/4$. The quasistatic fold gives $b = 8/27$. Consequently the undamped step threshold is only $\sqrt{27/32} \simeq 0.919$ times the slow-ramp pull-in voltage. A device operated between the two voltages can survive a ramp but collapse after an abrupt step. Dissipation and the actual rise time change this prediction.

Reconstruct the prepared state from a frequency measurement

Take a 100 µm square electrode in vacuum, $g = 2.00$ µm, $k = 2.00$ N/m and $m = 5.00 \times 10^{-10}$ kg. The predicted pull-in voltage is 7.32 V, the zero-bias capacitance 44.3 fF and the zero-bias natural frequency 10.07 kHz. On the low branch $s_0 = 0.20$ gives $x_0 = 0.400$ µm and voltage 6.80 V. Then $k_{\text{eff}} = 1.00$ N/m and the small-signal frequency is 7.12 kHz. A measured frequency ratio f/f_0 can be inverted via $s = (1 - r)/(3 - r)$, where $r = (f/f_0)^2$. The result is independent of absolute optical displacement calibration if the mass and underlying spring stiffness have not changed during the bias sweep.

At the same voltage the other physical root is $s = 0.48769$. A numerical force balance at this root would give the same supply reading but a negative tangent stiffness. The ideal voltage-controlled potential in units kg^2 is $u(s) = s^2/2 - \Lambda/(1 - s)$. The barrier height $kg^2[u(0.48769) - u(0.20)]$ for this example is 7.26×10^{-14} J. A sufficiently energetic disturbance can carry the plate out of the stable basin even below static pull-in. This is different from loss of the static equilibrium itself. A quasistatic model predicts the existence and local stiffness of the equilibrium; a transient simulation must additionally specify initial displacement, velocity, drive ramp and damping.

Change the preparation to fixed charge

Disconnect a perfect isolated capacitor after placing a known charge Q on it, neglecting leakage and parasitic capacitance. Then $F_Q = Q^2/(2\epsilon A)$ is independent of the remaining gap, because $D = Q/A$ is fixed. Static equilibrium is $x_0 = Q^2/(2\epsilon A k)$, with incremental stiffness exactly k. At the same initial voltage and gap the instantaneous force agrees with the voltage-controlled value, since $Q = C(x_0)V$. The derivatives governing subsequent motion differ. At $x_0 = 0.400$ µm the required charge in the numerical example is 0.376 pC. After ideal electrical isolation the small-signal frequency returns to the underlying elastic value even though the loaded static position stays the same.

Ideal charge isolation is delicate in a small device. A fixed parasitic capacitance C_p from the isolated node to a reference means the conserved charge belongs to $C(x) + C_p$. Motion changes the fraction of total charge residing on the actuator. The electrical energy becomes $Q_{\text{total}}^2/[2(C + C_p)]$, so the force is $Q_{\text{total}}^2 C'/[2(C + C_p)^2]$, generally displacement dependent. If $C_p \gg C$, the node voltage changes little with a small displacement and behavior is closer to voltage control. Interpreting an observed softening after disconnecting the supply as evidence against electromagnetic force balance would overlook this boundary change.

A different practical preparation puts an intentional series capacitor C_s between a fixed voltage supply and the actuator. Its series combination is $C_{\text{ser}} = \epsilon A/[g - x + \epsilon A/C_s]$. For static mechanical work at fixed supply voltage use $F = V_s^2 C'_{\text{ser}}/2$. Defining an effective electrical spacing $g_e = g + \epsilon A/C_s$, the static fold occurs at $x = g_e/3$ if this lies within the open physical gap. If $\epsilon A/C_s \geq 2g$, contact would occur before any such static fold in the ideal model. This calculation shows a direct connection between passive circuit design and allowed mechanical travel, while making clear that the maximum actuator voltage can differ from the voltage printed on the supply.

Why a sudden voltage change can reach contact below static pull-in

For a rapid electrical step the plate has a position and velocity inherited from the previous preparation. Suppose it starts at rest at its zero-bias position, the supply steps to a constant V much faster than a mechanical period, and mechanical damping is initially negligible. Immediately after the step, energy in the mechanical potential $u(s) = s^2/2 - \Lambda/(1 - s)$ is $u(0) = -\Lambda$ in units of kg^2. Motion under this constant voltage can reach the force barrier if the initial value exceeds the potential at the unstable

stationary point. This question can be solved by comparing two energies without integrating an entire time history.

Let s_b be the unstable root of $\Lambda = s_b(1 - s_b)^2$. At threshold the initial state is on the separatrix, the trajectory separating oscillations in the well from excursions to the closing gap. Set $u(0) = u(s_b)$, subtract the two expressions and cancel s_b from the nontrivial solution. The two conditions become

$$\Lambda = \frac{s_b(1 - s_b)}{2},$$

$$\Lambda = s_b(1 - s_b)^2.$$

Thus $s_b = 1/2$, $\Lambda = 1/8$, and the ideal undamped step threshold is

$$V_{\mathrm{step}}/V_{\mathrm{pi}} = \sqrt{27/32} = 0.919.$$

In our example this is 6.72 V. A slow increase to 6.80 V leads to the observed stable 0.40 µm deflection, whereas a sudden ideal voltage step to the same value from rest at the origin contains enough energy to escape the well. Starting on the biased equilibrium before applying a small perturbation is a different experiment. The direction of the threshold shift makes physical sense: damping removes mechanical energy during the first excursion, and a slow ramp allows the equilibrium to move with the plate. The undamped value specifies a particular ideal initial-value experiment, rather than a voltage rating for an unspecified drive waveform.

One can check a simulated step by monitoring $m\dot{x}^2/2 + \mathcal{U}_V$ after the supply settles. With viscous damping its derivative is $-b\dot{x}^2$, so any sustained increase during a constant-voltage segment points to a numerical or modelling error. Before the step ends there is an explicit drive term $-CV\dot{V}$ in this energy balance. The mechanical potential already includes the source work. Adding $V\dot{Q}$ to the same balance a second time gives an artificial energy imbalance. A transient solver should stop at a physically specified minimum gap instead of marching across the singularity; a statement about contact time depends on what counts as contact.

A finite source resistance changes what a ringdown measures

A dc supply with series resistance R can maintain the static voltage accurately while failing to hold the actuator voltage fixed over a mechanical cycle. Let its steady node voltage be V, with equilibrium capacitance $C = C(x_0)$. A small sinusoidal displacement δx causes current $i\omega(C\,\delta v + VC'\delta x)$ into the actuator. The small-signal supply voltage is zero, so $\delta v = -Ri$. Eliminating current gives

$$\delta v = -\frac{VC'}{C}\frac{i\omega\tau}{1 + i\omega\tau}\delta x,$$

$$\tau = RC.$$

Linearise $F_e = V^2C'/2$ allowing both voltage and position to vary. The direct derivative is $K_{e0} = V^2C''/2$, while the change from node voltage is $VC'\,\delta v$. For an ideal parallel plate $C''/2 = (C')^2/C$, so the two terms combine to the simple complex relation $\delta F_e = K_{e0}\delta x/(1 + i\omega\tau)$.

At low frequency the electrical force follows displacement with its fixed-voltage slope. At high frequency the slope vanishes, as it must for an isolated ideal plate carrying fixed charge over one oscillation. At intermediate frequency a motion-induced current dissipates heat in the resistor.

Bring δF_e to the left side of the mechanical equation. Its real part subtracts $K_{e0}/[1+(\omega\tau)^2]$ from the mechanical stiffness; its imaginary part adds $K_{e0}\tau/[1+(\omega\tau)^2]$ to the viscous damping coefficient. This damping is positive for a passive resistor. At $s = 0.20$ the static electrical stiffness is 1.00 N/m, the operating capacitance is 55.3 fF and $R = 400$ MΩ gives

$$\tau = 22.1\,\mu\text{s}.$$

A 7.2 kHz interrogation has $\omega\tau \simeq 1$. Only about half the static electrical slope survives and the added damping is roughly $11\ \mu\text{N}\,\text{s}/\text{m}$. Treat these as frequency-dependent coefficients in the driven susceptibility. Substituting the low-frequency stiffness into a ringdown fit at this frequency would give the wrong displacement when the fitted frequency is inverted. Fitting the complex response at several frequencies avoids that ambiguity.

An experiment can separate the circuit effect from mechanical nonlinearity. Keep the same static bias and displacement, insert two known series resistances, then measure both in-phase and quadrature response to a small sinusoidal force. The displaced equilibrium should remain essentially unchanged at dc if leakage stays small. A stiffness dispersion and dissipative peak that shift in proportion to $1/R$ support an electrical cause. Then repeat at a smaller oscillation amplitude. Amplitude-dependent frequency shift that survives the change in resistance can arise from nonlinear spring or force curvature, which the first-order susceptibility leaves out. A simple change to the external circuit has turned the slope of an energy curve into a prediction for a measured phase lag.

Compare force intersections for voltage and charge control

The initial gap is 2.00 µm, the area is a 100 µm square and the mass is 0.50 µg. Use the voltage ratio to move the force curve through the fold. At 93% of pull-in the low-displacement fixed-voltage intersection has a positive restoring slope. The high-displacement intersection has a negative slope. The charge-controlled line is prepared at the selected voltage at the original open gap. It gives the same initial force but a different subsequent curve. The readout reports both open-gap roots even if the upper root lies beyond the plotted interval. At the baseline stiffness, static pull-in is 7.32 V.

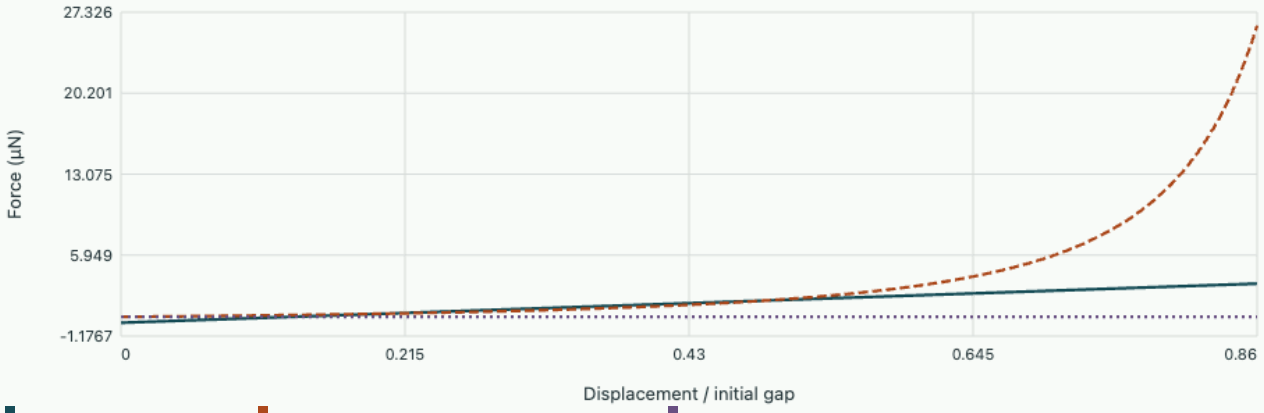
Change the spring stiffness while holding the voltage ratio fixed. The dimensionless locations of the roots stay in place, but their dimensional force and small-signal frequency change. This checks the scaling that eliminated the physical dimensions in the fold equation. Then set the ratio between the dynamic step threshold and unity. Use the force intersections to locate the potential maximum and sketch the area between attraction and spring reaction from the initial position. Its signed integral supplies the work which distinguishes a bounded excursion from crossing the maximum. The displayed curves predict initial-value behaviour only when combined with a choice of initial kinetic energy and damping.

Open this experiment online

Try the calculation

Bias as fraction of static pull-in **0.93**

Spring stiffness (N/m) **2**



Bias 6.805 V; static pull-in 7.317 V. Stable x/g = 0.200, unstable x/g = 0.487, small-signal frequency 7.11 kHz.

Tutorial · distinguish stability from force balance

Infer a gap fraction and a bias from a resonance

An otherwise identical actuator shows $f/f_0 = 0.80$ at a stable fixed voltage. Find the deflection as a fraction of gap, the voltage relative to pull-in, and the independent capacitance change. What could spoil this comparison?

▼ **Work through the solution**

Here $r = 0.64$ and $s = (1 - 0.64)/(3 - 0.64) = 0.1525$. The bias ratio is $\sqrt{(27/4)s(1-s)^2} = 0.860$ approximately. The parallel-plate capacitance should rise by $1/(1-s) - 1 = 18.0\%$. Measure the change relative to the active capacitance after removing any constant wiring capacitance. Disagreement can come from changing mode shape, a nonlinear spring, a tilted plate, a measurement frequency above the electrical equilibration bandwidth, or an incorrect extraction of mechanical stiffness from a strongly damped resonance. With a measured gap and mode shape these explanations yield different quantitative corrections.

Choose a series capacitor to move the static fold

The original 44.3 fF zero-bias actuator should remain on its stable slope as far as $x = 0.60g$, ignoring contact and other limits. Find the series capacitance whose fold falls exactly at this displacement. How

much supply voltage appears across the actuator at that point?

▼ **Work through the solution**

Set $g_e/3 = 0.60g$, giving $\epsilon A/C_s = 0.80g$ and $C_s = C(0)/0.80 = 55.4$ fF. At $0.60g$ the actuator capacitance is $C(0)/0.40 = 110.7$ fF. Series charge is identical in both capacitors, so

$$V_{\text{act}}/V_{\text{supply}} = C_s/(C_s + C_{\text{act}}) = 1/3.$$

Choosing exactly this value places operation at vanishing ideal stiffness, so a strictly positive measured restoring slope at that displacement requires a smaller series capacitance or a different margin. The result is sensitive to additional capacitance connected between the series node and ground.

Further reading

- Derive capacitor pressure from field stress and work

Electromechanics, optics and measurement · 2. Which part of a sample changes a four-electrode impedance measurement?

Driving one electrode pair and measuring another yields a transfer impedance whose spatial sensitivity can be positive, negative or nearly zero. A second field solution supplies the sensitivity without perturbing every element of a numerical mesh.

Distinguish the current terminals from the voltmeter terminals

Consider a bounded two-phase electrical sample in a benign laboratory characterisation cell. Drive harmonic current $+I$ through electrode a and collect $-I$ through b. Two independently selected electrodes c, d read the difference $U_c - U_d$ with negligible voltmeter current. The measured transfer impedance is

$$Z_{cd,ab} = (U_c - U_d)/I.$$

A four-terminal measurement reduces some lead-voltage errors, but finite-area electrodes still alter the field and contact processes can affect it. Reversing either pair reverses the signed transfer reading. Interchanging both pairs leaves it unchanged in a reciprocal linear sample.

Adopt phasors $e^{i\omega t}$ and a local complex admittivity $\gamma = \sigma + i\omega\epsilon$, with real positive scalar σ, ϵ for this first model. The total current density is $\mathbf{J} = -\gamma\nabla u$. In the electroquasistatic regime $\nabla \cdot (\gamma\nabla u) = 0$ away from injected current at the boundary. Magnetic induction and propagation are negligible at the chosen cell dimensions and frequencies; checking electrode and cable dynamics remains necessary even when the sample itself is quasistatic. Perfectly conducting measurement electrodes are equipotentials. Inactive electrodes have zero *net* current, which allows charge redistribution over their finite surfaces; a strictly insulating uncovered wall instead requires zero normal current locally.

Use an outward normal $\mathbf{n}$ from the sample. Define positive terminal current into the sample by $I_i = \int_{S_i} \gamma\partial_n u \, dA$; it equals minus the outward conduction-plus-displacement flux. The pair currents sum to zero, and only voltage differences matter, so fix one reference or a mean voltage. Integrate by parts against any test voltage v constant on each ideal electrode, giving

$$\int_\Omega \gamma \, \nabla u \cdot \nabla v \, dV = \sum_i I_i \, v_i.$$

This is a complex bilinear identity for reciprocity and linear sensitivity. Real average heating is obtained separately by conjugating the physical fields when computing power. Confusing those two products can give an incorrect phase or an incorrect sign for an imaginary admittivity perturbation.

Perturb the sample while keeping injected currents fixed

Let ψ_{ab} be the potential per unit current driven from a to b, and ψ_{cd} the solution when current is instead driven between the measurement electrodes. Using each as test function for the other shows directly

that $Z_{cd,ab} = Z_{ab,cd}$. Now change material admittivity by a small distribution $\delta\gamma$ and let the drive field change by $\delta\psi_{ab}$. Holding all currents and electrode geometry fixed, differentiate the weak equation:

$$\int_\Omega \gamma \nabla \delta\psi_{ab} \cdot \nabla v \, dV = -\int_\Omega \delta\gamma \, \nabla\psi_{ab} \cdot \nabla v \, dV.$$

Choose $v = \psi_{cd}$ and apply the unperturbed measurement-pair equation to $\delta\psi_{ab}$. Its left side becomes the change in voltage difference per drive current, hence

$$\delta Z_{cd,ab} = -\int_\Omega \delta\gamma(\mathbf{x}) \, \nabla\psi_{ab}(\mathbf{x}) \cdot \nabla\psi_{cd}(\mathbf{x}) \, dV.$$

The minus sign has an immediate check in a conducting bar: increasing conductivity lowers its resistance at fixed current. The sensitivity density is the overlap of the drive and reciprocal fields, not simply the magnitude of the drive field. If the fields are locally perpendicular a small isotropic admittivity perturbation is invisible to first order in this channel. If the fields are opposed the local real sensitivity can have the opposite sign to nearby regions. For tensor perturbations replace the product by $-\nabla\psi_{cd} \cdot \delta\boldsymbol{\gamma} \nabla\psi_{ab}$. Reciprocity in the above form requires symmetric material tensors.

A one-dimensional experiment tests the sign, normalisation and scale

Take a uniform real-conductivity bar of length 20 mm, cross-section $A = 100$ mm² and conductivity 0.20 S/m. Assume end electrodes cover its faces and ideal voltage taps select the full length in this limiting four-wire experiment. The impedance is

$$L/(\sigma A) = 1000\ \Omega.$$

The drive and reciprocal gradients per ampere have magnitude $1/(\sigma A)$. Increase conductivity in a full cross-section segment 2.0 mm long by 0.020 S/m. The first-order formula predicts

$$\delta R = -\ell \delta\sigma / (\sigma^2 A) = -10.0\ \Omega.$$

Direct series integration of $1/(\sigma A)$ gives a change from 100.0 to 90.91 Ω in the segment, or $-9.09\ \Omega$.

The 0.91 Ω difference is consistent with truncating at first order for a 10% conductivity change. Recompute at half the material perturbation: the exact change becomes $-4.762\ \Omega$, only 0.238 Ω away from the first-order $-5.00\ \Omega$. The residual decreases by about four when the step halves. Repeating at several positive and negative perturbations and taking a centred difference provides a sharper test of the adjoint code. Varying only the mesh resolution with a fixed large material contrast cannot remove a genuine nonlinear remainder.

The same one-dimensional geometry also demonstrates an absolute identifiability limit. Interchanging two equal-length full-cross-section inserts with different conductivities leaves the end-to-end resistance unchanged, since the integral of reciprocal conductivity is independent of ordering. Perfect

measurement precision cannot recover the order. A voltage tap between the two inserts or an alternative contact geometry is needed to break that symmetry.

Interpret real and imaginary voltage readings together

Even if each local σ, ϵ is real, the fields ψ in an inhomogeneous sample usually carry spatially varying phase. A change $\delta\sigma$ can therefore change both the real and imaginary transfer impedance, as can $i\omega\delta\epsilon$. Treat a complex reading as two real measurements with their calibrated covariance. To first order one finite-element cell with piecewise-constant parameters contributes coefficients $-\int_{\text{cell}} \nabla\psi_{ab} \cdot \nabla\psi_{cd}\, dV$ for $\delta\sigma$ and $i\omega$ times that coefficient for $\delta\epsilon$. The units of the two unknowns differ, so rescale with plausible physical parameter changes before comparing singular values.

As a simple frequency check choose a uniform engineered dielectric-conductor composite with $\sigma = 0.010$ S/m and $\epsilon_r = 1000$. At $f = \sigma/(2\pi\epsilon) \simeq 180$ kHz, $\gamma = \sigma(1 + i)$. The same bar geometry then gives $Z = (L/A)/\gamma = 10.0(1 - i)$ kΩ, a phase of -45°. At low frequency the phase tends to zero and the real impedance to 20.0 kΩ. A constant cable delay produces phase proportional to frequency independent of the sample parameters, so record a calibrated reference at each frequency before attributing an observed phase change solely to the specimen.

Derive a spatial sensitivity that can be checked without a mesh

Consider a homogeneous, thick conducting calibration block with a flat, electrically insulating top except at four small contacts on the same line. Coordinates are x, y along the surface and $z > 0$ into the block. If a unit current enters through a point at the surface, it spreads over hemispheres of radius r. Uniform normal current through a hemisphere requires

$$J_r = 1/(2\pi r^2).$$

The radial field is J_r/σ; integrating from r to infinity gives potential $1/(2\pi\sigma r)$. The coefficient differs from a point source in the interior where an entire sphere carries the current. Subtract a corresponding solution for the terminal extracting the current to satisfy conservation.

Let the drive pair be at $x = \mp a$ and the sense pair at $x = \mp c$, with positive terminal at negative x in each case. At surface points separated from the point contacts the baseline transfer impedance becomes

$$Z_0 = \frac{1}{\pi\sigma}\left(\frac{1}{a - c} - \frac{1}{a + c}\right) \qquad (0 < c < a).$$

For $a = 15$ mm, $c = 5$ mm and $\sigma = 0.20$ S/m this is 79.58 Ω. A 1 mA real current gives 79.58 mV. The same number follows on interchanging the drive and measurement pairs. The large individual contact potentials of an ideal point source are singular at the driving contact itself, yet the transfer potential evaluated at a distinct contact is finite. A two-terminal impedance obtained by setting $c = a$ is

divergent in this point-contact approximation. To make such a measurement calculable one must assign physical electrode radii, contact laws and current distributions.

Place a small spherical inclusion of radius 1.0 mm at $x = y = 0$ and depth z, with conductivity just 0.020 S/m above background. At the centreline the vertical field components cancel in each paired solution. Differentiating the two point-source potentials horizontally gives a gradient magnitude $a/[\pi\sigma(a^2 + z^2)^{3/2}]$ for a drive half-spacing a; replace a by c for the reciprocal measurement field. The first-order change in impedance is the product of the two signed gradients times minus the conductivity perturbation and the sphere volume. The centre sample approximates the volume integral when both background gradients vary slowly over the sphere.

At $z = 8$ mm the result is -3.86 mΩ, a $-3.86\,\mu\mathrm{V}$ perturbation at 1 mA, about 48 parts per million of baseline. Increasing depth to 16 mm leaves only -0.320 mΩ. A point midway between one source and one sensing contact can experience a very different gradient alignment from a point on the common centreline. This is why a general inclusion shift should be calculated by differentiating the vector field before taking the dot product. Replacing each gradient by its magnitude would forbid the experimentally possible positive changes. A point inclusion moved twice as deep does not, in general, change the answer by one universal inverse power. Each field samples a different combination of depth and contact separation.

Retain unknown contact impedance as a separate physical parameter

A metal current terminal is nearly equipotential internally but can have an interface voltage drop at the sample. Let U_i be its metal potential, u the potential on the adjacent sample, $j_i = \gamma \partial_n u$ positive into the body and z_i an area-specific contact impedance in Ω m². A simple local interface law is $U_i - u = z_i j_i$, together with $\int j_i \, dA = I_i$. At an inactive metal terminal only this integral is zero. Current can enter on one side and return on the other if the sample potential varies appreciably across its face. A high-impedance voltmeter does not by itself make that metal patch equivalent to an absent electrode.

For sample and electrode test fields (v, W), integration by parts and the contact law give

$$B((u,U),(v,W)) = \int_\Omega \gamma \nabla u \cdot \nabla v \, dV + \sum_i \int_{S_i} \frac{(U_i - u)(W_i - v)}{z_i} \, dA = \sum_i I_i W_i.$$

Here the current and potential gauges are chosen consistently on both drive and reciprocity solves. The contact product is as symmetric as the bulk product, so finite reciprocal contact impedances retain equality upon drive/sense exchange. If the contact changes, differentiating $1/z_i$ introduces a minus, and the minus from differentiating the full field equations cancels it. The additional first-order sensitivity is $+\sum_i \int \delta z_i j_{i,d} j_{i,m} \, dA$, with both current densities normalised to unit terminal current. In a uniform two-terminal contact of area A, the two normalised currents are $1/A$ and one contact contributes $+\delta z/A$, as an ordinary series contact should. This independent limit fixes both the positive sign and the square-metre convention.

For a controlled reconstruction, form one column per candidate sample perturbation and another per uncertain contact coefficient. Weight measured channels by their noise covariance. Two nearly proportional columns then warn that bulk variation and degrading contact cannot be separated by those channels over that bandwidth. Reciprocity catches lead swaps and some drift, but a reciprocal change in a contact can pass this check. Repeat with a different electrode pattern, or calibrate against a homogeneous reference block at the same frequency. To verify a numerical sensitivity, perturb the contact alone by equal positive and negative amounts and compare the centred impedance difference with the surface integral. Then perturb the sample alone and compare with the volume integral. A successful combined test could otherwise conceal equal and opposite implementation errors.

Move a weak inclusion beneath four surface contacts

The block is treated as a homogeneous half-space except for a 1 mm radius sphere with a positive conductivity perturbation. Each plotted point uses the two unperturbed analytical vector gradients at the sphere centre. The second curve repeats the calculation at twice the selected depth. At 8 mm and 5 mm sensing half-spacing the predicted centre perturbation is −3.86 mΩ against a baseline of 79.58 Ω. Look for lateral positions where the sign changes before interpreting increased conductivity as a uniformly smaller transfer impedance.

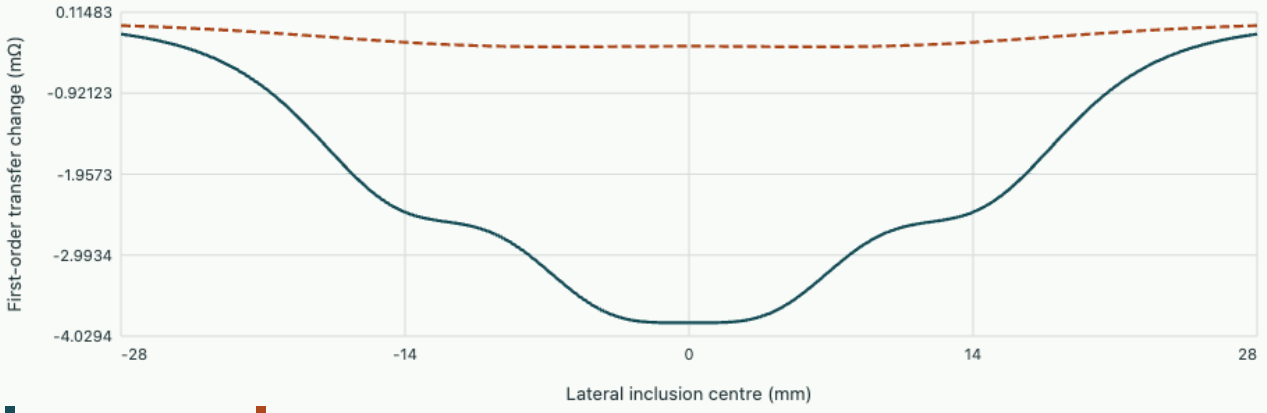
Widen the sensing pair and predict how both the transfer baseline and the local sensitivity will respond. A larger transfer voltage does not guarantee a proportionately larger fractional change for a chosen deep inclusion. The ideal point-contact fields vary steeply close to electrodes. When the inclusion radius approaches the distance over which the gradients change, volume quadrature supplies a better approximation than evaluating a single point. A finite laboratory specimen also needs boundaries sufficiently distant compared with the patterned contact spacing.

Open this experiment online

Try the calculation

Inclusion depth (mm) 8

Sensing half-spacing (mm) 5



Centre perturbation -3.858 mΩ; unperturbed transfer 79.58 Ω. Sphere radius 1 mm, conductivity increase 0.020 S/m.

Tutorial · bound a perturbation and design another observation

Predict a transfer change without solving again

A field computation for unit drive and unit reciprocal current in a small inclusion gives approximately parallel real field gradients of magnitudes 1500 and 400 V/(m A). The inclusion volume is 2 mm³. Its conductivity rises by 0.010 S/m. Predict the resistance change and the observed voltage change at a 5 mA drive. What changes if only the measurement electrodes are reversed?

▼ **Work through the solution**

The overlap is $6.0 \times 10^{5}\ \mathrm{V}^{2}/(\mathrm{m}^{2}\mathrm{A}^{2})$. Multiplying by $2 \times 10^{-9}\ \mathrm{m}^{3}$ and the material perturbation gives $\delta Z = -1.2 \times 10^{-5}\ \Omega$, or -12 µΩ. At 5 mA the transfer voltage changes by -60 nV. Reversing only c, d reverses the reciprocal field and the transfer change. The result assumes nearly uniform overlap inside the inclusion and small perturbation. Subdividing the inclusion or independently perturbing the forward model tests these assumptions differently. A voltmeter's microvolt accuracy would be inadequate for the proposed single measurement.

Do more electrodes resolve two unknown defects?

Two calibrated real channels have sensitivity rows proportional to $(1, 0.8)$ and $(0.8, 1)$ for two dimensionless defect amplitudes. Which combination is measured poorly? Would two additional

measurements that simply reverse the existing electrode signs supply a new material constraint?

▼ **Work through the solution**

The common pattern has gain 1.8 and the difference pattern gain 0.2; their singular-value ratio is nine in these units. Distinguishing which defect changed is harder than detecting a common material change. Sign reversals duplicate the same rows up to a minus sign. They can cancel offsets or improve precision by averaging independent noise, but do not increase the rank of the noise-free sensitivity matrix. A drive/measurement pair with opposing sensitivities to the two spatial regions would directly strengthen the weak difference direction.

Further reading

- Derive electrostatic reciprocity from a boundary-value problem
- Check complex field conventions with an independent power balance
- Somersalo, Cheney and Isaacson · existence and uniqueness for the complete electrode model

Electromechanics, optics and measurement · 3. Measuring the force on a sliding dielectric

A suspended strip slides between two electrodes without touching them. Predict the pull, infer the air clearance from a capacitance trace and find where an electrical measurement can detect a change in mechanical stiffness.

Reduce a three-dimensional field to a capacitance gradient

A light insulating strip is attached to a translation stage by a spring. Two stationary metal plates extend a length L in the direction of motion and have width w and separation d. The leading face of the strip is at coordinate x, measured from the entrance to the plates. The strip is longer than the active length, has thickness $t < d$, and fills the width in the interior to good approximation. The combined air clearance above and below it is $d - t$. Use V for the terminal voltage and increasing x for insertion. Electrode lengths and widths appreciably exceed the gap. Which information about the detailed electrostatic field is needed to predict a force in the horizontal direction?

First consider one square metre of plate well inside the overlap region. A pillbox straddling an air–solid interface contains no free charge, so the normal displacement D has the same value in air and solid. The fields are D/ϵ_0 and $D/(\epsilon_0\epsilon_r)$. Integrating the field through the layers gives the series law per unit area. Another square metre outside the strip has the gap filled entirely with air.

$$c_f = \frac{D}{V} = \frac{\epsilon_0}{d - t + t/\epsilon_r},$$

$$c_a = \frac{\epsilon_0}{d}.$$

Adjacent columns share the same voltage. For a small interior displacement dx, area $w\,dx$ changes from the air value to the filled value. Thus $dC = w(c_f - c_a)\,dx$. Define $K = w(c_f - c_a)$, measured in farads per metre. For a rigid straight edge well inside the plates it is nearly constant. Any fixed capacitance from leads adds to the measured C and drops out of K. Guard electrodes, if fitted, must be included in the electrical boundary conditions. Moving the guard or measuring a different pair of terminals can change the gradient itself.

For $L = 30$ mm, $w = 20$ mm, $d = 0.50$ mm, $t = 0.40$ mm and $\epsilon_r = 4.0$, the series thickness is 0.20 mm. The effective relative permittivity of a filled column is 2.50. The ideal empty capacitance is 10.63 pF and the filled capacitance is 26.56 pF. The slope is 0.5313 pF/mm. A naive average of permittivity by volume gives 3.4 and overestimates the force. It would apply to columns side by side in a uniform tangential field. The orientation of the interface supplies the missing piece of information.

Account for the power supply during a displacement

Imagine changing x very slowly at fixed voltage. The source transfers $dQ = V\,dC$ through voltage V, supplying $V^2 dC$. The energy in the field increases by $\tfrac{1}{2}V^2 dC$. Their difference is the mechanical work $F\,dx$ delivered to the moving strip. For an electrically isolated pair, Q is constant and energy $Q^2/(2C)$ decreases with increasing insertion. Differentiating either description gives

$$F_V = \frac{1}{2} V^2 C'(x),$$

$$F_Q = \frac{Q^2}{2C(x)^2} C'(x).$$

Their instantaneous values agree when $Q = C(x)V$. Their evolution after a displacement generally differs. At 80 V the plateau force is $1.700\,\mu\mathrm{N}$. A spring of $0.20\,\mathrm{N/m}$ allows an extra $8.50\,\mu\mathrm{m}$ of insertion if the slope stays constant. The source supplies 102.0 nJ over a complete ideal 30 mm sweep. Mechanical work is 51.0 nJ and the field gains 51.0 nJ. Make this independent check by evaluating each endpoint energy separately. With the charge prepared on empty plates then disconnected, the final voltage is

$$80/2.5 = 32.0\,\mathrm{V}.$$

The final plateau force approached from the interior falls to $0.272\,\mu\mathrm{N}$. Once the slab is fully inside, the edge term makes the force decay toward zero.

How can a vertical field pull a slab horizontally? Deep in either uniform column the local translational symmetry prevents a longitudinal push on a uniform piece of material. There is a transition near boundaries where the field curves and the polarisation changes. The work calculation moves material through this transition while keeping the remote uniform regions trackable. It predicts the integral of the force without locating each contribution. A force calculation based only on a vertical component times a horizontal normal lacks the tangential and normal stress components on a closed surface. Evaluating a vacuum Maxwell-stress integral on a contour around a finite strip gives a physically independent check of the net result when the supporting mechanical contact is accounted for separately.

Infer an edge profile from a measured trace

An abrupt switch in C' at the end of a plate would imply an unlimited second derivative. There is a finite interaction length around any real edge. A convenient interpolation for fitting data starts from the ideal rectangular overlap derivative and smooths each step over a length ℓ. Take the measured empty capacitance, including any fixed wiring, to be C_b. A symmetric fit for the measured gradient and its integral is

$$C'(x) = \frac{K}{2}\left[\tanh\!\left(\frac{x}{\ell}\right) - \tanh\!\left(\frac{x-L}{\ell}\right)\right],$$

$$C(x) = C_b + \frac{K}{2}[L + \ell \ln\cosh(x/\ell) - \ell \ln\cosh((x-L)/\ell)].$$

At large negative x the bracket tends to zero, at large positive x it tends to $2L$. The area under the gradient therefore produces the correct total increment KL for every ℓ. This normalisation is important. A fit that reproduces the centre of each transition but changes the area also changes the predicted work in a complete insertion. The two edges can have different widths near asymmetric supports. A fit

should then keep the capacitance endpoints and the physical separation of the stations as independent experimental checks.

For $L \gg \ell$ the first isolated transition reaches 10% and 90% at $x/\ell = \mp\,\mathrm{atanh}(0.8)$. Their separation is 2.1972ℓ. An observed 1.10 mm separation implies $\ell = 0.501$ mm. At the entrance the voltage-controlled gradient of force is

$$F_V' \simeq V^2 K/(4\ell);$$

the spring sees $k_{\mathrm{eff}} = k - F_V'$. At the exit the slope reverses and the oscillation frequency increases. For the numerical stage the entrance subtracts 0.00170 N/m from its 0.20 N/m spring. The ratio of loaded to zero-bias resonance frequencies is about 0.9957, if the moving mass is unchanged. The middle of the strip gives the largest static displacement but essentially no frequency shift under ideal voltage control. Measuring displacement and frequency at the same point distinguishes a force from a force gradient.

Estimate a derivative with enough resolution to trust its sign

A bridge returns C at positions separated by a calibrated step h. For the central derivative $D_h = [C(x+h) - C(x-h)]/(2h)$, expansion of both observations about their midpoint gives

$$D_h = C'(x) + h^2 C'''(x)/6 + \cdots.$$

With independent capacitance noise of standard deviation s_C per reading, the standard deviation of the slope is $s_C/(\sqrt{2}h)$. Shrinking h reduces truncation bias but magnifies random fluctuations. This competition reverses the familiar intuition that the smallest encoder step necessarily gives the most accurate force. A slowly drifting bridge offset can cancel between close readings, whereas a drift proportional to time can imitate a slope if all positions are visited in only one direction.

Suppose each measurement has 0.005 pF rms noise and $h = 0.25$ mm. The slope noise is 0.0141 pF/mm, 2.7% of the plateau. At fixed 80 V this corresponds to 45 nN rms in a single force estimate. Twenty-five independent pairs bring this contribution down to 9 nN. An uncertainty of 0.5% in voltage causes a 1% scale uncertainty in force shared by all the pairs. Repeated measurement cannot cancel a common scale uncertainty. At the exact centre of an isolated symmetric edge the symmetric difference of the integrated profile returns exactly $K/2$: opposite gradient values sum to K. The surrounding curve can still suffer marked smoothing. A correct midpoint alone provides a weak validation of a fitted transition length.

A complementary measurement clamps the stage at positions separated by several millimetres and obtains the force from a calibrated spring deflection. Fit the measured forces against V^2 at each position with an intercept free to capture a mechanical preload. A force caused by a contact potential V_c would instead have its parabola centred at $V = V_c$. Measurements of both voltage polarities reveal this offset; a single magnitude and a zero point cannot distinguish it from a biased slope. Perform both insertion and withdrawal sweeps. Hysteresis in the measured spring position with almost identical $C(x)$ indicates mechanical friction or creep rather than a change of the electrostatic energy law.

From a fitted edge to a field calculation

A two-dimensional cross-section can test which part of the interpolation is determined by geometry. In the air and in the strip solve $\nabla \cdot (\epsilon \nabla \phi) = 0$. Prescribe metal potentials, extend the exterior region far enough to include fringing field and match continuous potential and normal displacement at each material boundary. At each x, calculate $C(x)$ in two independent ways. Integrate the normal displacement on the driven electrode to get Q/V. Integrate $\epsilon |\nabla \phi|^2$ over every dielectric region and divide by V^2 to get the energy definition of capacitance. Both quantities per unit width must be multiplied by the same model width. Integrating only over the material strip removes the energy of the air gap, precisely the storage mechanism that reduced the effective permittivity.

To find force by differentiating numerical energies, use the same domain, mesh quality and quadrature on displacements either side of the evaluation point. A remeshing error uncorrelated from point to point enters like the measurement noise in the preceding calculation. Vary the displacement step and repeat with a finer mesh. A range of steps where the force moves little under both changes is stronger evidence than obtaining a smooth potential plot. Resolve thin clearance layers explicitly or represent them using a validated thin-layer boundary condition. Test the sharp-edge idealisation by changing the radius of the metal edge. The integrated force can converge even while a pointwise maximum field remains sensitive to this radius.

Finally, ask which geometric parameters can be determined from the plateau. Its single slope measures $d - t + t/\epsilon_r$ if w and d are known. It cannot separately determine thickness and relative permittivity. The electrical endpoint change provides KL, which is the same measurement multiplied by L; including both in a fit as independent material constraints can produce an artificially small confidence interval. Measuring t mechanically, or repeating with material samples of independently known thickness, resolves the ambiguity. The observed edge widths provide other geometric information but require a field model of the support and nearby shields before they can be interpreted as a direct permittivity measurement.

Measure curvature with a small carrier modulation

Capacitance-gradient force can be checked while a stage is held near a prescribed operating position. Bias the plates at V_0 and add a small sinusoidal voltage $v \cos \omega t$, where v is a peak amplitude in this experiment. With the stage almost stationary, expand the square of this voltage. The constant force is $C'(V_0^2/2 + v^2/4)$, the force at ω has peak amplitude $C' V_0 v$, and the force at 2ω has amplitude $C' v^2/4$. The latter persists at zero dc bias. Reversing the bias reverses the first harmonic while leaving the second harmonic unchanged. These are experimentally separable predictions of the local energy law even if the absolute mechanical preload is poorly known.

On the plateau of the example, choose $V_0 = 40.0$ V and $v = 2.0$ V. The first-harmonic force is 42.5 nN and the second-harmonic force is 0.531 nN. Well below mechanical resonance a 0.20 N/m spring turns these into peak oscillations of 0.213 µm and 2.66 nm. Close to resonance the spring response instead multiplies each force by its own complex susceptibility at ω or 2ω. A measured ratio of displacement harmonics should therefore be divided by the ratio of those susceptibilities before attributing any

difference to dielectric nonlinearity. Sweep the modulation frequency slightly or use a mechanical shaker calibration to measure the transfer function independently.

One subtle source of false harmonics is the motion itself. Near the entrance C' changes over a distance of order ℓ. A vibration that appreciably samples this length modulates the force even at constant bias. To use the harmonic test above, verify that the measured oscillation is small compared with ℓ and that any mean position shift due to bias has been accounted for. On withdrawing the dielectric entirely, both force harmonics should tend to the background associated with moving cables or the support. This empty-stage control tests the often implicit assumption that the wire capacitance is independent of stage position. A fixed added cable capacitance changes a charge-controlled experiment, but only a position-dependent contribution can imitate a capacitance gradient at fixed voltage.

Compare a connected and an isolated moving strip

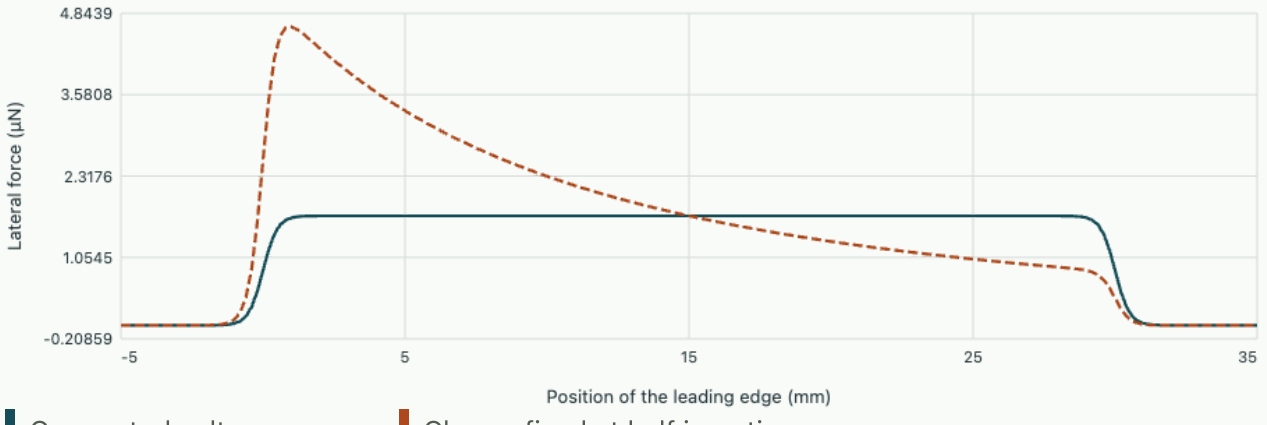
Follow the leading edge from outside the plates to beyond the exit. In the connected experiment the interior pull stays near 1.70 µN at 80 V. In the isolated experiment the charge is prepared at half insertion and kept fixed; no extra cable capacitance is included here. Find the common point of the two curves, then increase the fitted transition length. The peak displacement derivative of force changes even though the integrated voltage-controlled work over a complete traversal remains the same. Predict the sign of the resonance shift on each side of the device.

Open this experiment online

Try the calculation

Bias at preparation (V) **80**

Edge transition length (mm) **0.5**



Interior fixed-voltage pull 1.700 µN; entrance force gradient 1.700 mN/m. The two preparations coincide at 15 mm.

Tutorial · infer a material property and test the energy balance

Recover a clearance and assign an uncertainty

The plateau is 0.500 ± 0.015 pF/mm. Width and plate separation retain their nominal values; a mechanical gauge gives $t = 0.400$ mm. What permittivity follows? If instead $\epsilon_r = 4$ is accepted, what total clearance follows?

▼ **Work through the solution**

Calculate the equivalent thickness from $d_e^{-1} = d^{-1} + K/(\epsilon_0 w)$. The observed K gives $d_e = 0.2073$ mm. With known thickness,

$$\epsilon_r = t/(d_e - d + t) = 3.73.$$

Differentiation gives $|\delta d_e| = d_e^2 |\delta K|/(\epsilon_0 w) = 0.00364$ mm, corresponding to approximately 0.13 in relative permittivity with other quantities held fixed. A positive fluctuation of slope gives smaller equivalent thickness and larger inferred permittivity.

With known permittivity and unknown clearance $a = d - t$, write $d_e = a + (d - a)/4$. Then $a = (4d_e - d)/3 = 0.1097$ mm, with uncertainty 0.0049 mm. Substitution into the original series expression reproduces the observed slope. These two inferences answer different experimental questions. The same pair of endpoints cannot establish both estimates simultaneously without the extra information specified in each part.

Compare two preparations over one short motion

At half insertion connect 80 V, then isolate the terminals including 5.00 pF of fixed wiring. Use the ideal interior geometry. Estimate force after a further 5.00 mm motion and calculate the released mechanical work directly from endpoint energies.

▼ **Work through the solution**

The initial total capacitance is $10.63 + 7.97 + 5.00 = 23.60$ pF, so $Q \simeq 1.888$ nC. The final value is 26.25 pF and the terminal voltage falls to 71.9 V. The final force is $1.37\,\mu\mathrm{N}$. The energy released is $Q^2(1/C_i - 1/C_f)/2 \simeq 7.65$ nJ. Independently integrate $Q^2 K/[2(C_i + Kx)^2]$ over the 5 mm path. The antiderivative is $-Q^2/[2(C_i + Kx)]$ and gives the same result. The mean force of $1.53\,\mu\mathrm{N}$ lies between the initial 1.70 and the final 1.37. Leaving the wiring out of this calculation leaves the voltage-controlled plateau unchanged but predicts an incorrect final voltage and energy release in isolation.

Further reading

- Field force from a closed stress surface

- MIT 6.013, chapter 6 · capacitor work and dielectric forces

Electromechanics, optics and measurement · 4. Designing a displacement bridge at its noise limit

A moving electrode changes two capacitances in opposite directions. Derive the displacement signal, reconstruct its noise in metres and select a carrier voltage consistent with measured mechanical stiffness and electrical losses.

Find the voltage of the moving electrode before calculating sensitivity

Consider three plane electrodes with common active area. At the centred position the middle conductor is separated by g from each outer electrode and each gap has capacitance C_0. Displacement x toward the positive drive electrode reduces one gap and increases the other. Use $s = x/g$, where $|s| < 1$. Drive the outer electrodes with coherent sinusoidal voltages $+V_d$ and $-V_d$, with V_d the rms amplitude of either electrode relative to ground. The middle conductor leads to a high-impedance amplifier. Its cable and input provide a fixed total capacitance C_p to ground. Leakage is initially negligible over one carrier period; the input draws negligible signal current. All formulas for carrier voltages in this project use rms amplitudes.

$$C_+ = \frac{C_0}{1 - s},$$

$$C_- = \frac{C_0}{1 + s}.$$

The middle node has zero net charge at the carrier frequency. Its instantaneous ac charge is $C_+(V_n - V_d) + C_-(V_n + V_d) + C_p V_n$. Set the sum to zero and solve the resulting linear equation for V_n. After combining the gap capacitances the result simplifies considerably:

$$\frac{V_n}{V_d} = \frac{C_+ - C_-}{C_+ + C_- + C_p} = \frac{2C_0 s}{2C_0 + C_p(1 - s^2)}.$$

For zero parasitic capacitance the response is exactly $V_d x/g$ throughout the ideal geometry. Each individual capacitance is strongly curved near an electrode. Charge conservation divides one nonlinear combination by another and removes that curvature from their voltage ratio. Additional capacitance reduces the small-signal gain and introduces an odd cubic term. Let $\eta = 2C_0/(2C_0 + C_p)$. Expanding about the centre gives

$$V_n/V_d = \eta s[1 + (1 - \eta)s^2 + \cdots].$$

The derivative at zero is $K = \eta V_d/g$ in volts per metre. A small-signal calibration taken only at the origin implicitly accepts this cubic distortion at larger displacements.

For $C_0 = 2.00$ pF, $C_p = 4.00$ pF, $g = 100\,\mu\text{m}$ and $V_d = 1.00$ V, $K = 5000$ V/m. A displacement of 100 nm produces 0.5000 mV. At 20 µm, the exact signal is 0.10204 V against the linear prediction 0.10000 V. The 2.04% curvature would be apparent in a calibration over the wider range. A single proportional calibration cannot remove it. A fit to the ratio itself has a physical parameter, $C_p/(2C_0)$,

which can also be checked by measuring total input capacitance with the mechanical element held at centre.

Translate each readout fluctuation into equivalent displacement

Represent the amplifier near the carrier by an input series voltage noise density e_n and a shunt current noise density i_n. With the drives treated as small-signal grounds for a noise perturbation, the central node presents $C_T = 2C_0 + C_p$ at the centre. The impedance magnitude for current fluctuations is $1/(\omega C_T)$. For mutually independent noise sources and a narrow demodulation band the corresponding input-referred displacement amplitude spectral density is

$$S_{x,e}^{1/2} = \frac{1}{K}\sqrt{e_n^2 + \left(\frac{i_n}{\omega C_T}\right)^2}.$$

Use noise densities and gain referred to the same detection channel. An rms sine amplitude, a peak-amplitude display and a lock-in reading with an unreported normalisation can differ by factors involving $\sqrt{2}$. Here noise figures denote the effective one-sided densities referred to the recovered rms carrier channel. For a white spectrum and an equivalent noise bandwidth B_e the displacement standard deviation equals the density times $\sqrt{B_e}$. The displayed cut-off frequency of a multi-pole lock-in filter need not equal its equivalent noise bandwidth. A calibration using a known injected sideband measures both the gain convention and the actual band response.

At 100 kHz, $e_n = 10\,\mathrm{nV}/\sqrt{\mathrm{Hz}}$, $i_n = 10\,\mathrm{fA}/\sqrt{\mathrm{Hz}}$ and $C_T = 8.00$ pF, current noise produces $1.99\,\mathrm{nV}/\sqrt{\mathrm{Hz}}$. Adding variances gives $10.20\,\mathrm{nV}/\sqrt{\mathrm{Hz}}$, or $2.04\,\mathrm{pm}/\sqrt{\mathrm{Hz}}$ at the stated gain. A 100 Hz equivalent noise bandwidth gives 20.4 pm rms of electrical readout noise. Cable capacitance reduces the voltage made by current noise but also reduces signal gain. In fact $C_T K = 2C_0 V_d/g$, so their ratio for current noise is independent of C_p in this model. The voltage-noise contribution grows with cable capacitance. Higher carrier frequency initially reduces the current contribution but reaches a plateau set by voltage noise.

Derive backaction for a floating sensing plate

Electrical drive can change the mechanical stiffness of the sensor. For each gap take half the squared rms gap voltage times its capacitance derivative. This follows either by averaging the instantaneous plate pressure over a carrier cycle or by differentiating electrical coenergy with the middle node at its charge-balanced voltage. Mechanical motion must be slow compared with the carrier. Since C'_- is negative, the two signed forces cancel at the centre. For a small positive s, write $V_n \simeq \eta V_d s$,

$$C'_+ \simeq (C_0/g)(1+2s),$$

$$C'_- \simeq -(C_0/g)(1-2s).$$

The leading imbalance is

$$F = \tfrac{1}{2}C'_{+}(V_d - V_n)^2 + \tfrac{1}{2}C'_{-}(-V_d - V_n)^2 \simeq \frac{2C_0V_d^2}{g^2}(1-\eta)x.$$

The electromagnetic stiffness $K_e = 2C_0V_d^2(1-\eta)/g^2$ subtracts from the mechanical restoring stiffness k. If $C_p = 0$, the equal field magnitudes on both sides cancel exactly for every displacement in ideal plane geometry. To check directly, the positive gap field is

$$[V_d(1-s)]/[g(1-s)] = V_d/g.$$

The negative gap field has the same magnitude. A charge amplifier holding the central electrode at virtual ground would change this condition and have a different backaction; its calibration must use its own circuit. For a finite C_p, the measured change of resonance with carrier voltage can identify electrical coupling independently of the signal voltage.

With $k = 0.020$ N/m the nominal configuration has $K_e = 0.00020\,\mathrm{N/m}$ at 1 V and $0.00080\,\mathrm{N/m}$ at 2 V. At 2 V the resonance ratio for the same effective mass is

$$\sqrt{1 - 0.0008/0.020} = 0.980.$$

A 2% frequency decrease measures roughly a 4% reduction of stiffness. If the displacement is imposed by a very stiff external positioner this effect changes the force needed to hold position. If the sample is itself a force sensor, the same effect changes the mechanical conversion between applied force and displacement. Quoting an electronic noise floor without specifying which mechanical situation is intended can hide the larger uncertainty.

Choose a feasible drive and include Brownian motion

Raising the carrier at fixed frequency increases displacement signal. It may also heat the dielectrics, exceed amplifier headroom or significantly soften the spring. Suppose each gap at centre has an effective loss tangent $\tan\delta$, with a real conductance $\omega C_0 \tan\delta$ at the carrier. Its dissipated power is conductance times the squared rms voltage. Add both gaps to find

$$P = 2\omega C_0 \tan\delta V_d^2.$$

Fixed parasitic capacitance at the stationary middle node has negligible carrier voltage at exact balance in this model. An actual shield or cable dielectric connected directly to one of the drive nodes will have its own loss. A calorimetric or current phase measurement should include that extra load.

With effective $\tan\delta = 0.010$, the two active gaps dissipate 25.13 nW per squared volt at 100 kHz. A 100 nW heat budget gives $V_d \le 1.995$ V. A driver that remains linear to 2.50 V and a softening allowance $K_e \le 0.1k$ permit 2.50 V and 3.16 V respectively. The thermal bound sets the largest practical drive under these assumptions. For the electrical readout alone, the best feasible setting is

thus 1.995 V and the electrical floor is about $1.02\,\mathrm{pm}/\sqrt{\mathrm{Hz}}$. A separate limit on the electric field or measurement amplitude could be introduced as another experimentally justified constraint.

Now let the mechanical element have viscous damping $b = 1.00 \times 10^{-6}\,\mathrm{N\,s/m}$ at $T = 300$ K. In thermal equilibrium the one-sided Brownian force density is

$$\sqrt{4k_B T b} = 1.29 \times 10^{-13}\,\mathrm{N}/\sqrt{\mathrm{Hz}}.$$

Far below mechanical resonance its displacement density is this force divided by $k - K_e$. At 1 V it is $6.50\,\mathrm{pm}/\sqrt{\mathrm{Hz}}$, already greater than the electrical term. At 1.995 V it is about $6.70\,\mathrm{pm}/\sqrt{\mathrm{Hz}}$. The combined density adds in quadrature, giving about 6.81 at 1 V and 6.78 at the heat limit. A minimum of the total can occur between them. For an imposed position of a rigid stage the Brownian motion of this compliant probe may be outside the measurement model; for a freely suspended sensing mass it is part of the signal uncertainty. The optimisation criterion follows the physical quantity the instrument measures.

Use the phase and polarity of a calibration to track false signals

Middle-node leakage to ground with conductance G changes the circuit equation to $[G + i\omega C_T]V_n = i\omega(C_+ - C_-)V_d$ at small displacement. The ideal gain acquires a factor $i\omega C_T/(G + i\omega C_T)$. For a 10 MΩ leakage path and 8 pF, the corner is 1.99 kHz. At 100 kHz the magnitude reduction is about 0.02% and the phase lead about 1.14°. At 2 kHz both quadratures matter. A drift in humidity that lowers the resistance can look like a gain change if only the in-phase channel is recorded. Measure a known displacement at two carrier frequencies and fit both quadratures before interpreting it as a change in geometry.

Suppose the two actual drives are $V_d(1 + a)$ and $-V_d(1 - a)$. At centre the output becomes $\eta V_d a$, equivalent in the small-signal calibration to displacement ag. An amplitude imbalance of one part in ten thousand gives a 10 nm offset at $g = 100\,\mu\mathrm{m}$, many orders above a short-band noise floor expressed in picometres. Reverse the mechanical calibration displacement to isolate odd signal, measure the voltages at the electrode terminals and compare the nulled bridge under exchange of the drive channels. Reversing both carrier phases simply reverses both desired signal and this coherently driven offset; by itself it cannot distinguish them. An offset stable over a short scan can be estimated from two symmetric calibration displacements, whereas a drifting imbalance requires a reference or simultaneous drive measurement.

Find the minimum for a compliant probe instead of guessing at it

It is possible to optimise the free probe analytically up to a scalar root. Write $y = V_d^2$, $K_e = hy$, and a for the readout displacement density at unit drive multiplied by one volt. Let $d_F = \sqrt{4k_B T b}$ be the Brownian force density. At displacement frequencies well below the resonance, the total variance density has an electrical term falling as $1/y$ and a mechanical term that grows as the spring softens:

$$S_x(y) = \frac{a^2}{y} + \frac{d_F^2}{(k - hy)^2},$$

$$\frac{dS_x}{dy} = -\frac{a^2}{y^2} + \frac{2hd_F^2}{(k - hy)^3}.$$

On the stable interval the first derivative strictly increases when $h > 0$. The first term starts at negative infinity and the second diverges at the stiffness boundary. Hence there is one unconstrained minimum. Solve a bracketed scalar equation for y, then compare with each experimental upper bound in volts squared. At zero parasitic capacitance the ideal floating plate has $h = 0$; total noise then falls monotonically toward an asymptotic Brownian floor. A numerical routine that divides by h would fail precisely at this informative physical limit. In either case, a force-noise specification referred to the external sample can produce a different optimum because force conversion multiplies displacement noise by stiffness.

With the baseline values $a = 2.039 \times 10^{-12}\ \mathrm{m\,V/\sqrt{Hz}}$, $h = 2.00 \times 10^{-4}\ \mathrm{N/(m\,V^2)}$, $d_F \simeq 1.287 \times 10^{-13}\ \mathrm{N/\sqrt{Hz}}$. Substitution brackets the stationary point between 1.45 and 1.50 V. At roughly 1.47 V the density is about $6.72\,\mathrm{pm/\sqrt{Hz}}$, a shallow minimum compared with the heat-limited result. A tiny uncertainty in amplifier noise or in the support damping could shift the exact optimum appreciably while having very little effect on achievable resolution. Reporting a numerically optimised voltage to six decimals would imply a knowledge of the physical system absent from these inputs.

A direct bench experiment can test whether the excess really comes from compliance. Compare the demodulated spectrum with the centre plate tightly held and with it free. The electrical floor should be similar if the clamping keeps cable capacitance and carrier coupling fixed. The free probe should acquire a mechanical resonance which moves with V_d^2, and the low-frequency component should track the inferred static stiffness. A large peak locked to carrier-drive amplitude modulation in both experiments suggests coherent feedthrough. Also check that the noise estimate comes from a frequency band above drift yet below resonance, and that the inferred amplitude density times the square root of the bandwidth predicts repeated stationary readings. These practical checks distinguish a readout-limited displacement estimate from a calibrated measurement of actual thermal motion.

Explore the usable voltage range of the bridge

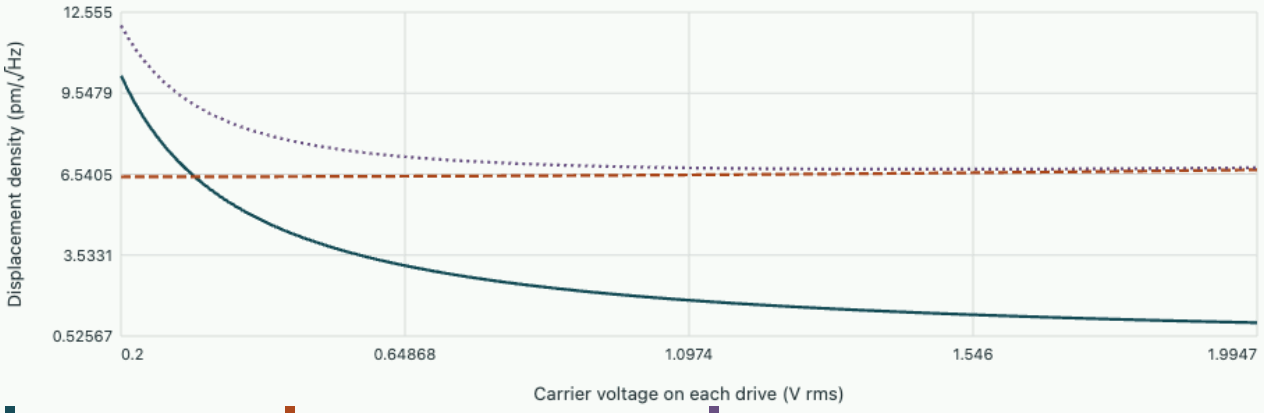
The horizontal axis ends at the first of the heat, driver and mechanical limits. With 4 pF fixed parasitic capacitance at 100 kHz the heat ceiling is 1.995 V rms, while a freely suspended probe reaches its minimum combined noise near 1.47 V rms. Reduce the added capacitance to zero and explain why a finite optimum arising from mechanical softening disappears. Then lower carrier frequency. The current-noise term grows and dielectric heating at a given voltage falls. Observe which effect changes the allowed voltage range and which changes the height of the electrical noise curve.

Open this experiment online

Try the calculation

Input and stray capacitance (pF) 4

Carrier frequency (kHz) 100



Maximum allowed drive 1.995 V rms. Minimum combined noise 6.72 pm/√Hz at 1.472 V rms.

Tutorial · separate electronic resolution from mechanical response

Find the frequency at which current and voltage noise contribute equally

Retain the baseline input capacitances and noise sources. Calculate the crossover frequency and the effect of doubling cable capacitance from 4 pF to 8 pF. What happens to input-referred current-noise displacement at fixed frequency?

▼ **Work through the solution**

Set $i_n/(2\pi f C_T) = e_n$. With $C_T = 8$ pF the crossover is 19.9 kHz. The longer cable gives $C_T = 12$ pF and a crossover at 13.3 kHz. At 100 kHz, the current noise at the input falls to $1.33\,\mathrm{nV}/\sqrt{\mathrm{Hz}}$ but gain falls from 5000 to 3333 V/m. The current contribution remains $0.398\,\mathrm{pm}/\sqrt{\mathrm{Hz}}$. The voltage contribution increases from 2.00 to 3.00 pm/√Hz. Both results follow independently by substituting $K = 2C_0V_d/(gC_T)$ into the noise formula and cancelling C_T in only one of the two terms.

Diagnose a frequency shift and a noise claim

At 2.00 V the resonance changes from 500.0 Hz to 490.0 Hz. Determine the implied stiffness reduction. A second experiment quotes 10 pm rms in a 100 Hz noise bandwidth for the freely suspended probe at 300 K. Can thermal equilibrium and the measured spring and damping account for this number?

▼ **Work through the solution**

At unchanged moving mass $k_{\mathrm{eff}}/k = (490/500)^2 = 0.9604$. The measured electrical stiffness is 0.000792 N/m, consistent with the 0.00080 N/m prediction. At frequencies well below resonance the Brownian density is approximately 6.70 pm/√Hz, and a flat 100 Hz equivalent band would contain approximately 67 pm rms of thermal motion alone. Ten picometres rms would correspond to about 2.2 Hz equivalent noise bandwidth at this density, or require a changed mechanical condition, frequency band or calibration. To discriminate experimentally, measure the mechanical resonance spectrum with a known input-force calibration and integrate the noise with the actual filter transfer. Include mechanical susceptibility over the band if the filter extends close to resonance.

Further reading

- Maxwell stress and electrical coenergy in mechanical force balances
- MIT · Woodson and Melcher, lumped-parameter electromechanics, chapter 3

Electromechanics, optics and measurement · 5. A moving-coil galvanometer as an electrical and mechanical system

A scale division records an angle, yet the quantity marked on the dial is electric current. A spring, a magnetic field and the resistance of the external measuring circuit connect the two. Derive the calibration, predict how a pointer approaches its reading, and find which experiment measures the charge of a short pulse.

Convert the force on two straight sides into a torque

A light rectangular coil has N turns, active length l, width w, and area per turn $A = lw$. It pivots about an axis parallel to its long sides. Shaped pole pieces confine an approximately radial magnetic field of magnitude B to an air gap. Over the working angular range the magnetic field is perpendicular to the active wire and lies approximately in the plane of the coil. An elementary length carrying conventional current i experiences $d\mathbf{F} = i\,d\mathbf{l} \times \mathbf{B}$. The two long sides carry current in opposite directions and experience forces of equal magnitude $NilB$. Acting with lever arms $w/2$, the forces make a couple whose torque is $NiAB$. Their net force is approximately zero. The short ends supply negligible torque about the pivot under the ideal geometry.

Write $K = NAB$, and choose the positive sense of current to give positive torque. Its units are $\mathrm{N\,m/A}$. In a uniform Cartesian field an ordinary rigid loop instead gives torque $NiAB\sin\alpha$, where α is the angle between its normal and the field. The radial gap maintains the factor equivalent to $\sin\alpha$ close to unity as the pointer turns. This is a design choice that produces a nearly linear scale. If a measured calibration curve flattens at a large angle, field nonuniformity and a nonlinear torsion spring are candidate causes that can be tested separately.

For a soft torsion spring with stiffness κ, the return torque is $-\kappa\theta$ at small deflections from the zero-current setting. At static equilibrium $\theta = Ki/\kappa$. With $N = 200$, $A = 1.00\,\mathrm{cm^2}$, $B = 0.250\,\mathrm{T}$ and $\kappa = 8.0 \times 10^{-4}\,\mathrm{N\,m/rad}$, the torque constant is $0.0050\,\mathrm{N\,m/A}$ and the current sensitivity is $6.25\,\mathrm{rad/A}$. A $5.0\,\mathrm{mA}$ current turns the pointer through $0.03125\,\mathrm{rad}$, about 1.79°. A mirror mounted on the same axle deflects a reflected laser through twice this angle. At a screen distance of $0.50\,\mathrm{m}$ the spot shifts $0.50\tan(2\theta) = 31.3\,\mathrm{mm}$, making the small mechanical rotation easy to resolve.

Recover the reciprocal voltage from work

Now rotate the coil through a small positive angle while it carries positive current. The electromagnetic torque does mechanical work $Ki\,d\theta$. The voltage associated with the motion must therefore draw electrical work $ie_{\mathrm{back}}\,dt$ of equal magnitude when the motor torque assists that motion. This gives the back-emf relation $e_{\mathrm{back}} = K\dot\theta$, measured as a positive drop in the motor sign convention. Its coefficient has units $\mathrm{V\,s/rad}$, numerically the same SI coefficient as the torque constant. One can also derive it from the motional emf on the two active sides. Each moves at speed $(w/2)\dot\theta$, crosses field B, and generates a voltage $Bl(w/2)\dot\theta$ along its wire. The two contributions add over every turn.

Let J denote the rotational inertia, b the mechanical viscous damping coefficient, L the coil inductance and R the sum of winding plus external series resistance seen by a voltage source $v(t)$. The electromechanical equations are

$$J\ddot{\theta} + b\dot{\theta} + \kappa\theta = Ki,$$

$$L\dot{i} + Ri + K\dot{\theta} = v(t).$$

Multiplying the first equation by $\dot{\theta}$ and the second by i eliminates the coupling power $Ki\dot{\theta}$. The result says that source power vi equals the rate of increase of $J\dot{\theta}^2/2 + \kappa\theta^2/2 + Li^2/2$, plus $b\dot{\theta}^2 + Ri^2$. This identity fixes the relative signs of the torque and back emf. If a sign mistake turns a passive closed coil into a self-accelerating pointer, the same mistake produces a residual coupling term in this power balance. Mechanical friction and winding heat represent distinct sinks even though both can damp the observed displacement.

Predict overshoot and find a critical external resistance

If the electrical relaxation time L/R is short compared with the oscillation time $1/\sqrt{\kappa/J}$, set $i \simeq (v - K\dot{\theta})/R$. Substituting into the mechanical equation increases its effective damping to $b_{\mathrm{eff}} = b + K^2/R$. Set $v = 0$ when discussing free relaxation with the electrical terminals connected through a resistor. A moving shorted coil generates a current that opposes its motion. Opening the circuit instead suppresses that current and leaves the mechanical damping. An ideal current source holding specified current through all pointer motions also changes the back-emf response because its output voltage adjusts to enforce that current.

The undamped angular frequency is $\omega_0 = \sqrt{\kappa/J}$ and the damping ratio is

$$\zeta = b_{\mathrm{eff}}/(2\sqrt{\kappa J}).$$

Take $J = 2.0 \times 10^{-6}\,\mathrm{kg\,m^2}$, $b = 1.6 \times 10^{-5}\,\mathrm{N\,m\,s/rad}$, and the preceding K, κ. Then $\omega_0 = 20.0\,\mathrm{rad/s}$, $2\sqrt{\kappa J} = 8.0 \times 10^{-5}\,\mathrm{N\,m\,s/rad}$, and an open circuit gives $\zeta = 0.20$. With $R = 1.00\,\Omega$ the electric contribution to damping is $2.50 \times 10^{-5}\,\mathrm{N\,m\,s/rad}$, giving $\zeta = 0.5125$. For a voltage step the ideal fractional overshoot in the reduced model is

$$\exp[-\pi\zeta/\sqrt{1-\zeta^2}] = 0.153.$$

The first peak occurs after $\pi/(\omega_0\sqrt{1-\zeta^2}) = 0.183\,\mathrm{s}$.

Critical damping occurs when $b + K^2/R = 2\sqrt{\kappa J}$, which requires a total resistance of about $0.391\,\Omega$. A winding resistance of $0.300\,\Omega$ therefore leaves $0.091\,\Omega$ for external source and leads. If the winding alone exceeds the target resistance, a simple passive external series resistor cannot reach this damping in the reduced model. A finite L must also be checked: with $L = 5.0\,\mathrm{mH}$ and $R = 1.0\,\Omega$, $\omega_0 L/R = 0.10$, so the approximation provides a useful starting estimate. Reducing R indefinitely eventually invalidates the elimination of current. The full pair of equations then predicts the damping and frequency dependence.

Distinguish a charge impulse from a slow current reading

Suppose a brief imposed current pulse ends long before the pointer has turned appreciably. Integrating the torque equation over that interval gives

$$J\Delta\dot{\theta} \simeq K\int i\,dt = Kq.$$

The initial signal is now angular velocity proportional to total transmitted charge. For weak subsequent damping, the first excursion is approximately $Kq/(J\omega_0)$. A dose of $20\,\mu\mathrm{C}$ gives $2.50\,\mathrm{mrad}$ with the instrument above, corresponding to about $2.50\,\mathrm{mm}$ on the mirror scale. Two current pulses of identical charge but different shapes give nearly the same reading if both are short on the mechanical time scale. Their peak currents can be entirely different.

For appreciable damping, use the impulse solution $\theta(t) = Kq\,e^{-\zeta\omega_0 t}\sin(\omega_d t)/(J\omega_d)$, with $\omega_d = \omega_0\sqrt{1-\zeta^2}$ for an underdamped pointer. Its maximum obeys $\tan(\omega_d t_p) = \omega_d/(\zeta\omega_0)$ in the first quarter cycle. Substitution corrects the ballistic calibration instead of treating the damped peak as an undamped amplitude. The state of the external circuit after the pulse matters because it determines ζ during the throw. A calibration pulse should leave the measuring circuit connected in the same way as the unknown pulse.

Measure the torque constant without assuming the magnetic field

The preceding design calculation multiplies turn count, active area and a nominal air-gap induction. An independent calibration can measure the same constant without knowing the field distribution along every wire. Move the pointer through a small controlled angle while measuring its open-circuit voltage with a high-impedance instrument. In the same working interval the voltage is $K(\theta)\dot{\theta}$ up to a polarity choice. Integrating the voltage over the sweep gives $\int_{\theta_1}^{\theta_2} K(\theta)\,d\theta$. If K is constant this is simply $K\Delta\theta$, independent of sweep speed. It is often easier to integrate a recorded voltage pulse accurately than to differentiate the angle trace to obtain instantaneous speed.

For a sweep through $0.0800\,\mathrm{rad}$, suppose the measured voltage integral is $0.401\,\mathrm{mV\,s}$. The generator constant is $5.01\times10^{-3}\,\mathrm{V\,s/rad}$. Independently add a known small torque to the spring and measure its static angle. A torque $32.0\,\mu\mathrm{N\,m}$ rotates the pointer by $0.0400\,\mathrm{rad}$, giving $\kappa = 8.00\times10^{-4}\,\mathrm{N\,m/rad}$. Combining the two measurements predicts a current sensitivity of $6.27\,\mathrm{rad/A}$. Splitting the sweep into smaller equal angular intervals tests whether the measured K depends on angle. Sweeping backwards should reverse the integrated voltage. A voltage offset instead contributes its offset times duration, so repeating at two sweep speeds helps separate it.

A dynamic cross-check uses free decay under two load conditions. Measure the exponential decay rate α_{open} with a high-impedance voltage probe and α_R with a known total resistance in the closed circuit. In the short-electrical-time limit, subtraction of the two damping laws yields

$$K^2 = 2JR(\alpha_R - \alpha_{\mathrm{open}}).$$

With $J = 2.0 \times 10^{-6}\,\mathrm{kg\,m^2}$, $R = 1.00\,\Omega$, and decay rates 4.0 and $10.25\,\mathrm{s^{-1}}$, this gives

$$K = 0.0050\,\mathrm{N\,m/A}.$$

The method needs two identifiable decay rates and independent inertia. If the loaded response is overdamped, the envelope of two oscillation peaks is no longer available; fit the full two-real-pole response to the measured displacement.

Keep the third dynamical variable in a frequency-response experiment

For a sinusoidal voltage at angular frequency ω the exact linear transduction law follows by eliminating the complex current after transforming both differential equations. The mechanical impedance in angular-displacement form is $\kappa - J\omega^2 + i\omega b$; the winding impedance is $R + i\omega L$. Using phasors with time dependence $e^{i\omega t}$ gives

$$\frac{\Theta}{V} = \frac{K}{(R + i\omega L)(\kappa - J\omega^2 + i\omega b) + i\omega K^2}.$$

At zero frequency the gain is $K/(R\kappa)$ and the phase tends to zero, as the static calibration requires. At a sufficiently high frequency both the electrical and inertial impedances grow. For $L > 0$ the magnitude approaches $K/(LJ\omega^3)$. The reduced model with the current eliminated algebraically falls only as $1/\omega^2$. The change of the asymptotic slope provides an experimental way to distinguish finite inductance from an incorrectly adjusted viscous damping constant. Beyond the working band of a real instrument, elastic modes of the pointer or parasitic capacitance can enter before that asymptote is resolved.

At the nominal undamped frequency $20\,\mathrm{rad/s}$, with $R = 1.0\,\Omega$ and $L = 5.0\,\mathrm{mH}$, the stiffness and inertia terms cancel. The denominator becomes $-\omega^2 L b + i\omega(Rb + K^2)$, or approximately $-0.000032 + i\,0.000820$ in consistent SI units. Its magnitude gives about $6.09\,\mathrm{rad/V}$. A sinusoid of $1.0\,\mathrm{mV}$ peak produces about $6.09\,\mathrm{mrad}$ peak, whereas the static response to $1.0\,\mathrm{mV}$ is $6.25\,\mathrm{mrad}$. The phases differ radically despite their similar amplitudes: near this frequency the pointer lags by about 92.2°. A gain-only calibration at a single frequency would miss the phase lag.

Change the electrical load and compare two step models

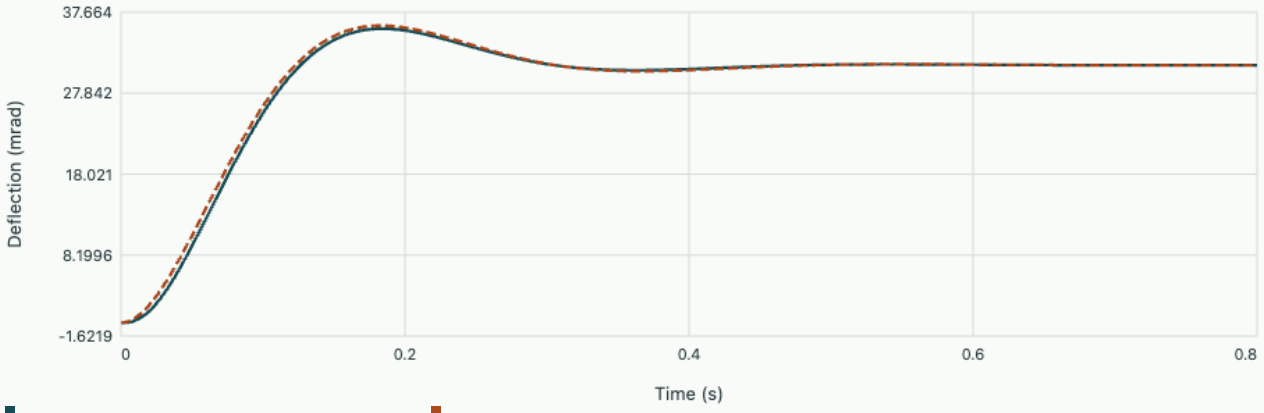
In the live graph the source voltage is chosen anew at each resistance to give a final current of $5.0\,\mathrm{mA}$ after the pointer settles. That convention keeps the final angle common to all curves and isolates the transient response of the load. The full model retains $i, \theta, \dot\theta$; the second curve sets $L\dot i = 0$. Predict first which trace should start flatter. With finite inductance the current initially vanishes and increases at a finite rate. The initial torque and angular acceleration therefore vanish, while the reduced model applies a finite torque immediately. Increasing the inductance makes that distinction easier to see, especially when the electrical response time becomes comparable to the period of mechanical oscillation.

Open the live experiment

Try the calculation

Total resistance (Ω) 1

Winding inductance (mH) 5



Coupled winding and pointer Short electrical time approximation

The reduced damping ratio is 0.512. The largest deflection in the first 0.80 s is 35.67 mrad. The common static limit is 31.25 mrad.

How could a student change the static range of the instrument without changing its suspension or its torsional stiffness?

▼ **Work through the solution**

For a dc ammeter, connect a calibrated shunt resistance in parallel with the coil, allowing only a known fraction of total current into it. With a coil winding resistance $0.300\,\Omega$ and a $0.0333\,\Omega$ shunt, the coil carries about ten percent of a steady terminal current and the indicated full-scale terminal current increases about tenfold. The total circuit seen by a motional voltage during a pointer oscillation depends on the shunt and source impedance, so the static range multiplier does not by itself give the new damping. For a voltmeter, a series resistance instead sets the current produced by an applied terminal voltage. In both cases record the resistance network whenever reporting a dynamic response.

Estimate the back action on the signal being measured

A galvanometer becomes part of the circuit it observes. Suppose a source with open-circuit voltage $10.0\,\mathrm{mV}$ and internal resistance $2.00\,\Omega$ drives a coil of resistance $0.300\,\Omega$. After settling, the current is $4.35\,\mathrm{mA}$ and the pointer turns by $27.2\,\mathrm{mrad}$. The undisturbed short-circuit current of the source would have been $5.00\,\mathrm{mA}$. Interpreting the indicated value as the current that would flow with a perfect zero-resistance meter underestimates that quantity by about thirteen percent. Measuring the open-circuit voltage instead requires a sufficiently large input resistance, another electrical boundary condition.

During pointer motion the disturbance includes the back emf as well as winding resistance. If the same coil is briefly turning at $0.40\,\mathrm{rad/s}$ it develops a $2.0\,\mathrm{mV}$ back emf. Neglecting inductance for that estimate, the resulting current is

$$(10.0 - 2.0)\,\mathrm{mV}/2.30\,\Omega = 3.48\,\mathrm{mA}.$$

The deflection therefore contains information about both the source and the pointer's earlier motion. A static calibration alone cannot recover a rapid source waveform. A known source resistance and the two coupled dynamic equations provide a way to estimate the waveform from synchronised angle and current measurements.

Tutorial on calibration and transient identification

A current source produces a static mirror shift of $12.5\,\mathrm{mm}$ on a screen $0.50\,\mathrm{m}$ away. Estimate the current and identify a reversible test for an angular zero offset.

▼ **Work through the solution**

Use $\theta = \frac{1}{2}\arctan(0.0125/0.50) = 0.01250\,\mathrm{rad}$ and $i = \kappa\theta/K = 2.00\,\mathrm{mA}$. Repeat with reversed current of equal magnitude. Half the difference of the two angles cancels a fixed angular zero offset and isolates the response odd in current. A changing temperature during reversal can alter the spring or winding resistance, so alternate the order and record the zero afterwards if the required uncertainty is small.

For an open-circuit free decay the ratio of two successive same-side positive peak angles is 3.60. Their time separation is $0.321\,\mathrm{s}$. Recover the mechanical parameters that can be inferred if J is known.

▼ **Work through the solution**

The logarithmic decrement is $\ln 3.60 = 1.281$. The decay rate is $\alpha = 1.281/0.321 = 3.99\,\mathrm{s}^{-1}$, and the damped angular frequency is

$$2\pi/0.321 = 19.57\,\mathrm{rad/s}.$$

Then $\omega_0 = \sqrt{\omega_d^2 + \alpha^2} = 19.97\,\mathrm{rad/s}$,

$$b = 2J\alpha = 1.60 \times 10^{-5}\,\mathrm{N\,m\,s/rad},$$

$$\kappa = J\omega_0^2 = 7.98 \times 10^{-4}\,\mathrm{N\,m/rad}.$$

This identification assumes viscous damping and a sufficiently high impedance to make the electrical damping negligible.

Explore how motion generates voltage in the induction chapter.

Electromechanics, optics and measurement · 6. Eddy-current braking, magnetic penetration and the heat left behind

A conducting loop moves above a row of magnetic poles. The drag first increases with speed, but a rapid crossing need not generate proportionally greater braking. Trace the work done against the Lorentz force into circuit energy, heat and a measurable temperature change. Then decide which features of a solid plate the single-loop model can capture.

Generate a voltage from a spatially periodic field

Let a rectangular loop of height h along y and width w along x translate to the right above a stationary magnetic pattern. At the loop let the normal induction be $B_z(x) = B_0 \cos(kx)$, with $k = 2\pi/\lambda$. Its two active sides are centred symmetrically about the coordinate x_c. Assume the field varies negligibly along y over this height. Integrating through the loop gives

$$\Phi = h \int_{x_c - w/2}^{x_c + w/2} B_0 \cos(kx)\, dx = [2hB_0 \sin(kw/2)/k] \cos(kx_c).$$

A uniform translation $x_c = ut$ therefore produces an external emf with peak amplitude $E_{\mathrm{pk}} = Ku$, where $K = 2hB_0 |\sin(kw/2)|$.

This spatial averaging explains an initially surprising design feature. A loop spanning precisely one full spatial period always links zero net flux from the sinusoidal field and therefore generates no emf in this ideal geometry. A loop of half a period has maximum coupling at a specified height. If w is much smaller than the period,

$$\sin(kw/2) \simeq kw/2,$$

$$K \simeq hwB_0 k.$$

This is exactly the small-loop result from using its area times the local gradient of induction. Reversing velocity reverses the emf at a fixed position. At a fixed positive speed the temporal frequency is $f = u/\lambda$, so the same conductor experiences different electrical frequencies at different mechanical speeds.

Include finite inductance and derive the drag curve

Model the current path by a constant resistance R and self-inductance L. Its steady periodic current solves $L\dot{i} + Ri = \mathcal{E}(t)$. In phasor notation its magnitude is $E_{\mathrm{pk}}/\sqrt{R^2 + (\omega L)^2}$, lagging the emf by $\arctan(\omega L/R)$, where $\omega = ku$. The current develops field energy $Li^2/2$ and dissipates Ri^2. Multiplying the circuit equation by i and averaging over a period eliminates the derivative of stored energy. The average mechanical power delivered against the drag is therefore the mean Joule heating $P = E_{\mathrm{pk}}^2 R/[2(R^2 + \omega^2 L^2)]$. Dividing by the speed gives the drag magnitude

$$F(u) = \frac{K^2 u}{2R[1 + (u/u_c)^2]},$$

$$u_c = \frac{R}{kL}.$$

At low speed the drag is proportional to velocity. At the crossover $u = u_c$ it reaches $K^2 u_c/(4R)$, and at much larger speeds it falls approximately as $1/u$ within the assumed lumped model. The incoming mechanical power then tends to a constant rather than growing without bound. Why is there a maximum? Increasing speed raises the emf, but it also raises the reversal frequency. An inductive current increasingly lags the driving emf, and its component in phase with the emf does the net dissipative work. A measured turnover therefore tests both an electrical time scale and the spatial scale of the magnet pattern.

Use $h = 50\,\mathrm{mm}$, $w = 25\,\mathrm{mm}$, $\lambda = 0.100\,\mathrm{m}$, $B_0 = 0.20\,\mathrm{T}$, $R = 0.050\,\Omega$ and $L = 0.150\,\mathrm{mH}$. Then $K = 0.01414\,\mathrm{T\,m}$, $u_c = 5.31\,\mathrm{m/s}$, and maximum mean drag is $5.31\,\mathrm{mN}$. At $u = 2.0\,\mathrm{m/s}$ the field alternates at $20\,\mathrm{Hz}$, giving an emf of $28.3\,\mathrm{mV}$ peak. The current is $0.529\,\mathrm{A}$ peak and its phase lag 20.7°. The resistor receives approximately $7.00\,\mathrm{mW}$, and the motor maintaining translation supplies a mean force of $3.50\,\mathrm{mN}$. Using peak current in I^2R without its factor one half would overstate the mechanical force by a factor two.

Determine whether the current penetrates a real plate

A continuous metal plate contains many possible current paths, unlike a preformed loop. Their resistances, inductances and mutual couplings depend on the plate boundary, magnet geometry and frequency. For a good homogeneous conductor the magnetic diffusion equation gives a skin depth $\delta = \sqrt{2/(\mu\sigma\omega)}$ under sinusoidal excitation. At a depth δ a field entering a locally planar half-space has lost a factor e in amplitude and acquired a phase delay of one radian. The frequency to use is the frequency experienced by the moving material; the fact that the magnets are stationary in the laboratory does not make this frequency zero.

For copper with $\sigma = 5.8 \times 10^7\,\mathrm{S/m}$ and permeability close to μ_0, the skin depth is about $14.8\,\mathrm{mm}$ at $20\,\mathrm{Hz}$ and $1.48\,\mathrm{mm}$ at $2.0\,\mathrm{kHz}$. A $2.0\,\mathrm{mm}$ plate therefore sees little through-thickness attenuation in the first experiment but may need a diffusion calculation in the second. The plate's lateral current pattern can still matter when the through-thickness current density is nearly uniform. Slots interrupt wide current loops and usually reduce drag even when the mass and the bulk conductivity change little. Comparing a slotted and an unslotted plate directly tests the importance of current closure.

If a plate experiences sharply separated poles, its applied field in the moving frame contains a fundamental and higher harmonics. Harmonic n has a skin depth smaller by $\sqrt{n}$, so checking only the fundamental can miss surface concentration associated with narrow features. A Hall scan along the track supplies the actual spatial field spectrum. Multiplying each spatial wavenumber by the speed converts it into a temporal angular frequency for a constant-speed pass. Once the speed changes significantly over one pole spacing, a time-domain calculation using the measured position trace is preferable to this fixed-frequency conversion.

Close a mechanical and thermal energy budget

Take a rotating brake as a second experiment. A flywheel of known inertia $J_{\mathrm{rot}} = 0.020\,\mathrm{kg\,m^2}$ slows from 120 to $80\,\mathrm{rad/s}$ while no drive supplies power. The released rotational kinetic energy is

$$J_{\mathrm{rot}}(120^2 - 80^2)/2 = 80.0\,\mathrm{J}.$$

A separate run with the magnet removed measures bearing and air losses. Suppose the corresponding speed-dependent losses integrated over the magnetic braking trajectory total $8.0\,\mathrm{J}$. Then the electromagnetic channel receives $72.0\,\mathrm{J}$. Using the reference run's total energy over an arbitrary equal time could give a different answer, since the two speed histories affect the parasitic losses.

A calorimeter enclosing the conducting rotor has effective heat capacity $C = 60\,\mathrm{J/K}$ and a thermal link of conductance $G = 0.12\,\mathrm{W/K}$ to an environment at constant temperature T_a. Its balance is

$$C\,dT/dt = P_{\mathrm{deposited}} - G(T - T_a).$$

During a $20\,\mathrm{s}$ run, suppose the time-averaged rise above ambient is $0.50\,\mathrm{K}$. Then $1.20\,\mathrm{J}$ flowed through the thermal link. If all electromagnetic heat entered the calorimeter, its final rise from an ambient start is

$$(72.0 - 1.20)/60 = 1.18\,\mathrm{K}.$$

A measured rise near $0.80\,\mathrm{K}$ would leave an energy discrepancy of approximately $23\,\mathrm{J}$. Check conduction into a shaft, heat stored outside the instrumented volume, and the estimate of parasitic torque before adjusting the electromagnetic theory.

Find the spatial features that dominate a measured braking signal

A single Fourier component of field already produces an informative turnover. In a tracked experiment the field often has a measurable third harmonic. Let $B(x) = B_1 \cos kx + B_3 \cos(3kx + \varphi)$, with constant translation speed. Flux integration across the finite loop multiplies each harmonic by its own width factor. The corresponding emf peak is $2h|B_n|u|\sin(nkw/2)|$, and its temporal angular frequency is nku. The linear RL equation treats the two drives independently. Orthogonality over a complete fundamental period makes the mean of their product vanish, so total mean heat can be found by adding the individual resistive powers. Within one period the interference terms do affect instantaneous torque and power.

Suppose $B_3/B_1 = 0.20$ and keep the preceding $w = \lambda/4$. Here $\sin(kw/2)$ and $\sin(3kw/2)$ both have magnitude $1/\sqrt{2}$. At low speed the third harmonic therefore adds about four percent to mean drag. At $u = u_c$, however, its angular frequency sees inductive impedance $3R$ while the fundamental sees R. The third-harmonic share relative to the fundamental becomes $0.20^2(1+1)/(1+9) = 0.008$, only 0.8%. A peak-to-peak field reading can change visibly without a comparable change in mean drag. Conversely, if the loop width happens to null one spatial harmonic, another smaller harmonic can supply most of the signal. A field map and the loop geometry together determine what source drives the circuit.

In a solid plate, predicting force from field and speed needs a field solution that enforces current closure. In the slowly moving conductor, $\mathbf{J} = \sigma[-\nabla\phi + \mathbf{u} \times \mathbf{B}]$ when the imposed magnetic pattern is effectively time independent in the laboratory and the induced magnetic field can be neglected. Charge conservation then gives

$$\nabla \cdot [\sigma(-\nabla\phi + \mathbf{u} \times \mathbf{B})] = 0.$$

On an electrically insulated plate edge, enforce $\mathbf{n} \cdot \mathbf{J} = 0$. Solving this potential problem accounts for charge accumulation that redirects currents at a boundary. Simply setting $\mathbf{J} = \sigma\mathbf{u} \times \mathbf{B}$ can predict current flowing straight out of an insulating edge. The force follows from integrating $\mathbf{J} \times \mathbf{B}$ through the conducting volume, and Joule heat follows from $\int J^2/\sigma \, dV$.

A useful check on such a field calculation is a finite plate translating wholly inside an exactly uniform static magnetic field. Charges can rearrange until a uniform electrostatic field cancels $\mathbf{u} \times \mathbf{B}$. An isolated plate in this steady limit then has zero transport current and zero drag. Motion alone does not guarantee braking. At an entry edge, the moving conductor spans a spatial change of induction, and one scalar potential generally cannot cancel the motional drive around every closed path. Slits, thickness variations, a conducting contact at a boundary, and the induced field at higher speeds each change this test problem in an identifiable way.

Interpret a thermal transient without assuming it is instantaneous

If the brake runs at a stable speed and equilibrium electrical conditions, a local single-temperature model sees a nearly constant power. Its step response from ambient is $\Delta T = (P/G)[1 - \exp(-Gt/C)]$. Removing the drive gives an exponential decay with the same time constant C/G. Measuring that cooling tail fixes the ratio of heat capacity to conductance but does not set either one separately. A known heater power or an independent heat-capacity measurement supplies the missing absolute scale. A slope evaluated over a long interval without correcting leakage will underestimate the input power as the sample warms.

Take a small bench calorimeter enclosing the single test loop with $C = 1.20\,\mathrm{J/K}$ and $G = 0.020\,\mathrm{W/K}$. The $7.00\,\mathrm{mW}$ low-speed run gives a $0.350\,\mathrm{K}$ eventual rise and a $60\,\mathrm{s}$ time constant. After $30\,\mathrm{s}$ the rise is about $0.138\,\mathrm{K}$, whereas a thermally isolated calculation would give $0.175\,\mathrm{K}$. Its stored heat $0.166\,\mathrm{J}$ is less than the $0.210\,\mathrm{J}$ mechanical work over that interval; the thermal link accounts for the remainder. Loading the conductor thermally with an additional copper holder increases the response time and changes the initial slope without changing the final rise if conductance to the bath remains the same.

Compare predictions at a chosen travel speed

The live graph displays the force predicted by the finite-inductance loop alongside the resistive low-frequency extrapolation. Choose a speed, calculate the apparent excitation frequency, and compare the

returned skin depth to the actual conductor thickness before interpreting the prediction as a plate measurement. Try choosing an inductance twice as large. The location of maximum force halves in speed, but the low-speed slope at fixed geometry and resistance is unchanged. A real plate whose high-speed drag does not follow the single-loop curve can still agree with the model on its low-speed slope. Plotting the measured residuals against speed can reveal the point where extra current paths or through-thickness diffusion become important.

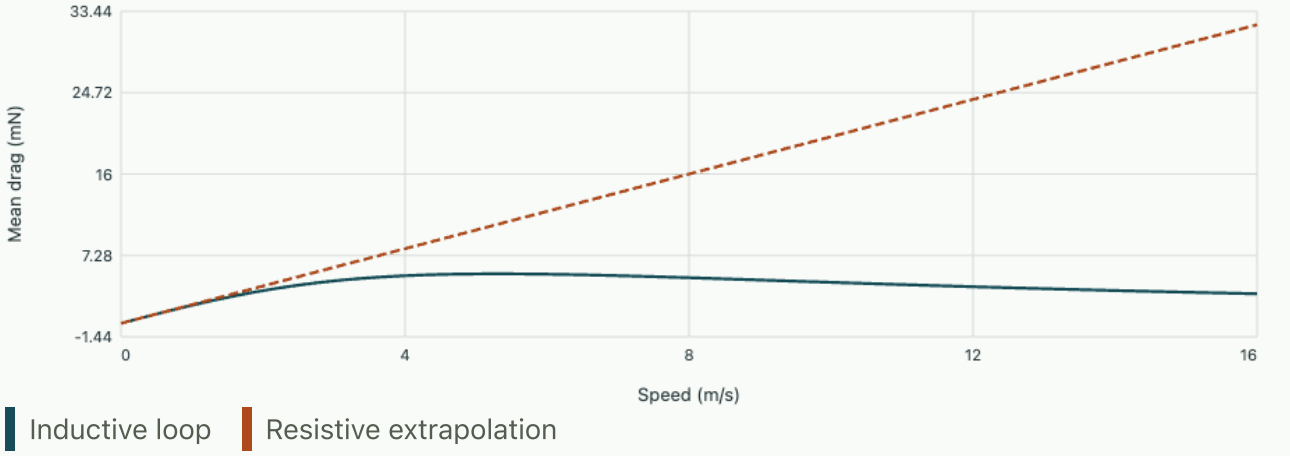
Open the live experiment

Try the calculation

Travel speed (m/s) **2**

Loop inductance (mH) **0.15**

Peak field (T) **0.2**



At 2.00 m/s the drag is 3.50 mN and the mean heat is 7.00 mW. The copper skin depth at 20.0 Hz is 14.78 mm. Peak drag occurs at 5.31 m/s.

A plate and holder cool from $0.240\,\mathrm{K}$ above ambient to $0.120\,\mathrm{K}$ in $42\,\mathrm{s}$ after a run. Can these two readings establish the braking power?

▼ **Work through the solution**

The half-life gives

$$C/G = 42/\ln 2 = 60.6\,\mathrm{s},$$

which agrees approximately with the small calorimeter example. It determines only a ratio. If an independent steady $10.0\,\mathrm{mW}$ heater then produces a $0.500\,\mathrm{K}$ temperature rise, $G = 0.0200\,\mathrm{W/K}$ and $C = 1.21\,\mathrm{J/K}$. A magnetic run that settles at $0.350\,\mathrm{K}$ now corresponds to $7.00\,\mathrm{mW}$, provided the thermal boundary and deposition pattern are sufficiently similar to the calibration.

Check the sign of instantaneous electromagnetic work

At a phase where the applied emf has just crossed zero, a finite-inductance loop may still carry considerable current. During part of a cycle the emf and current can have opposite signs. The product $\mathcal{E} i$ is then negative even though $R i^2$ remains positive. The difference is a negative derivative of the magnetic store $L i^2/2$. The loop briefly returns energy mechanically while its stored field decreases, and some of that release also becomes heat. A force transducer resolving separate pole passages can therefore see instantaneous variations that a mean braking-force estimate suppresses.

For the numerical $2.0\,\mathrm{m/s}$ case the peak field energy is $L I_{\mathrm{pk}}^2/2 \approx 21.0\,\mu\mathrm{J}$. The dissipated energy per full pole period is

$$7.00\,\mathrm{mW}/20\,\mathrm{Hz} = 350\,\mu\mathrm{J}.$$

These quantities serve different purposes. The first is a reversible instantaneous store; the second is net irreversible energy delivered each time the conductor moves one spatial period. Dividing the second by the spatial period of $0.100\,\mathrm{m}$ recovers the mean drag of $3.50\,\mathrm{mN}$ without using the translational speed explicitly.

Tutorial on braking measurements

At $u = 2.0\,\mathrm{m/s}$ the loop above experiences a mean drag of $3.50\,\mathrm{mN}$. Predict what halving the induction and doubling the speed does, keeping its geometry and electrical properties fixed.

▼ **Work through the solution**

Halving induction quarters K^2. The speed factor contributes $2[1+(2/5.31)^2]/[1+(4/5.31)^2] \approx 1.46$. The combined change gives a drag about 0.364 times the original, or $1.27\,\mathrm{mN}$. The mechanical power decreases less because speed has doubled. A linear-speed extrapolation would miss the inductive phase lag, already significant at $4\,\mathrm{m/s}$.

In a repeated flywheel test the brake becomes warmer with every run. Which electrical parameter change can explain a change of drag even with the magnets held fixed?

▼ **Work through the solution**

The resistance of an ordinary metal generally increases with temperature. At a fixed speed F is proportional to $R/[R^2+(\omega L)^2]$. Raising resistance reduces drag on the low-frequency resistive side and can increase it on the high-frequency inductive side. The maximum occurs at $R = \omega L$ if electrical geometry and inductance stay fixed. Measuring the temperature and resistance before each run helps distinguish this effect from a weakening field or a changed gap.

Compare a step-driven diffusion profile with sinusoidal skin penetration.

Electromechanics, optics and measurement · 7. Measuring magnetic core loss by a hysteresis loop and by calorimetry

A closed loop on a graph of magnetic induction against field encloses an area with units of energy per unit volume. A thermometer measures kelvins. Bring these two observations onto the same scale, account for the winding heat, and determine when the two experiments actually test the same material loss.

Infer the field and the induction from independent windings

Wind a toroidal specimen with a primary winding of N_p turns and a lightly loaded pickup of N_s turns. Let A be the representative iron cross-sectional area, ℓ the mean magnetic path length and $V_c = A\ell$ the magnetic volume. Neglect a gap and leakage initially. Ampère's law around a path through the core gives

$$H \simeq N_p i_p / \ell.$$

This relation is accurate when the toroid is slender enough that the spread of path radii is small and the pickup current is negligible. In a thick toroid $H(r) = N_p i_p/(2\pi r)$, so one point on a nominal loop can actually represent a range of local field values.

Faraday's law supplies the second observable. Choose winding polarity so the reported voltage is

$$v_s = N_s A \, dB/dt.$$

Integrating the voltage gives the change in cross-section-averaged magnetic induction. The pickup cannot determine a constant induction offset, because static flux induces no voltage. A closed loop area is insensitive to adding a constant to B or H, but a dc offset in the voltage integrates into a time-dependent ramp and prevents the reconstructed trajectory from closing. In steady periodic operation one can subtract the voltage mean over a complete period before integration. Applying that correction to a genuinely evolving magnetisation process would remove part of a real flux change.

Multiply the two measured field quantities in the appropriate order. The field work supplied per unit material volume on a small induction change is $H\,dB$. The source term associated with the magnetising flux is $i_p v_{p,\mathrm{induced}}\,dt$. Using $v_{p,\mathrm{induced}} \simeq (N_p/N_s) v_s$, its value is

$$i_p N_p A \, dB = V_c H \, dB.$$

Integrating around a settled cycle gives the magnetic loss

$$W_c = V_c \oint H \, dB,$$

$$P_c = f V_c \oint H \, dB.$$

The field can absorb positive work and return some of it later in the same cycle. The area measures the algebraic remainder. Reversing the polarity of a single signal flips the loop orientation. A passively

heated specimen must receive positive net energy when signs are defined for power entering the core. Simply taking the absolute value of all instantaneous products would count reversible storage twice and can grossly overestimate the heat.

Work an elliptical loop from time-domain signals

Suppose a nearly sinusoidal field is $H = H_p \cos \omega t$ and the induction lags it by a positive angle δ, $B = B_p \cos(\omega t - \delta)$. Differentiate the latter and multiply by H. Over one cycle $\cos \omega t \sin \omega t$ averages to zero, and $\cos^2 \omega t$ averages to one half. The resulting mean power density is $\omega H_p B_p \sin \delta / 2$, giving $\oint H \, dB = \pi H_p B_p \sin \delta$. With zero lag the two signals trace a line and the area vanishes, even if the peak values are large. A saturation-distorted loop need not be elliptical; the original time integral remains valid with synchronised data.

Take $H_p = 120\,\mathrm{A/m}$, $B_p = 0.200\,\mathrm{T}$ and $\delta = 12^\circ$. The energy per cycle and volume is $15.68\,\mathrm{J/m^3}$. A toroid with $\ell = 0.20\,\mathrm{m}$, $A = 2.0 \times 10^{-4}\,\mathrm{m^2}$ and $V_c = 40\,\mathrm{cm^3}$ dissipates $0.627\,\mathrm{mJ}$ per cycle. At $f = 200\,\mathrm{Hz}$ its power is $0.125\,\mathrm{W}$. With $N_p = 100$, the necessary current peak is $0.240\,\mathrm{A}$. With $N_s = 50$, the pickup voltage has peak $N_s A (2\pi f) B_p = 2.51\,\mathrm{V}$. These last two predictions allow the raw oscilloscope traces to be checked before a calculated loss in watts is trusted.

For sampled periodic data use $w = \sum_n (H_n + H_{n+1})(B_{n+1} - B_n)/2$, including the segment from the last point back to the first. This trapezoidal line integral computes an oriented polygon area. Plot the starting and ending points before adding the closing segment. Connecting widely separated endpoints by hand hides drift and can generate a fictitious wedge whose area depends on acquisition timing. Repeat at higher sampling rates to see whether corners or switching features carry appreciable extra area. When a periodic excitation has harmonics the time increment must resolve the highest significant harmonic in both measured signals.

Compare a thermal measurement with the magnetic area

Consider first a calorimeter that receives heat only from the core. Let the heat capacity of specimen, holder and sensor be C_{eff}. Let the leakage conductance to an ambient bath be G, and let $\Delta T = T - T_a$. The thermal balance $C_{\mathrm{eff}} \dot{\Delta T} = P_c - G \Delta T$ predicts a steady offset P_c/G and an initial heating slope P_c / C_{eff}. A small thermometer lag or poor thermal contact can make the earliest measured slope misleading even though environmental losses are then small. A separate electrical heater placed where the core deposits its heat can calibrate the effective thermal response.

For $C_{\mathrm{eff}} = 20\,\mathrm{J/K}$, $G = 0.015\,\mathrm{W/K}$, and a $2.0\,\mathrm{K}$ rise above ambient, the magnetic loss $0.125\,\mathrm{W}$ would give a slope of about $0.00477\,\mathrm{K/s}$. The heat already leaking to the bath is $0.030\,\mathrm{W}$, too large to discard in a ten-percent comparison. If the winding is inside the same calorimeter, its Ohmic heat must enter the balance as well. With primary resistance $1.50\,\Omega$ and the computed sinusoidal current, winding heating is

$$(0.240/\sqrt{2})^2 (1.50) = 0.0432\,\mathrm{W}.$$

The expected slope of the combined package at the same temperature is now $0.00693\,\mathrm{K/s}$. Subtraction of winding heat recovers the core result only when the estimated resistance represents the winding at its operating temperature and frequency.

A thermal estimate drawn from a whole interval is often more robust than a derivative from two adjacent temperature samples. Integrating gives

$$Q_{\mathrm{deposited}} = C_{\mathrm{eff}}[\Delta T(t_2) - \Delta T(t_1)] + G\int_{t_1}^{t_2} \Delta T\, dt.$$

Divide by the duration for mean power, then remove other measured heat sources. A drifting ambient must be recorded explicitly because the calorimeter stores energy relative to its own absolute temperature. If the core and coil equilibrate slowly with each other, a single fitted heat capacity can depend on the fitting time window. A two-temperature model or a longer dwell then supplies an independent diagnostic.

Separate reversible exchange from hysteretic and induced currents

A single measured loop at finite frequency gives the total energy dissipated by the core at that prescribed waveform and temperature. The loop can include irreversible domain processes, eddy currents and other rate-dependent effects. It does not by itself split these contributions. To probe their different scaling hold the peak induction and waveform shape fixed, then change frequency. Under a restricted low-frequency model the quasi-static hysteresis energy per cycle is approximately constant, while classical thin-lamination eddy-current power scales as $f^2 B_p^2$. Its energy per cycle therefore scales roughly as f. Plotting the measured loss per cycle and volume against f tests whether such an intercept-plus-slope description fits the chosen range.

Suppose the area is $12\,\mathrm{J/m^3}$ at $100\,\mathrm{Hz}$ and $20\,\mathrm{J/m^3}$ at $300\,\mathrm{Hz}$, at the same peak induction. A straight line gives intercept $8\,\mathrm{J/m^3}$ and slope $0.040\,\mathrm{J\,s/m^3}$. It predicts $16\,\mathrm{J/m^3}$ at $200\,\mathrm{Hz}$, near the elliptical-loop calculation. Two points always determine a line. A third and fourth frequency, together with uncertainties, are required to test the law. Different losses can share similar frequency scaling over a short interval, and temperature-dependent conductivity can bend a nominally simple curve.

Use the pickup to reject the reversible part of terminal power

Measuring primary terminal voltage and current with a power analyser provides a separate electrical route to loss, but the wanted number can be a small difference between terms. The applied voltage contains winding resistance, induced magnetising voltage, leakage-inductance voltage and possible parasitic contributions. In steady periodic operation the energy stored in a fixed linear leakage inductance returns after each cycle, while winding resistance dissipates energy permanently. The secondary pickup preferentially measures the core-linked flux. Forming $p_c(t) = (N_p/N_s) i_p(t) v_s(t)$ and averaging over a full cycle estimates core power without directly including the primary's copper

voltage drop. It relies on both windings linking the same relevant flux and on negligible power drawn by the pickup.

For the elliptical example the primary magnetising voltage has peak $5.03\,\mathrm{V}$ and leads the induction by ninety degrees. Its phase relative to the current is

$$90^\circ - \delta = 78^\circ.$$

The core branch's apparent power is $V_{\mathrm{rms}} I_{\mathrm{rms}} \approx 0.603\,\mathrm{VA}$; its mean dissipative part is about $0.125\,\mathrm{W}$, and the reactive part is about $0.590\,\mathrm{var}$. Only the mean part contributes net heating of the magnetic volume. Including the winding voltage adds about $0.043\,\mathrm{W}$ of real power to the terminal reading. A simple product of peak current and peak secondary voltage, without the turns ratio, factor one half and phase factor, has no reason to agree with either measured loss.

Consider a nearly ideal core with the same peak signals but a lag of only one degree. Its loss is about $10.5\,\mathrm{mW}$, while the much larger reversible power exchange is almost unchanged. A time offset of $10\,\mu\mathrm{s}$ at $200\,\mathrm{Hz}$ adds 0.72°, causing a relative loss error of approximately 72% for that small lag. Calibrate the relative channel delays using a reference signal through the actual current transducer and voltage chain, including their filters. Adjusting traces on screen until a core loop appears narrow assumes the very loss one is trying to measure. A synchronous measurement over many periods suppresses random noise but does not remove a persistent delay bias.

Test reconstruction on a waveform with a third harmonic

Let $H(t) = H_1 \cos \omega t + H_3 \cos 3\omega t$ while $B(t) = B_1 \cos(\omega t - \delta_1) + B_3 \cos(3\omega t - \delta_3)$. With these definitions δ_n is the phase lag of the nth harmonic in its own sinusoid. Multiplying H by $\dot{B}$ and integrating over an integer number of fundamental periods eliminates products of different harmonics. Each surviving harmonic contributes the number of its own cycles in one fundamental period. The area per fundamental period is therefore $\pi[H_1 B_1 \sin \delta_1 + 3 H_3 B_3 \sin \delta_3]$. This identity tests whether a numerical area calculation tracks the full waveform. It does not assume that a real material is linear; here the two signals are supplied as measured periodic functions.

Use the earlier fundamental values and add $H_3 = 20\,\mathrm{A/m}$, $B_3 = 0.030\,\mathrm{T}$ and $\delta_3 = 30^\circ$. The third harmonic contributes $2.83\,\mathrm{J/m^3}$ in each fundamental period. This represents an additional $0.0226\,\mathrm{W}$ for the chosen specimen and frequency. A fundamental-only sine fit would miss nearly fifteen percent of the resulting total area. An apparent jagged loop can also arise from asynchronous sampling or an offset. Distinguish genuine harmonics by checking that they are phase locked to the drive and persist under a change in sampling rate and analogue bandwidth.

Sweep phase and read the oriented loop

The live experiment reconstructs the H, B trajectory and compares it with a zero-lag reference. It uses the same peak field and induction for the two curves. At fixed peaks changing frequency leaves an assigned phase lag and therefore the prescribed energy per cycle unchanged, while watts rise with the

number of cycles per second. A real core can change its lag and waveform with frequency; the graph separates this independent variable so that the meaning of the two scaled quantities is clear. Add a timing offset and predict the direction of the area error before checking its reported size. Near zero lag even the direction of an apparent loop can be controlled by a small electronic offset.

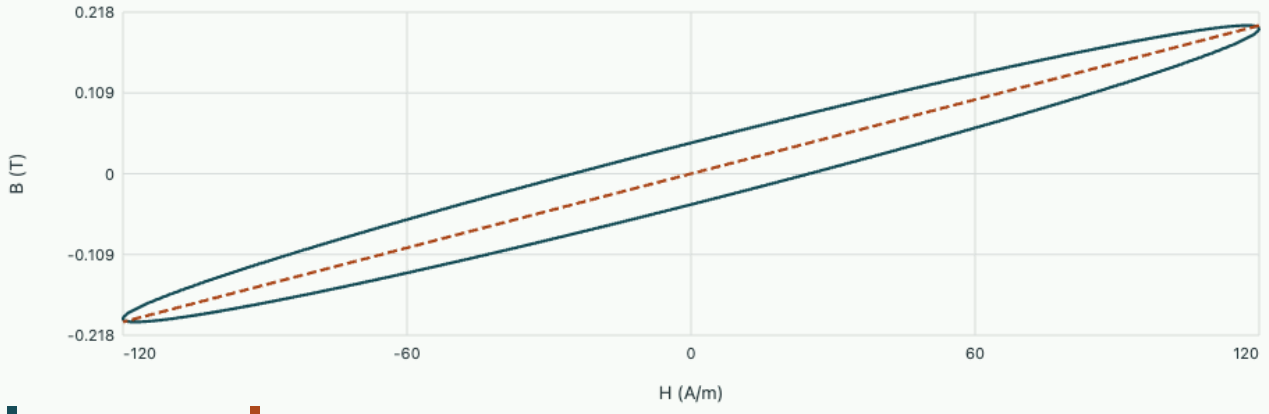
Open the live experiment

Try the calculation

Physical induction lag (°) **12**

Frequency (Hz) **200**

Induction channel delay (µs) **0**



True loop area 15.68 J/m³ per cycle. The recorder indicates 15.68 J/m³. Physical heating of the 40 cm³ specimen is 0.125 W.

Two toroids are made of the same nominal material with equal cross sections but different mean path lengths. How should a result reported only as watts be compared?

▼ **Work through the solution**

Determine actual magnetic volume for each toroid and calculate the energy per unit volume per cycle, $P/(fV_c)$. Also check that both experienced the same induction waveform, frequency and temperature. Equal primary currents need not give equal field when the path lengths differ; equal primary applied voltages need not give equal core induction if turns, winding voltage drops or area differ. Reproducing the actual $B(t)$ with feedback on the pickup is a more direct way to match excitation. Report dimensions and peak induction with the result so a reader can reconstruct what material condition was tested.

A saturated sample shows a small loop during a biased excitation that never crosses zero induction. Does the area formula still apply?

▼ **Work through the solution**

A settled periodic minor loop encloses an area representing the net cyclic energy under exactly that bias and excursion. Adding a static induction offset does not change $\oint H\,dB$, but the bias can alter the trajectory, differential permeability, and width of the minor loop itself. Do not infer the full major-loop energy from its area. The pickup returns only changes of induction unless an independent dc measurement or a known magnetic preparation supplies the offset. A bias winding may additionally heat the calorimeter, so include its measured power when comparing with thermal loss.

Tutorial on comparing two loss measurements

A data logger reports H_p and B_p correctly but adds an uncorrected $10\,\mu\mathrm{s}$ delay to the induction channel. Estimate the fractional area error of the elliptical example.

▼ **Work through the solution**

At $200\,\mathrm{Hz}$ the extra apparent lag is

$$2\pi f\Delta t = 0.01257\,\mathrm{rad} = 0.72^\circ.$$

The reported area is multiplied by $\sin(12.72^\circ)/\sin(12^\circ)$, about 1.059. An uncorrected delay of only one hundred-thousandth of a second overstates the core loss by about six percent. For a very low-loss specimen with much smaller physical lag, the same delay produces a far larger relative error.

A thermal run on the combined winding and core reports a slope $0.0070\,\mathrm{K/s}$ at $\Delta T = 2.0\,\mathrm{K}$. Recover the core power and the volume-specific loss area at $200\,\mathrm{Hz}$.

▼ **Work through the solution**

Heat deposition in the package is

$$20(0.0070) + 0.015(2.0) = 0.170\,\mathrm{W}.$$

Subtract the estimated $0.0432\,\mathrm{W}$ of winding heating to obtain $0.1268\,\mathrm{W}$ in the core. Dividing by $200 \times 4.0 \times 10^{-5}$ gives $15.85\,\mathrm{J/m^3}$ per cycle. Its closeness to $15.68\,\mathrm{J/m^3}$ should be evaluated against the uncertainties of heat capacity, thermal conductance, resistance, dimensions and electrical phase alignment.

Vary the magnetic circuit and identify the induction scale used by the specimen.

Electromechanics, optics and measurement · 8. A diamagnetic specimen in a gravitational and magnetic trap

A suspended specimen can have exactly the right vertical magnetic force and still slide sideways out of its apparent equilibrium. Derive the force on induced magnetisation, impose gravity, and use the curvature of a measured field to decide whether small disturbances return the specimen to its starting point.

Derive the force on an induced magnetic dipole

Take a small, isotropic, weakly magnetic particle of volume V, mass density ρ and SI volume susceptibility $\chi < 0$. In vacuum or air the imposed field is $\mathbf{B}$, and to first order in χ its magnetic moment is

$$\mathbf{m} = \chi V \mathbf{B}/\mu_0.$$

The field must vary little over the particle for a centre-of-mass dipole description. A permanent magnetic moment aligned with a field would have interaction energy $-mB$. Applying that formula directly with an induced m varying with B doubles the predicted force. Build the induction from zero at fixed source-current control: the energy change at a small increment of imposed field is $-\mathbf{m}\cdot d\mathbf{B}$. Since the induced moment itself increases linearly with field, integration gives

$$U_{\mathrm{mag}} = -\frac{\chi V}{2\mu_0} B^2,$$

$$\mathbf{F}_{\mathrm{mag}} = \frac{\chi V}{2\mu_0} \nabla B^2.$$

Because χ is negative, energy rises with squared induction and the particle moves toward weaker field. The factor one half can also be checked using the instantaneous force $m_j \partial_i B_j$ on a small dipole in a current-free region, inserting the actual induced moment only after the field derivative. For an anisotropic solid the scalar susceptibility must be replaced by its orientation-dependent tensor and the material can rotate. For a strongly magnetisable body the internal field is appreciably changed by its own magnetisation. These effects alter both equilibrium and stiffness. The weak isotropic model provides a controlled starting point for a specimen with calibrated response.

Include gravity by choosing z upward and taking $U = \rho V g z - \chi V B^2/(2\mu_0)$. Equilibrium requires zero horizontal gradients of B^2, and $\partial_z B^2 = 2\mu_0 \rho g/\chi$. The right-hand side is negative: the imposed squared field must decrease upwards at the equilibrium point. Volume cancels because gravity and the weak induced moment are both proportional to volume. A larger sample of identical density and susceptibility ideally levitates at the same height. Real finite-size changes in field averaging supply a way to test whether the point-particle approximation has broken down.

Solve a three-dimensional quadrupole trap

A local source-free field satisfying both divergence and curl constraints is $\mathbf{B} = b(x\,\hat{x}/2 + y\,\hat{y}/2 - z\,\hat{z})$, where b has units of $\mathrm{T/m}$. Its trace of derivatives is

$$b/2 + b/2 - b = 0.$$

Squaring gives

$$B^2 = b^2[(x^2 + y^2)/4 + z^2].$$

In zero gravity the induced magnetic energy therefore has an isolated minimum at the origin. Although each Cartesian component of a static current-free field is harmonic, the sum of their squares need not be. This mathematical fact permits a stable low-field-seeking diamagnet in three dimensions.

Completing the square in the vertical potential puts the equilibrium at $z_e = -\mu_0 \rho g/(|\chi| b^2)$. The two horizontal spring constants are $k_x = k_y = |\chi| V b^2/(4\mu_0)$ and the vertical one is $k_z = |\chi| V b^2/\mu_0$. Divide by mass and take square roots to obtain

$$\omega_z = b\sqrt{|\chi|/(\mu_0 \rho)},$$

with $\omega_x = \omega_y = \omega_z/2$. Gravity shifts the equilibrium in this exactly quadratic potential without changing the frequencies. More general magnetic geometries have curvature that changes with position; in those a gravity-induced shift can move the particle into a region with different stiffness.

Take an illustrative isotropic specimen with $\rho = 2200\,\mathrm{kg/m^3}$, $\chi = -4.0 \times 10^{-4}$, and $b = 200\,\mathrm{T/m}$. The predicted equilibrium is $1.70\,\mathrm{mm}$ below the field zero. The vertical oscillation frequency is $12.1\,\mathrm{Hz}$, the horizontal frequencies are about $6.05\,\mathrm{Hz}$, and the local induction magnitude at the equilibrium is $0.339\,\mathrm{T}$. A check independent of susceptibility is $g = \omega_z^2 |z_e|$ in this ideal quadrupole, obtained by eliminating $b^2|\chi|/(\mu_0\rho)$. A measured $12.1\,\mathrm{Hz}$ and $1.70\,\mathrm{mm}$ give approximately $9.83\,\mathrm{m/s^2}$. Agreement tests the consistency of position and dynamical measurements with the quadratic trap assumption.

Check radial stability from an axial field map

Practical magnets rarely generate a pure quadrupole over the entire useful volume. Suppose a smooth axisymmetric current-free field has on-axis induction $B_0(z)\hat{z}$. Expand about the axis using reflection symmetry: $B_r = a(z) r + O(r^3)$ and $B_z = B_0(z) + c(z) r^2 + O(r^4)$. The zero divergence condition gives $2a + B_0' = 0$. The azimuthal curl condition $\partial_z B_r - \partial_r B_z = 0$ then gives $a' - 2c = 0$, hence $a = -B_0'/2$ and $c = -B_0''/4$. Squaring both components yields the near-axis expansion

$$B^2 = B_0^2 + r^2 \left[\frac{(B_0')^2}{4} - \frac{B_0 B_0''}{2} \right] + O(r^4).$$

Thus the axial curvature of squared induction is $2[(B_0')^2 + B_0 B_0'']$, and each transverse curvature is $(B_0')^2/2 - B_0 B_0''$. A weak isotropic diamagnet needs both to be positive for stable harmonic motion. An axial field profile can satisfy vertical balance and produce positive axial curvature while the transverse curvature is negative. With no symmetry one needs the full Hessian matrix of B^2. Positive diagonal elements alone are insufficient if off-diagonal couplings tilt the unstable direction. Its

eigenvectors give normal-mode directions; eigenvalues multiplied by $|\chi| V/(2\mu_0)$ give the corresponding linear restoring constants.

At one test position take $B_0 = 0.800\,\mathrm{T}$,

$$B_0' = -84.75\,\mathrm{T/m}.$$

The product is approximately $-67.8\,\mathrm{T^2/m}$, close to the value required for the numerical specimen above. Let $B_0'' = 5000\,\mathrm{T/m^2}$. The transverse curvature is about $3591 - 4000 = -409\,\mathrm{T^2/m^2}$, while axial curvature is about $22365\,\mathrm{T^2/m^2}$. The particle can satisfy vertical balance yet move away under a small horizontal displacement. Reducing B_0'' to $1000\,\mathrm{T/m^2}$ at the same local induction and slope makes the transverse curvature about $2791\,\mathrm{T^2/m^2}$, while the axial curvature remains positive. A field value and a gradient alone cannot distinguish these two cases.

Design measurements that can resolve second derivatives

An axial Hall scan at equally spaced positions $z - h$, z, $z + h$ estimates B_0' from the centred first difference and B_0'' from the centred second difference. For independent induction noise with standard deviation σ_B, the noise of the gradient estimate is $\sigma_B/(\sqrt{2}h)$, and the noise of the second derivative is $\sqrt{6}\,\sigma_B/h^2$. Halving the spacing while leaving the noise fixed improves the leading truncation error from smooth spatial variations but multiplies second-derivative noise by four. Repeated measurements, a justified fit across several points and a probe smaller than the desired spatial scale can improve the estimate. A fitted polynomial with small residuals at the recorded points does not guarantee a sharply determined curvature.

For $h = 0.50\,\mathrm{mm}$ and $\sigma_B = 0.10\,\mathrm{mT}$, the three-point second-derivative uncertainty is approximately $980\,\mathrm{T/m^2}$. In the first test geometry above the radial curvature lies only $409\,\mathrm{T^2/m^2}$ below zero, while its contribution from B_0'' uncertainty alone is $0.8 \times 980 \approx 784\,\mathrm{T^2/m^2}$. Such a scan cannot establish the sign convincingly from those three readings. Independently displacing a specimen sideways and tracking whether it returns is a direct stability check. Air drag may make a growing instability look slow, so fit a damped or unstable equation over sufficient time and monitor nearby surfaces that might mechanically support the specimen.

Measure susceptibility from dynamics and compare with force balance

An oscillation measurement can determine susceptibility if the field curvature and density are known. For a weak isotropic sample the matrix of squared angular frequencies is $|\chi|\,\mathcal{H}(B^2)/(2\mu_0\rho)$, with $\mathcal{H}$ evaluated at the equilibrium position. An observed oscillation along an eigenvector with curvature $h_j > 0$ gives

$$|\chi| = 2\mu_0\rho\,\omega_j^2/h_j.$$

Simultaneously, the static force-balance equation gives

$$\chi = 2\mu_0 \rho g / (\partial_z B^2).$$

The two estimates use different derivatives of the same field map. Their agreement is more informative than fitting both readings by adjusting unmeasured field parameters independently.

For a measured pure quadrupole gradient $b = (200 \pm 2)\,\mathrm{T/m}$, density $2200 \pm 22\,\mathrm{kg/m^3}$, and vertical oscillation frequency $12.10 \pm 0.10\,\mathrm{Hz}$, the dynamical estimate is

$$|\chi| = \mu_0 \rho (2\pi f_z / b)^2 \approx 4.00 \times 10^{-4}.$$

If the quoted errors are independent standard uncertainties, the relative uncertainty is $\sqrt{(0.01)^2 + (2 \times 0.10/12.10)^2 + (2 \times 2/200)^2}$, about 2.8%. The gradient calibration enters squared. Recording more frames of the oscillation improves the frequency measurement only until the field calibration and density dominate. A traceability statement for b, the camera time base and the measurement position is therefore part of the susceptibility result.

If the motion is viscously damped, the observed oscillation frequency is

$$\omega_d = \sqrt{\omega_0^2 - \alpha^2},$$

where the amplitude envelope decays as $e^{-\alpha t}$. A fit to oscillation frequency alone therefore underestimates the undamped stiffness. If $\omega_d = 70\,\mathrm{s^{-1}}$ and $\alpha = 20\,\mathrm{s^{-1}}$, the undamped angular frequency is $72.8\,\mathrm{s^{-1}}$. Since the inferred susceptibility is proportional to frequency squared, using the uncorrected frequency would give only $4900/5300 = 92.5\%$ of the correct value. Visually observing a stable position gives no direct measurement of this dynamic correction. A repeated small displacement at several amplitudes also tests whether cubic restoring terms contaminate the fit.

Account for the finite volume and orientation of a specimen

For a particle that is weakly perturbed by the field but too large for point sampling, the magnetic energy is the spatial integral of the local energy density over its translated volume. For a uniform spherical specimen of radius a centred at $\mathbf{R}$, Taylor expand $B^2(\mathbf{R} + \mathbf{s})$. Inversion symmetry eliminates the linear term and $\langle s_i s_j \rangle = a^2 \delta_{ij}/5$, so the average is $B^2(\mathbf{R}) + a^2 \nabla^2 B^2(\mathbf{R})/10 + O(a^4)$. Differentiating this average yields the leading force correction. In a perfectly linear quadrupole B^2 is quadratic and its Laplacian is spatially constant, so a spherical specimen adds an energy offset but leaves the translational force and stiffness unchanged. A large particle in a nonquadratic trap need not share that property.

Consider an additional on-axis quartic contribution to the field energy density, proportional locally to z^4, as one illustrative component of a measured three-dimensional expansion. Averaging it over a sphere gives $Z^4 + 6Z^2 a^2/5 + \langle s_z^4 \rangle$. The last term is independent of position and drops out of the force. The term proportional to $Z^2 a^2$ modifies even the small-amplitude stiffness. Such a size dependence could be mistaken for different susceptibilities if two samples have materially different diameters. A realistic

numerical calculation should average the measured three-dimensional squared field over the actual shape. Extending a one-dimensional polynomial to three dimensions arbitrarily can violate the source-free Maxwell constraints used above.

For an anisotropic small specimen the energy is $-V\,\mathbf{B}\cdot\boldsymbol{\chi}\mathbf{B}/(2\mu_0)$ in the material's orientation. A thin crystalline platelet can experience a torque that changes which susceptibility component contributes to the force. For a weak isotropic ellipsoid with demagnetising factor N_d along an axis, uniform magnetisation satisfies $M=\chi(H_{\text{applied}}-N_dM)$, giving $\chi_{\text{apparent}}=\chi/(1+N_d\chi)$. This correction is small for the numerical weak susceptibility used here, but the shape and tensor response of a real sample still need to be recorded for a quantitative comparison across different orientations.

Test a local field map before declaring a trap stable

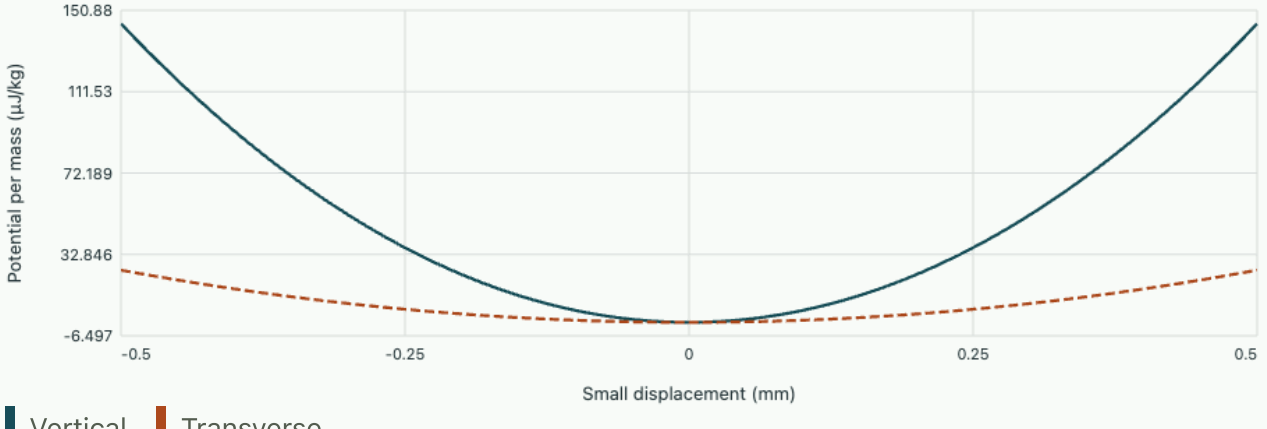
The live calculation varies axial curvature at fixed specimen response, equilibrium field and gradient. It plots the change of total potential per unit mass for a small vertical displacement and a transverse displacement. For the vertical curve the linear magnetic term cancels gravity by construction. Predict which curve will first turn down as positive axial field curvature is increased. At a transverse curvature of zero the quadratic plot is locally flat and higher powers or experimental imperfections decide the outcome. The calculation cannot declare stability at that marginal point. Move the control clearly onto each side of it and compare the resulting real oscillation frequency or exponential growth rate.

Open the live experiment

Try the calculation

Axial B curvature (T/m²) **1000**

Equilibrium field (T) **0.8**



Force balance fixes B′ at -84.75 T/m. Vertical motion: 5.41 Hz oscillation. Transverse motion: 2.26 Hz oscillation.

Is a vertically balanced particle exactly at a magnetic field zero possible in this static weak-diamagnet model with gravity?

▼ **Work through the solution**

Where a smooth imposed field vanishes,

$$\nabla B^2 = 2\sum_j B_j \nabla B_j = 0.$$

The induced magnetic force therefore vanishes at that point, while gravity remains finite. A pure quadrupole displaces the equilibrium away from its zero and creates the required nonzero gradient of squared induction. If a photograph seems to show a specimen at the field zero, test the location of the zero independently, check the imaging perspective and consider other forces such as buoyancy, electrostatic charging or a support. None follows merely from the existence of a zero of magnetic induction.

Test the effect of a nearby fluid

A specimen immersed in a weakly magnetic carrier fluid displaces that fluid as it moves. To first order in the susceptibilities, the magnetic energy change on exchanging equal volumes is proportional to the susceptibility contrast $\chi_{\mathrm{particle}} - \chi_{\mathrm{fluid}}$. The gravitational energy similarly depends on the density contrast. A neutrally buoyant particle has almost no net gravitational weight in the fluid even though it retains inertia and can experience a substantial magnetic force. Oscillatory experiments in liquid also require drag and possibly added inertia of surrounding fluid, so the simple vacuum frequency cannot be applied merely by substituting a density difference everywhere.

For example, take a particle of density $2200\,\mathrm{kg/m^3}$ in a liquid of density $1000\,\mathrm{kg/m^3}$ with magnetic susceptibility small relative to the particle. Its leading gravitational force is only $1200/2200 = 0.545$ of that in air. Under the same ideal linear quadrupole and negligible magnetic-fluid contrast correction, its equilibrium sag shrinks from $1.70\,\mathrm{mm}$ to about $0.93\,\mathrm{mm}$. This change in a static measurement could otherwise be misidentified as an increase in particle susceptibility. Comparing in-air and immersed equilibria therefore requires conditions for both buoyancy and magnetisation of the surrounding material.

Tutorial on force balance and stability

A particle oscillates vertically at $10\,\mathrm{Hz}$ in a pure quadrupole trap. What gravitational displacement is predicted, and how would a measured displacement twice that large challenge the model?

▼ **Work through the solution**

The vertical angular frequency is $2\pi(10) = 62.83\,\mathrm{s}^{-1}$, so the predicted shift is $g/\omega_z^2 = 2.48\,\mathrm{mm}$ below the field zero. A measured shift near $5.0\,\mathrm{mm}$ would require testing the location of the field zero, the measured frequency, and the curvature variation over the gravitational displacement. Adjusting susceptibility alone cannot reconcile both observations in the quadratic model because it changes stiffness and inverse shift together.

Two specimens have equal volume and identical density. The magnitude of susceptibility of the second is one quarter that of the first. What changes in the ideal quadrupole?

▼ Work through the solution

The second specimen sags four times as far because the restoring force at a given displacement is one quarter as large. Each frequency falls to one half. Its larger sag can take it outside the region where the quadrupole expansion is accurate even if the first specimen is well described. A volume change alone would leave both predicted quantities intact for specimens of equal density and susceptibility.

Michael Berry and Andre Geim derive local magnetic conditions for diamagnetic levitation.

Connect induced magnetisation to its current and external field.

Electromechanics, optics and measurement · 9. Optical trapping and Brownian calibration of a dielectric bead

An image of a bead remaining near a focus does not establish the strength of its trap. Derive the force pulling a small dielectric sphere into a bright region, compare it with the forward force from scattering and learn what a motion record can tell you about stiffness, drag and temperature. The model here uses an inert dielectric sphere in a homogeneous Newtonian liquid.

From two dielectric boundaries to the energy of an induced dipole

A sphere of radius a and relative permittivity ϵ_b sits in a liquid of relative permittivity ϵ_m. Assuming the sphere is small compared with a wavelength in the liquid, solve its local electric problem in an almost uniform applied field E. Rotational symmetry about the field admits an interior potential proportional to $r\cos\theta$. The exterior consists of the imposed potential $-Er\cos\theta$ and an induced dipolar term proportional to $\cos\theta/r^2$. Equality of potential and of normal displacement at the surface gives the local-field and dipole factors

$$E_{\mathrm{in}} = \frac{3\epsilon_m}{\epsilon_b + 2\epsilon_m} E,$$

$$p = \alpha E,$$

$$\alpha = 4\pi\epsilon_0\epsilon_m a^3 \frac{\epsilon_b - \epsilon_m}{\epsilon_b + 2\epsilon_m}.$$

The field doing the polarising work is the external field in the host at the particle position before inserting it. To turn that work into a potential, build up the dipole from zero rather than assuming a permanent dipole moment. Quasistatic assembly gives

$$-\int_0^E \alpha E'\, dE' = -\alpha E^2/2.$$

For a harmonic peak field average the square over an optical period. In a nearly lossless liquid of refractive index n_m, the peak field is related to travelling-wave intensity by $I = n_m\epsilon_0 c|E|^2/2$. The resulting conservative force is

$$U = -\frac{\mathrm{Re}\,\alpha}{4}|E|^2 = -\frac{\mathrm{Re}\,\alpha}{2n_m\epsilon_0 c} I,$$

$$\mathbf{F}_{\mathrm{grad}} = -\nabla U.$$

The two factors of two have different origins: induced-dipole assembly and time averaging of a sinusoid. Using a permanent-dipole potential with a peak field would miss both. A bead of higher refractive index than the liquid has positive real polarizability and is attracted to increasing intensity. A lower-index inclusion reverses this local tendency. For large particles, strong absorption or rapidly structured fields, a dipole with real static polarizability no longer specifies the force; a field or multipole calculation of the complete momentum balance is required.

Investigate the small-sphere dipole response and its dependence on particle size

Compute a transverse stiffness and test how local it is

Assume the beam near its focal plane has intensity $I(x) = I_0 e^{-2x^2/w^2}$, with power P, waist w defined at $1/e^2$ intensity and $I_0 = 2P/(\pi w^2)$. Put $U_0 = \mathrm{Re}\,\alpha I_0/(2n_m\epsilon_0 c) > 0$. The potential measured above its minimum is $U_0[1 - e^{-2x^2/w^2}]$. Expanding to second order and equating its leading term to $\kappa_x x^2/2$ gives

$$\kappa_x = 4U_0/w^2.$$

Stiffness therefore scales linearly with power, as the third power of sphere radius and as the inverse fourth power of waist at fixed indices. Each scaling applies within the stated approximations.

For a 40 nm radius bead with $n_b = 1.59$, take $n_m = 1.33$, $w = 0.65$ micrometres, vacuum wavelength 1064 nm, $P = 90$ mW and $T = 298$ K. The index contrast factor is 0.1252 and the waist intensity is 1.36×10^{11} watts per square metre. The predicted depth 3.03×10^{-20} J is 7.36 times the thermal energy. The lateral stiffness is 2.87×10^{-7} N/m. A displacement of 50 nm then requires approximately 14.3 fN of transverse balancing force. At a displacement of half a waist, the exact restoring force is the harmonic estimate multiplied by $e^{-1/2} = 0.607$; a Hookean calibration cannot be extrapolated that far.

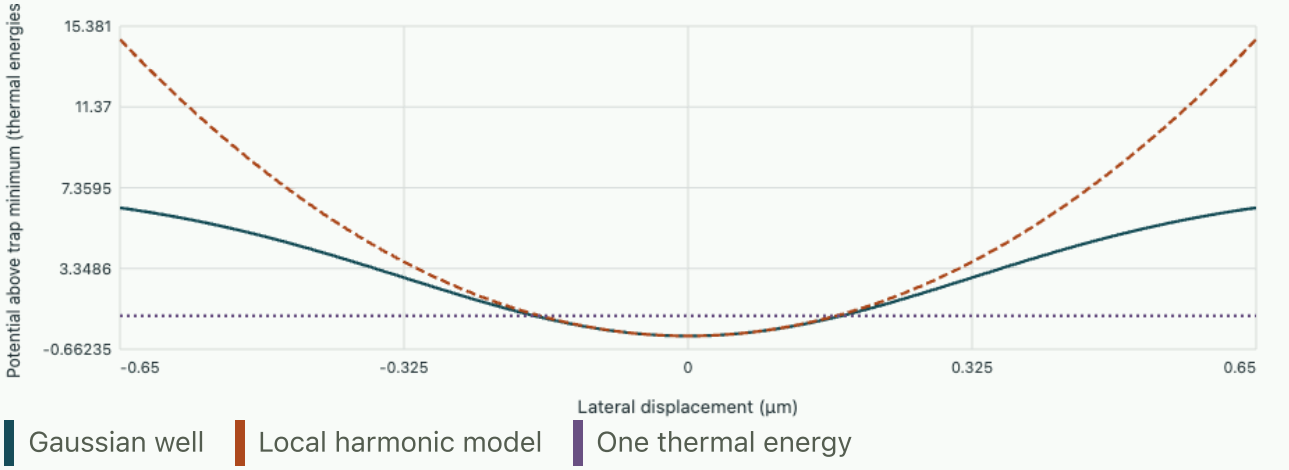
Open the live experiment

Try the calculation

Bead radius (nm) **40**

Optical power (mW) **90**

Beam waist (µm) **0.65**



The well depth is 7.36 kBT. The local model gives an rms displacement of 119.8 nm and a corner frequency of 60.5 Hz at 298 K.

Use the two curves to identify the interval in which the local quadratic energy is within ten percent of the Gaussian prediction. First lower power at fixed waist. Both curves shrink together in energy units while the harmonic thermal displacement grows. Next increase bead radius at fixed power and watch the well deepen, but also evaluate the size parameter $2\pi n_m a/\lambda_0$. It is 0.314 at the default and grows linearly with radius. Stronger trapping predicted by this simplified model does not establish the accuracy of the dipole approximation at arbitrary sizes.

Compare axial restoring force with radiation pressure

An induced dipole reradiates a portion of the incident field. In a uniform host use the Rayleigh scattering cross section $\sigma_s = (8\pi/3)k_m^4 a^6 |(\epsilon_b - \epsilon_m)/(\epsilon_b + 2\epsilon_m)|^2$. In a common travelling-wave momentum-flux model for a bead in a stationary nondispersive liquid the axial scattering force is approximately $F_s = n_m I \sigma_s / c$; absorption would add a further contribution. This estimate uses the total scattering cross section because the leading dipole pattern has vanishing mean forward cosine. For a larger forward-scattering sphere a transport cross section weights the deflected momentum instead.

In the default case the cross section is roughly 2.05×10^{-18} square metres. The forward force at the waist is about 1.23 fN. A Gaussian axial profile has $I(0,z) = I_0/[1 + (z/z_R)^2]$ with $z_R = \pi n_m w^2/\lambda_0 = 1.66$ micrometres. Its local axial stiffness $2U_0/z_R^2 = 2.20 \times 10^{-8}$ N/m is much smaller than its transverse stiffness. Balancing the constant forward force with that local stiffness predicts an equilibrium about 56 nm downstream of the waist. The small displacement relative to the Rayleigh length supports the linearisation.

Both the axial stiffness and forward scattering force scale with power in this simple model. A power sweep can thus increase confinement while barely shifting the equilibrium offset, a useful discriminating prediction. At fixed focus the offset grows rapidly with bead size because the scattering force scales with the sixth power and the gradient force with the third power. A stable lateral position alone does not establish stable three-dimensional capture. Check the axial restoring slope at a force zero and verify that thermal escape and fluid flow are negligible over the acquisition interval.

Extract stiffness from fluctuations or from a relaxation time

Near a stable point in one Cartesian direction, let x denote displacement from the mean and ζ the viscous drag. At sufficiently low frequencies the inertial term is negligible and the overdamped Langevin equation is

$$\zeta \dot{x} = -\kappa x + \xi.$$

At equilibrium the fluctuating force has zero mean and white covariance $2k_B T \zeta \delta(t - t')$ over the frequencies considered. The deterministic relaxation time is

$$\tau = \zeta/\kappa.$$

Multiplying the equation at positive delay by $x(0)$ and averaging removes the uncorrelated later noise and gives the decaying covariance. Equipartition sets its initial value.

$$C(t) = \frac{k_B T}{\kappa} e^{-|t|/\tau},$$

$$f_c = \frac{\kappa}{2\pi\zeta},$$

$$S_x^{(1)}(f) = \frac{4 k_B T \zeta}{\kappa^2 + (2\pi f \zeta)^2}, \quad f \geq 0.$$

The stated spectrum is one-sided in ordinary frequency. Its integral from zero to infinity equals $C(0)$; doubling another time would double the variance. In an unbounded fluid with viscosity 1.00 mPa s, Stokes drag is $6\pi\eta a = 7.54 \times 10^{-10}$ N s/m. The default predicts $f_c = 60.5$ Hz and rms displacement 120 nm. The latter is roughly 0.18 waist, so the outer part of a long thermal trajectory may sample appreciable anharmonicity. A finite-depth well in an unbounded bath does not have a globally normalisable trapped equilibrium. These local equilibrium predictions apply to a sufficiently long-lived, locally sampled trapped state.

If a voltage detector gives $V = gx$, the spectral corner and normalised autocorrelation time do not depend on the displacement gain g. They determine only κ/ζ. Equipartition using a calibrated spatial variance gives κ independently of drag, provided mechanical fluctuations are in equilibrium and sufficiently resolved. If the viscosity or nearby-wall drag is uncertain, combining a known stage oscillation with the Brownian spectrum can determine further calibration quantities. Keep a stage-driven coherent peak out of the noise integral used for equipartition.

Account for exposure, sample size and unobserved motion

A camera typically reports the position averaged during an exposure of duration t_e. Its variance is the double integral of the covariance over the exposure interval divided by t_e^2. Evaluating the exponential local model and introducing $u = t_e/\tau$ gives a multiplicative factor $2(u - 1 + e^{-u})/u^2$. At $u = 1$ the reported physical-motion variance is only 0.736 of the instantaneous variance. Interpreting it as the full variance would overestimate stiffness by approximately 36 percent. Independent pixel-localisation noise adds additional variance with the opposite sign of bias.

Estimate that localisation noise with an effectively immobilised reference bead at a comparable brightness. Test the averaging correction by changing exposure duration at constant sampling frequency where possible. A camera that reports overlapping exposures has correlated measurement errors and needs a different covariance model. A long series of closely spaced frames also contains fewer independent thermal configurations than its frame count suggests. Compare estimates across several blocks substantially longer than the relaxation time; residual low-frequency drift can dominate even when high-frequency position precision looks excellent.

A separate check uses a known uniform liquid flow. At a steady small displacement x_s, force balance gives

$$\kappa x_s = \zeta u_{\mathrm{flow}}.$$

For the default drag and stiffness a flow of 10 micrometres per second gives an offset of 26.3 nm. Repeat with reversed flow and use half the displacement difference to cancel an unknown zero-force position. Near a wall, the local flow at the bead and wall-corrected drag may differ from a stage velocity and the unbounded Stokes value. Those effects alter the mechanical calibration even if the optical field is unchanged.

A known stage oscillation calibrates position in a fluid

Brownian fluctuations alone determine the product of several unknown calibration parameters. A weak sinusoidal translation of the sample cell adds a known mechanical signal at a chosen frequency. Work in laboratory coordinates with a fixed optical trap and with fluid moving uniformly at velocity $u(t)$ near the bead, well away from walls in the idealised model. The drag is now $-\zeta(\dot{x} - u)$. Superposing a stage displacement $A\cos\omega t$ on thermal fluctuations gives a deterministic response whose complex amplitude satisfies $(\kappa - i\omega\zeta)\widetilde{x} = -i\omega\zeta A$ in the negative-exponential convention. Therefore its amplitude ratio is

$$\frac{|\widetilde{x}|}{A} = \frac{\omega\tau}{\sqrt{1+\omega^2\tau^2}}.$$

At the trap corner the bead displacement amplitude is the known stage amplitude divided by the square root of two. A calibrated 80.0 nm stage oscillation there produces a predicted bead amplitude of 56.6 nm. If a position-sensitive receiver records a coherent peak amplitude of 0.170 V, its displacement gain is 3.01 mV/nm. At very low drive frequencies the fluid velocity is small for fixed stage amplitude and the trap holds the bead nearly stationary. At high enough frequency the bead follows the fluid displacement within the overdamped model, but finite hydrodynamic, optical and electronic bandwidths eventually matter.

After determining the gain, convert the surrounding voltage spectrum into spatial units and use the area of the stochastic fluctuation spectrum to find stiffness. Exclude the calibrated line and account for the finite spectral averaging window; a narrow drive that leaks into neighbouring bins can inflate the inferred thermal variance. Dividing measured stiffness by the independently determined corner rate then gives drag, which can be compared with the known viscosity and sphere radius. This avoids assuming free-space Stokes drag in the first step of a near-wall measurement.

There are two limiting systematic effects that a good fit to a single drive frequency cannot resolve. A frequency-dependent stage calibration changes the actual fluid displacement, and motion of the optics relative to the cell generates a direct detector background even with the bead immobilised. Repeat the drive above and below the corner, compare coherent phase as well as amplitude and acquire a trapped and immobilised reference. Correct conversion should explain the entire complex response with one spatial gain and one corner time. A single calibration number obtained at one frequency can hide a phase lag in the stage controller or in the optical position channel.

One last cross-check reverses the stage drive phase by half a period. The coherent bead response must reverse, while thermal background power remains unchanged. A component that fails this reversal

could come from ambient vibration unrelated to the stage. Averaging the two traces with and without a sign change separates these contributions before either is used in an optical-force calibration.

Tutorial · Separate a unit-conversion error from excess noise

In a single-axis trap at 298 K a calibrated detector reports a variance of 2500 square nanometres after removal of localisation noise and exposure correction. An independent spectral fit gives a corner of 175 Hz. Infer stiffness, drag and the equivalent unbounded hydrodynamic radius for a liquid of viscosity 1.00 mPa s. Compare against a nominal 80 nm radius bead.

▼ **Infer the three quantities and test their consistency**

A nanometre squared is 10^{-18} square metres, so the variance is 2.50×10^{-15} square metres. Equipartition gives 1.65×10^{-6} N/m. Dividing by $2\pi f_c$ gives drag 1.50×10^{-9} N s/m and radius $\zeta/(6\pi\eta) = 79.5$ nm. The agreement supports the local overdamped description under the assumed temperature and viscosity. Forgetting the factor of 2π would predict a radius roughly six times larger and could be mistaken for a huge near-wall correction.

Now imagine that additional uncorrelated read noise had been left in the variance. This raises apparent variance, lowers the equipartition stiffness and would lower the inferred drag at the same fitted corner. Nearby-wall drag for a given radius instead normally raises hydrodynamic resistance for parallel translation. Their effects on the inferred radius thus differ in sign under the stated assumptions. Varying height and independently calibrating the measurement noise are appropriate diagnostics before attributing a discrepancy to bead dimensions.

Tutorial · Test a force-law inference with power and concentration controls

At fixed bead radius a trap is operated at two powers differing by a factor of two. Measured corner frequencies increase from 42 to 84 Hz, but rms displacement falls only from 110 to 87 nm. What does the harmonic model with fixed drag and temperature predict? Estimate a power-independent additive position-noise variance that could reconcile the two readings.

▼ **Use two variances to separate scale and offset**

The doubled corner gives doubled stiffness if drag is unchanged. Physical thermal variance should halve. The predicted rms at higher power would be 77.8 nm if the lower-power value were entirely physical. Let the low-power measured variance be $v + b$ and the high-power one $v/2 + b$, where b is a constant additive noise variance. Solving from 12,100 and 7,569 square nanometres gives $v = 9062$ and $b = 3038$ square nanometres, or approximately 55.1 nm rms noise.

This is a large inferred detector noise and demands an independent immobilised reference check. Power-dependent heating of the liquid changes temperature and viscosity, so an unchanged product

inferred from only two quantities cannot prove that heating is absent. Test several powers, reverse their order to reveal slow drift and vary bead concentration to exclude overlapping particles in the tracking window. The inferred additive term should remain constant across those controls if it comes from the specified detector model.

Tolić-Nørrelykke and colleagues · position and force calibration using thermal and driven measurements

Electromechanics, optics and measurement · 10. Coupled optical and mechanical resonances

A vibrating mirror can imprint its position on an optical field, while the stored light pushes back on the mirror. An apparent pair of peaks can indicate two hybrid modes, interference at a readout port or two unrelated resonances. Starting from energy in a moving cavity, derive the coupled response and learn which measurements establish a coupling strength and its uncertainty.

From a moving boundary to a force per photon

Take a nearly empty Fabry–Pérot cavity of optical length L with one moving end. A longitudinal resonance has $\omega_c = m\pi c/L$ for integer m, neglecting frequency-dependent mirror phase. For a small extension x, $\delta\omega_c = (\partial\omega_c/\partial x)x$ with signed slope $G_x = -\omega_c/L$. At fixed photon number n the optical energy is $n\hbar\omega_c(x)$. Its derivative gives the radiation-pressure force on the coordinate. For this mirror $F = -n\hbar G_x > 0$ pushes outward. The derivative must be at fixed photon number. Differentiating a driven steady-state photon number as though it were a closed-system energy would incorrectly include work exchanged with the pump.

For a 10 mm cavity resonant near 1064 nm the frequency slope magnitude in ordinary frequency is about 28.2 MHz per nanometre. A static shift of 10 pm therefore changes the optical resonance by approximately 282 kHz. One photon exerts a mean force $\hbar\omega_c/L \simeq 1.87 \times 10^{-17}$ N. An equivalent classical derivation counts a momentum change twice per normal reflection for each relevant round trip. The two descriptions yield the same mean force. The mirror displacement is the properly normalised mode coordinate; in a flexural device the optically sampled position and the total physical mass are generally different from centre-of-mass displacement and mass.

Introduce a single mechanical eigenmode with effective mass m_{eff}, angular frequency Ω_m and displacement scale $x_{\mathrm{zpf}} = \sqrt{\hbar/(2m_{\mathrm{eff}}\Omega_m)}$. The single-photon coupling magnitude is $g_0 = |G_x|x_{\mathrm{zpf}}$. This normalisation is convenient even when the observed vibrations are entirely classical. For $m_{\mathrm{eff}} = 10$ ng and $\Omega_m/(2\pi) = 1.0$ MHz, $x_{\mathrm{zpf}} = 9.16 \times 10^{-16}$ m and $g_0/(2\pi) = 25.8$ Hz for the stated optical geometry. The small displacement scale explains why a coherent pump is normally used to make the interaction measurable.

How a laser couples frequencies that are otherwise far apart

An optical carrier oscillates at hundreds of terahertz, whereas the mirror may vibrate at only megahertz. Direct comparison of these two bare frequencies would never suggest a resonant exchange. A strong coherent pump supplies a phase reference and converts a mechanical displacement into optical sidebands. Move into a frame rotating at the pump frequency and write the cavity amplitude as its large steady part plus a small perturbation. The leading frequency-shift interaction is proportional to photon number times displacement. Expanding the intensity around the large pump keeps terms linear in both the probe field and displacement. The resulting coupling is $G = g_0\sqrt{n_c}$, where n_c is mean intracavity pump photon number.

Tune the pump about one mechanical frequency below the optical cavity resonance. In the resolved-sideband and weak-fluctuation limit a near-resonant process moves one excitation between the

mechanical mode and an upper optical sideband. The rapidly rotating opposite-sideband terms average out. Now the two coupled frequencies are an optical sideband offset and the mechanical frequency, measured relative to a common rotating reference. The large carrier frequency has already been accounted for by the pump. The pump phase can be absorbed into the mode definitions, so G may be chosen positive for this isolated pair.

If instead the pump is placed near the upper sideband, the surviving interaction creates or annihilates excitations in pairs. The passive exchange equations below cease to apply and strong pumping can produce amplification or instability. A bare two-oscillator machine driven mechanically near a shared natural frequency often has analogous exchange equations without a carrier pump. Identical matrices can describe different energy supplies; identify the drive and rotating reference before assigning a literal photon-to-phonon energy conversion.

Derive complex poles and the effect of unequal damping

Let a, b be small energy-normalised optical and mechanical complex amplitudes. In a frame where the uncoupled optical sideband has zero frequency, let the mechanical detuning be δ. Let κ, Γ denote energy linewidths in angular frequency, so amplitude decay rates are half these values. With an optical probe s at offset ω, the linear system is

$$\begin{pmatrix} \kappa/2 - i\omega & iG \\ iG & \Gamma/2 - i(\omega - \delta) \end{pmatrix} \begin{pmatrix} a \\ b \end{pmatrix} = \begin{pmatrix} s \\ 0 \end{pmatrix}.$$

Zeros of the determinant give autonomous complex mode frequencies. In the lossless case the eigenvalues are $\delta/2 \pm \sqrt{G^2 + (\delta/2)^2}$. Far off resonance each branch approaches a bare mode. At zero detuning the two eigenvectors have equal optical and mechanical weights and the splitting is $2G$. The eigenvectors rotate continuously through the avoided crossing, an important discriminator from two uncoupled lines simply passing through one another.

At zero detuning with losses, completing the square in the determinant gives

$$\omega_{\pm} = -i(\kappa + \Gamma)/4 \; \pm \sqrt{G^2 - (\kappa - \Gamma)^2/16}.$$

The real parts separate once $G > |\kappa - \Gamma|/4$. The shared imaginary part above that threshold corresponds to a hybrid energy linewidth $(\kappa + \Gamma)/2$. Resolving two intensity features on a given instrument is a stronger, readout-dependent condition. The dimensionless cooperativity $C = 4G^2/(\kappa\Gamma)$ is yet another measure, comparing interaction against the product of dissipation scales. A value greater than one does not automatically prove two resolved normal-mode poles in a device with very unequal linewidths.

Use frequency numbers divided by 2π consistently from here for examples. With optical linewidth 240 kHz, mechanical linewidth 40 kHz and coupling 160 kHz, the real pole separation is

$$2\sqrt{160^2 - 50^2} = 304\,\mathrm{kHz}.$$

Both hybrid energy linewidths are 140 kHz, and cooperativity is 10.7. If coupling falls to 45 kHz, cooperativity is still about 0.844 and no real zero-detuning pole separation appears. At 50 kHz the square root reaches zero. Near that threshold even a small linewidth or detuning calibration error has a large effect on a coupling estimate inferred from a single splitting.

Compute what an optical or mechanical receiver actually sees

Invert the matrix. With $D = (\kappa/2 - i\omega)[\Gamma/2 - i(\omega - \delta)] + G^2$, the small amplitudes are $a = s[\Gamma/2 - i(\omega - \delta)]/D$ and $b = -iGs/D$. The poles are shared. Their numerators are different, so the two channels can show different apparent maxima. A port in reflection also has a directly reflected field that interferes with the leaking intracavity amplitude. Its intensity can display a narrow dip or asymmetric feature without a matching resonance-height pattern inside the cavity. A legitimate forward model must describe the measured port.

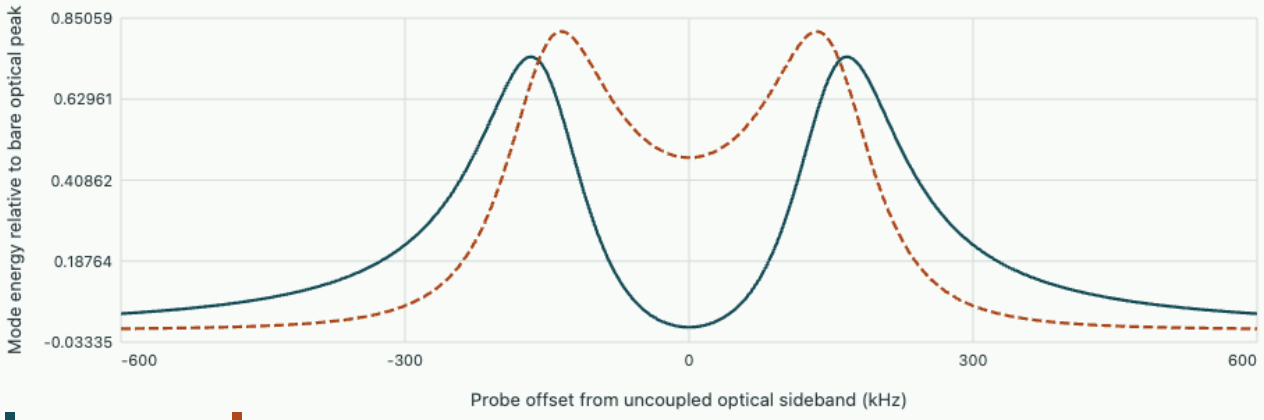
Open the live experiment

Try the calculation

Coupling G/(2π) (kHz) **160**

Optical linewidth κ/(2π) (kHz) **240**

Mechanical detuning (kHz) **0**



At zero bare detuning the real pole separation is 304.0 kHz. For the selected coupling and linewidths the cooperativity is 10.67. The mechanical linewidth is fixed at 40 kHz.

The graph plots the internal squared amplitudes relative to the bare on-resonance optical probe energy. Set the mechanical detuning to zero and reduce the coupling through 50 kHz. Compare the optical dip with the predicted real pole separation. Then set a substantial positive detuning and follow the transfer of mechanical response onto one branch. As a control set the coupling exactly to zero. The optical curve recovers the bare cavity Lorentzian and the mechanical probe-induced response vanishes. A

thermally excited mechanical background, absent from this driven calculation, could remain in a real detector.

At zero detuning and zero probe offset,

$$a/a_{\mathrm{bare}} = 1/(1+C).$$

For the default parameters the internal optical probe intensity at the centre is only $1/(1+10.67)^2 = 0.00735$ of the bare peak. This deep feature alone still does not establish the pole spacing. An incoherent background, a frequency-dependent detector transfer or coherent feedthrough can alter peak and dip positions. Fit complex quadratures across a detuning series when available, and verify bare linewidths by independent ringdown or far-detuned spectra.

Check how energy linewidth and amplitude ringdown are related for one isolated resonance

Watch energy exchange in time and identify the linewidth convention

In an ideal equal-linewidth system starting with optical perturbation $a(0) = a_0$, $b(0) = 0$ at zero detuning, change to symmetric and antisymmetric modes. Recombination gives

$$a(t) = a_0 e^{-\kappa t/2} \cos Gt,$$

$$b(t) = -i a_0 e^{-\kappa t/2} \sin Gt.$$

Their normalised total energy decays as $e^{-\kappa t}$, while energy moves back and forth between optical sideband and vibration. The first full transfer occurs at $t = \pi/(2G)$ if the rotating-wave approximation holds. For $G/(2\pi) = 100$ kHz, this is 2.50 microseconds. With a shared energy linewidth of 20 kHz in ordinary frequency the surviving energy fraction then is

$$e^{-2\pi(20\ \mathrm{kHz})(2.50\ \mu\mathrm{s})} = 0.730.$$

A gated excitation shorter than the exchange period but long enough to avoid unwanted modes can prepare an approximately optical initial perturbation. Independent detection of an optical revival and a delayed mechanical response tests coherent exchange more strongly than the presence of two peaks alone. Comparing times of maxima directly with one half the reciprocal measured optical linewidth misidentifies the exchange physics. Check the decay of the sum of appropriately calibrated energies and the relative phase of the exchange. Electrical or optical feedthrough can produce a prompt apparent response with no mechanical build-up.

Infer a coupling with propagated measurement errors

When the two hybrid pole frequencies have been obtained from a justified fit and zero bare detuning is established, the coupling follows from the measured real separation S:

$$G = \sqrt{S^2/4 + (\kappa - \Gamma)^2/16}.$$

All quantities here can be expressed in the same ordinary-frequency units. If $S = 300 \pm 8$ kHz, $\kappa = 240 \pm 10$ kHz and $\Gamma = 40 \pm 4$ kHz, the estimate is 158.1 kHz. Independent small errors give

$$\partial G/\partial S = S/(4G) = 0.474,$$

$$\partial G/\partial \kappa = -\partial G/\partial \Gamma = (\kappa - \Gamma)/(16G) = 0.0791.$$

Combining in quadrature gives about 3.9 kHz uncertainty. A common frequency calibration can correlate all three inputs, and a fitted detuning and splitting from one scan may also be correlated. Use their covariance rather than multiplying independent error bars blindly.

A second inference varies intracavity pump power. Since $G^2 = g_0^2 n_c$, plot the squared fitted coupling against independently calibrated n_c. A nonzero intercept could indicate an additional direct coupling, baseline fitting bias or a mode incorrectly assigned at low power. The linewidths themselves can vary with pump power because of heating or backaction, so fit or measure them across the scan. Incident optical power is not identical to stored photon number; cavity coupling, detuning and loss determine their relation.

A measured frequency shift and linewidth change reveal optical feedback

The same instrument can be operated below the resolved splitting regime and read out a dispersive shift of the mechanical response. Algebraically eliminate the optical amplitude in the two-mode equations while driving the mechanical mode weakly. Its inverse susceptibility acquires a self-energy contribution proportional to the optical susceptibility. Let x be probe frequency measured from the bare optical sideband and use the same linewidth convention as above. In the mechanical denominator the additional term is

$$\Sigma(x) = \frac{G^2}{\kappa/2 - ix} = \frac{G^2(\kappa/2 + ix)}{(\kappa/2)^2 + x^2}.$$

Its real part adds to the amplitude damping, while its imaginary part shifts the resonant condition. At very weak coupling one can evaluate it at the bare mechanical frequency $x = \delta$, because variation across the narrow mechanical peak is small. Near an avoided crossing or when the mechanical peak samples a large change in optical susceptibility, solve the coupled poles directly; simply adding a linewidth and shift then neglects the very hybridisation being tested.

In ordinary-frequency units choose $G = 10$ kHz, optical linewidth 200 kHz, mechanical linewidth 2 kHz and detuning $+100$ kHz. At that offset the optical amplitude half-width is 100 kHz, giving $\mathrm{Re}\,\Sigma = 0.50$ kHz and $\mathrm{Im}\,\Sigma = 0.50$ kHz. The full mechanical linewidth increases from 2.0 to approximately 3.0 kHz. Its centre moves upwards by about 0.50 kHz with the adopted matrix signs. Moving to minus 100 kHz

reverses the shift and preserves the added damping in this symmetric model. At zero detuning the predicted shift vanishes but the added linewidth is largest.

A scan on both sides is more discriminating than measuring broadening alone. A background rise in mechanical temperature changes integrated thermal noise and may change intrinsic loss, but need not reproduce this odd shift and even broadening pattern. Measure intrinsic linewidth far from the optical response and subtract that baseline. An unknown constant frequency offset can be removed with the two symmetric detunings, but an optical power dependence of cavity frequency can move the actual symmetry centre. Monitor the optical resonance during the scan.

The effective susceptibility describes classical feedback through the delayed optical field. It does not by itself specify the final mechanical temperature. A bath occupation or noise spectrum is also required to convert a damping change into an energy distribution. A driven response peak that broadens and lowers in amplitude is evidence for a changed susceptibility; thermal cooling additionally requires a calibrated measurement of the fluctuating mechanical displacement and its optical transduction.

Tutorial · A high cooperativity without resolved modes

A device has ordinary optical linewidth 1.00 MHz, mechanical linewidth 1.0 kHz and pump-enhanced coupling 30 kHz. Calculate cooperativity, compare the coupling with the real-splitting threshold and estimate the relative intracavity probe intensity at the central frequency. What observation would distinguish a narrow interference window from two separated poles?

▼ **Evaluate the three criteria independently**

In kHz units the cooperativity is

$$4(30)^2/(1000 \cdot 1) = 3.6.$$

The real-splitting threshold is $999/4 = 249.75$ kHz, far above the actual coupling. Yet the zero-detuning centre intensity is $1/(1+3.6)^2 = 0.0473$ relative to the bare optical peak. A narrow, deep structured feature is possible with no separated real pole frequencies in this model. The linewidth contrast permits mechanical response to interfere strongly within a broad optical susceptibility.

Acquire both amplitude and phase while scanning the absolute mechanical detuning and compare a coupled complex-response model with independently measured bare parameters. A pair of well-resolved poles should trace two consistent trajectories in both observables and can generate underdamped exchange in the time domain. A single optical intensity scan containing two flanks around a dip is insufficient to make that inference.

Tutorial · Diagnose an erroneous estimate of the single-photon

coupling

An independent linewidth analysis gives pump-enhanced couplings 80 and 160 kHz at photon numbers 4.0×10^6 and 1.6×10^7. Estimate $g_0/(2\pi)$ and predict the coupling at 9.0×10^6 photons. A calibration revision doubles all inferred photon numbers while leaving the measured spectra unchanged. Which conclusions move?

▼ **Use coherent amplitude scaling and separate calibration from spectroscopy**

Divide the respective couplings in ordinary frequency by the square roots of their photon numbers. Both give 40 Hz and the intermediate prediction is 120 kHz. Doubling all inferred photon numbers lowers the inferred single-photon coupling by $1/\sqrt{2}$, to 28.3 Hz. The observed enhanced couplings, pole locations and cooperativities computed from measured linewidths stay the same. A prediction labelled by fixed physical photon number changes; a prediction at a repeatable laser setting can still be calibrated empirically.

To test the absolute calibration, compare the inferred single-photon value with the independent cavity frequency slope times the mechanical zero-point displacement. This requires an effective mass appropriate to the measured displacement and the actual cavity optical overlap. An incorrect choice of mechanical mode normalisation can mimic an error in stored photon number. Agreement across a power ratio tests the square-root scaling but cannot by itself determine the absolute optical or mechanical calibration.

Aspelmeyer, Kippenberg and Marquardt · cavity optomechanics, linearisation and strong coupling

Electromechanics, optics and measurement · 11. Thermal radiance, étendue and detector calibration

A square millimetre of a heated object emits thermal radiation into an entire hemisphere. A detector sees only the rays accepted by its optics and only wavelengths to which it responds. Derive the equilibrium spectrum, follow it through an optical collection system and infer what temperature or emissivity a calibrated reading can actually determine.

Count optical states in a large equilibrium cavity

Take a cubic airless cavity of volume V in thermal equilibrium at temperature T. For its bulk mode density we can use periodic boundary conditions. Allowed wavevectors are separated by $2\pi/L$ in each coordinate. Count a spherical shell in wavevector space, divide by the volume per state and include two independent transverse polarisations. Substituting $k = 2\pi\nu/c$ gives

$$g(\nu)d\nu/V = 8\pi\nu^2 d\nu/c^3.$$

Using standing waves in an ideally reflecting large box gives the same leading volume density when directions and polarisations are counted consistently.

One oscillator mode of frequency ν can hold $m = 0, 1, 2, \ldots$ photons. Its thermal occupation has probabilities proportional to $e^{-mh\nu/k_BT}$. Summing the geometric series and taking its logarithmic derivative gives

$$\langle m \rangle = 1/(e^{h\nu/k_BT} - 1).$$

Multiplying by the density of modes and energy per photon gives spectral energy density u_ν. The zero-point contribution of a harmonic oscillator is not part of the thermal power exchanged between these black surfaces. At low frequency the result approaches an energy k_BT per mode; extending that classical limit to arbitrarily high frequency would make the integrated power diverge.

An isotropic distribution of energy travelling at speed c produces a normal flux through a small aperture weighted by the direction cosine. Per unit solid angle its radiance is $B_\nu = cu_\nu/(4\pi)$. Transform to equal wavelength intervals using $B_\lambda d\lambda = B_\nu |d\nu|$. The two useful spectral forms are

$$B_\nu = \frac{2h\nu^3}{c^2}\frac{1}{e^{h\nu/k_BT} - 1},$$

$$B_\lambda = \frac{2hc^2}{\lambda^5}\frac{1}{e^{hc/(\lambda k_BT)} - 1}.$$

The wavelength expression has units of watts per square metre per steradian per metre of wavelength. To express it per micrometre multiply by one millionth. At 400 K and 10 micrometres the result is 33.56 W per square metre per steradian per micrometre. At 295 K it is 9.14 in the same units. Equal wavelength and equal frequency bins carry different widths, so their distributions reach their maxima at different converted wavelengths. A spectrum's peak should always name its horizontal variable and spectral-density convention.

Distinguish emitter power from brightness in a chosen direction

For a black surface with angle-independent radiance into its outward hemisphere, integrate $\cos\theta\, d\Omega$. The result is π, not 2π. The emitted spectral power per unit area is πB_λ. Integrate over frequency using $x = h\nu/(k_B T)$. The remaining integral $\int_0^\infty x^3/(e^x - 1)\, dx = \pi^4/15$ follows by expanding $1/(e^x - 1)$ as a sum of exponentials and integrating term by term. This yields Stefan–Boltzmann exitance $M = \sigma T^4$ and identifies the constant $\sigma = 2\pi^5 k_B^4/(15 h^3 c^2)$.

A black patch of 1.0 square millimetre at 400 K emits about 1.45 mW into its entire outward hemisphere over all wavelengths. The same patch at 295 K emits about 0.429 mW. Replacing one by the other changes all-wavelength hemispherical power by about 1.02 mW. This is not the power a small infrared receiver sees through a narrow filter. The integrated emitter number is valuable for energy conservation, but by itself contains no receiver area, direction, passband or optical transmission.

The surface spectrum of a body in thermal equilibrium has directional spectral emissivity equal to its absorptivity in the corresponding reciprocal optical modes under the usual reciprocal-material conditions. An opaque diffuse grey surface with emissivity ϵ in an isotropically illuminated background can be modelled by $\epsilon B_\lambda(T) + (1 - \epsilon) B_\lambda(T_{\mathrm{bg}})$. It emits less than a black surface but also reflects background. A shiny object viewed in a warm room may consequently display a radiance temperature nearer the reflected scene than its own physical temperature. Specular surfaces require explicit directional knowledge of that scene.

Derive the geometric acceptance without counting the angle twice

An area element dA normal to the collection axis emits into $d\Omega$ at angle θ a spectral power $B_\lambda \cos\theta\, dA\, d\Omega$. For a uniformly filled cone of half-angle α and a uniform patch of area A, integrating gives $A\pi \sin^2\alpha$. This is its geometrical throughput in air when there is no vignetting. Optical étendue more generally uses $n^2 dA \cos\theta\, d\Omega$. A lossless passive optical relay in geometrical optics preserves this phase-space measure; correspondingly L/n^2 is conserved along a ray in transparent media under the usual stationary conditions.

A direct lens example makes the restriction tangible. An image relay enlarging a uniformly bright patch by a factor of two in each transverse direction forms an image four times the area. In a lossless paraxial design filling the original pupil, each image point then occupies one quarter the solid angle. A detector covering the whole enlarged image and accepting that cone can receive the original power. Placing a fixed small sensor at the image plane intercepts less area instead. Higher magnification has not created additional radiance, even if it makes a small detail easier to resolve.

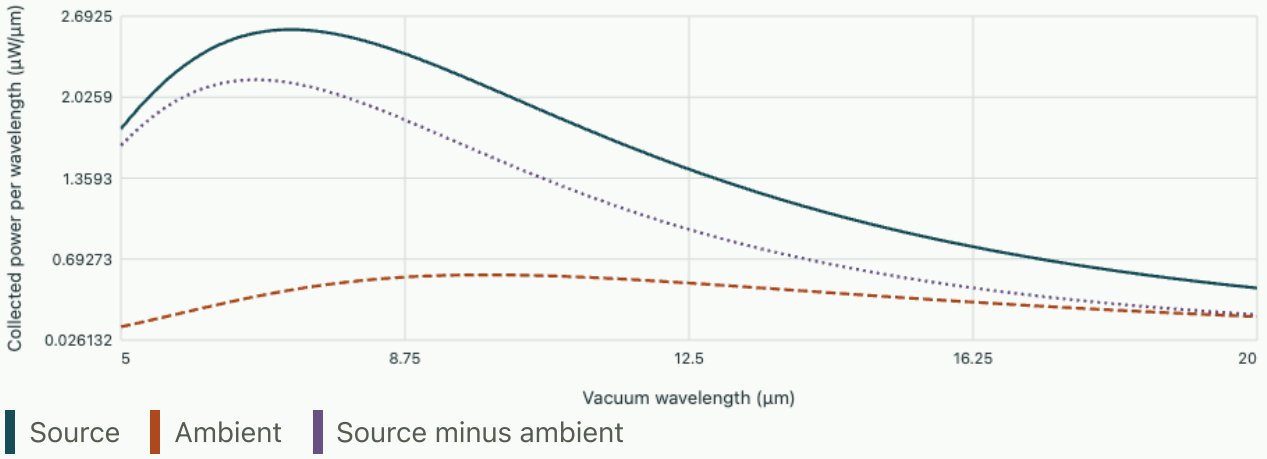
For the same 1.0 square millimetre patch seen within ten degrees, the projected acceptance is 9.47×10^{-8} square metre steradian. A wavelength-independent combined transmission and detector absorption of 0.65 leaves effective acceptance 6.16×10^{-8} square metre steradian. Integrating the Planck curve from 8 to 12 micrometres gives source and background band radiances 133.74 and 35.43 W per square metre per steradian. Their difference yields only 6.05 microwatts in the receiver. Keeping

a single midpoint radiance times four micrometres happens to be fairly close here, but there is no fixed universal midpoint correction across temperatures or filters.

Open the live experiment

Try the calculation

Source temperature (K)	400
Ambient temperature (K)	295
Collection half-angle (°)	10



The net 8–12 µm signal is 6.053 µW for a 1 mm² area and 65% throughput. Ideal source peak wavelength is 7.24 µm.

Set source and ambient temperatures equal. The emitted and ambient curves remain finite while the differenced instrument reading vanishes. Increase the cone half-angle from ten to twenty degrees and predict the scale factor $\sin^2 20^\circ / \sin^2 10^\circ = 3.88$. The spectral shape should stay fixed if transmission is separable from angle. If real data shift spectral shape with aperture, inspect filter angle dependence, source nonuniformity and stray light. The integral in the readout is computed on the specified 8–12 micrometre band even though the graph shows wavelengths beyond it.

Convert received power to calibrated voltage or counts

A thermal detector may respond to absorbed power through a temperature rise and an electrical responsivity. A photon-counting detector measures absorbed photons, so its count rate contains a factor $\lambda/(hc)$ multiplying spectral power before integration. Two receivers with identical geometric acceptance and nominal quantum efficiency can respond differently to a changing source temperature if one output is proportional to energy and the other to photon number. Calibrate the actual electrical transfer and make the time interval explicit for accumulated counts.

For an ideal linear power detector let $V = V_0 + gP$, with offset V_0 and gain g. Two calibrated sources spanning the use range determine both. A black reference port at the same ambient temperature can

also reject a common background in a chopped measurement. A filter, window or warm lens that absorbs thermal radiation also emits it. If these optics remain unchanged and stable, part of their own emission cancels in a reference difference. A reference traversing a different path generally leaves a residual input that is not captured by an electronic dark measurement.

Suppose effective source-minus-ambient powers of 2.00 and 8.00 microwatts yield 0.120 and 0.420 V. The fitted slope is 0.0500 V per microwatt with an offset of 0.020 V. A reading of 0.320 V implies 6.00 microwatts after offset correction. Substituting the same reading directly into a single-point gain with zero assumed offset would bias the inferred temperature. Rechecking a third reference near six microwatts tests linearity, while repeated zero-input readings at realistic instrument temperature test offset drift.

Invert the radiance and propagate uncertainties

A narrowband blackbody radiance measurement can be inverted analytically by solving Planck's expression for T. In a broad passband use numerical quadrature across the calibrated spectral response and solve a scalar monotone equation when emissivity and background are known. The derivative at a single wavelength is particularly informative for estimating precision. With $x = hc/(\lambda k_B T)$,

$$\frac{\partial \log B_\lambda}{\partial \log T} = \frac{x}{1 - e^{-x}},$$

$$T = \frac{hc/(\lambda k_B)}{\log[1 + 2hc^2/(\lambda^5 B_\lambda)]}.$$

At 10 micrometres and 400 K the logarithmic sensitivity is 3.70. A one-percent relative radiance uncertainty therefore gives about 1.08 K temperature uncertainty if all other quantities are exact. An unknown five-percent emissivity error can dominate that estimate. A two-colour temperature ratio may reduce uncertainty from an emissivity that is constant across the two narrow bands, but cannot cancel an arbitrary spectral emissivity or a large reflected ambient component.

As an example consider a grey object at 400 K and ambient 295 K with emissivity 0.70. At ten micrometres its outgoing radiance is $0.70(33.56) + 0.30(9.14) = 26.24$ in the earlier spectral units. Inverting as a perfect blackbody gives a brightness temperature of about 375 K. The difference is a physical radiance–temperature degeneracy. Repeat at known ambient temperatures while keeping the object thermally stabilised to constrain the reflected fraction. If heating the background changes the actual object temperature, a second independent temperature sensor or a transient thermal model is necessary.

When detector heat capacity sets the measured signal

Consider a thermal receiver of heat capacity C_d coupled to its surroundings with thermal conductance G_d. For small excursions its temperature obeys $C_d\dot{\theta} + G_d\theta = P_{\mathrm{abs}}(t)$, where θ is the excess above its operating point. A voltage thermometer with responsivity r_T converts this into output. Its frequency-

dependent power responsivity is $r_T/(G_d - i\omega C_d)$. The geometric and spectral calculations determine absorbed optical power, while this thermal equation determines how much of its modulation appears at the electrical output.

Take $C_d = 2.0$ microjoules per kelvin and $G_d = 0.10$ milliwatt per kelvin. The thermal time constant is 20 ms and ordinary corner frequency is 7.96 Hz. A sinusoidal absorbed-power amplitude of 6.0 microwatts would give a static temperature rise of 0.060 K. At 20 Hz the amplitude is reduced by $1/\sqrt{1 + (2\pi f\tau)^2} = 0.370$, leaving about 22.2 mK with a phase lag magnitude near 68 degrees. A receiver calibrated with a steady optical power is not automatically calibrated for this chopped experiment.

A square-wave chopper also changes the relation between time-domain peak differences and a lock-in's fundamental reading. For equal hot and reference dwell times, a square wave switching between powers P_1, P_0 has fundamental sinusoidal peak amplitude $2(P_1 - P_0)/\pi$, with different factors for rms and peak reports. The thermal transfer attenuates this component at the chopper frequency and the odd harmonics at their respective frequencies. Substituting the full hot-minus-reference power directly into the first-harmonic response would overestimate the expected signal.

Measure a frequency sweep on a stable reference and test whether amplitude and phase share a single time constant. A geometrical error rescales the amplitude but ordinarily leaves this thermal phase unchanged. A second thermal mass or an electronic filter can introduce another pole. Lowering chop frequency increases thermal signal until the static limit but can expose low-frequency environmental drift. Choose the frequency by comparing the calibrated response with the measured noise spectrum.

Finally, a reference and an unknown source must illuminate the same active area if responsivity varies across the receiver. Imaging one source as a small spot and the other as a filled patch can create a calibration bias even when total spectral powers agree. Translating a reference spot across the detector or imaging the same aperture successively at both temperatures tests that spatial uniformity assumption.

If the sensor is used on a source much smaller than the calibrated reference aperture, record an image or a field-stop scan to determine its filling fraction. Otherwise even exact knowledge of filter transmission and thermodynamic temperature leaves an unknown geometrical scale factor. Aperture filling is part of the measurement equation, not an electronic gain setting.

Tutorial · Infer emissivity using two controlled backgrounds

An opaque diffuse sample at fixed temperature is observed at 10 micrometres against two isotropic backgrounds with calibrated spectral radiances 8.00 and 16.00 W per square metre per steradian per micrometre. The resulting outgoing readings are 25.00 and 27.00 in the same units. Infer emissivity and the sample's blackbody-equivalent radiance. Estimate the significance of independent reading errors of 0.10 units.

▼ **Separate the reflected and emitted contributions**

The increased outgoing radiance is 2.00 for an 8.00 increase of background. Thus reflectivity is 0.250 and emissivity 0.750. The first measurement gives intrinsic blackbody radiance $[25.00 - 0.25(8.00)]/0.75 = 30.67$. The second returns the same value. With 0.10 independent uncertainty on each outgoing reading and exact backgrounds, the slope uncertainty is $\sqrt{2}(0.10)/8 = 0.0177$, as is the absolute emissivity uncertainty. Larger background separation can improve this slope estimate if sample temperature stays fixed.

If the sample transmits radiation, the residual fraction does not all correspond to reflection. A controlled change behind the sample helps detect that additional path. A directional specular reflector exposed to a warm enclosure also does not necessarily see the same angular average used in the diffuse model. Without these checks, a formally precise fitted emissivity can describe the experimental surroundings instead of the material.

Tutorial · Design a numerical spectral-integration check

An engineer tabulates spectral radiance per micrometre on a wavelength mesh. Another rewrites the detector model on an equally spaced frequency mesh, obtaining a signal that differs by several percent after independent mesh refinement. Explain what must transform, what stays dimensionless and how to compare a photon-counting channel with a power channel.

▼ Transform the complete measurement integral

The differential power $B_\lambda \, d\lambda$ must equal $B_\nu \, |d\nu|$, with $|d\lambda/d\nu| = c/\nu^2$. A dimensionless transmission curve becomes the same physical transmission at $\lambda = c/\nu$; it acquires no additional Jacobian. The integration bounds reverse when increasing wavelength is replaced by increasing frequency. A response specified per unit wavelength, or a calibrated gain integrating a particular finite bin, must instead be interpreted from how it was defined.

Evaluate a unit-transmission test using a very narrow band, then the full 8–12 micrometre band whose radiance values are given above. Refine each grid independently, treating sharp filter edges consistently and converting per-micrometre densities before using metres. For a photon counter divide each spectral power contribution by photon energy before summation. Replacing that energy by a single central-wavelength value is an approximation that should be checked against the full band and source temperature. Close agreement between two different meshes using the same incorrect density is not a valid units check.

NIST radiance-temperature calibrations · spectral radiance, sources and uncertainty

Electromechanics, optics and measurement · 12. Moving-mirror Doppler metrology

A moving mirror changes optical phase, shifts the reflected frequency and exchanges energy and momentum with the light. In many displacement measurements the classical phase rule is extraordinarily accurate. Derive its exact inertial-frame counterpart, identify which time a detector samples and find the practical uncertainties that usually matter well before a relativistic correction does.

Match phases on a boundary that moves

In a vacuum laboratory let an incident plane wave travel along $+x$ with phase $kx - \omega t$. A perfectly reflecting plane mirror has position $X(t)$, receding for positive velocity. The reflected wave travels along $-x$ with phase $-k_r x - \omega_r t + \phi_0$. At the moving conducting surface the tangential electric fields must cancel in the mirror rest frame. For a constant mirror speed this requires equality of the two phase rates evaluated on its trajectory. The phase reversal at reflection supplies a constant offset and disappears on differentiation.

$$kv - \omega = -k_r v - \omega_r,$$

$$\frac{\omega_r}{\omega} = \frac{1-\beta}{1+\beta},$$

$$\beta = v/c.$$

Here $k = \omega/c$ and $k_r = \omega_r/c$ are positive magnitudes. A receding mirror redshifts the reflected light and an approaching mirror blueshifts it. Another derivation boosts into the mirror frame, where incident and reflected frequencies are equal, reverses the wavevector and boosts back. This yields a product of two Doppler factors, one for each transformation. Multiplying the first factor by its inverse without reversing the wavevector would predict no shift.

Define the signed beat $f_b = f_i - f_r$. The exact and first-order relations with vacuum wavelength λ_0 are

$$f_b = \frac{2v}{\lambda_0(1+\beta)},$$

$$f_b \simeq \frac{2v}{\lambda_0},$$

$$v = \frac{\lambda_0 f_b}{2 - \lambda_0 f_b/c}.$$

At 633 nm and $v = 2.00$ mm/s the beat is 6319.12 Hz. The relative correction to the first-order expression is only 6.67×10^{-12}. Frequency scale, geometry and air refractive index are ordinarily much larger uncertainties in an uncorrected bench experiment. The same exact expression makes a genuinely different prediction at $\beta = 0.10$: $f_r/f_i = 0.81818$, whereas the first-order frequency ratio is 0.80. This latter value is a theoretical benchmark for the formula rather than a required moving-bench experiment.

Connect reflection time with the detector's interference phase

Put an ideal stationary beamsplitter and detector at the origin, and let the source continuously illuminate the mirror along the measurement arm. A wave arriving back at laboratory time t was reflected at t_r satisfying $t = t_r + X(t_r)/c$. It left the beamsplitter at $t_0 = t_r - X(t_r)/c$. Combining these gives

$$t - t_0 = 2X(t_r)/c.$$

With a stable source and a fixed reference arm, the accumulated return phase relative to the reference is proportional to $2kX(t_r)$ up to a constant and an electronic quadrature sign.

$$\phi(t) = \frac{4\pi X(t_r)}{\lambda_0} + \phi_{\mathrm{off}},$$

$$\frac{1}{2\pi}\frac{d\phi}{dt} = \frac{2v(t_r)}{\lambda_0[1 + v(t_r)/c]}.$$

The denominator comes from differentiating the arrival-time condition. It is not obtained from differentiating a geometrical arm length at detector time while keeping the reflection time fixed. For very slow motion and a modest arm one can replace the retarded trajectory by the present one to high accuracy. At higher bandwidth a fixed path delay can still matter even if the velocity correction is tiny. A one-metre mirror distance gives roughly 3.34 ns from reflection event to detection.

A sinusoidally driven mirror with amplitude 100 nm and ordinary mechanical frequency 1.0 kHz has phase amplitude $4\pi A/\lambda_0 = 1.99$ rad at 633 nm. The peak speed is 0.628 mm/s and peak signed beat about 1.99 kHz. The instantaneous beat changes sign at each mechanical turning point. A frequency counter returning a single unsigned average misses that directional information. Demodulating the phase or fitting the sinusoidal motion to both quadratures can recover position, speed and reversal times.

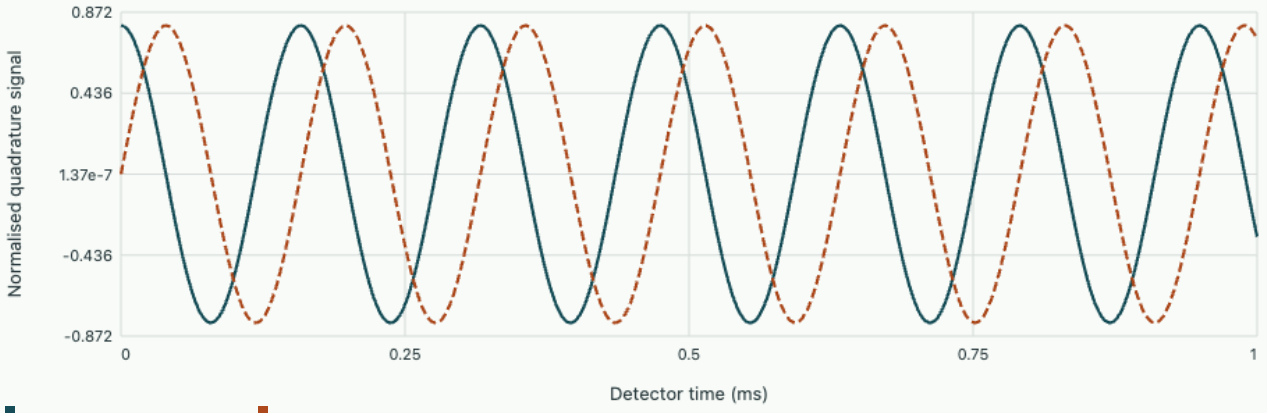
Infer displacement or signed speed without losing complete fringes

If stationary reference and returned fields overlap in polarisation, spectrum and space, their combined intensity contains a cross term proportional to $\cos\phi$. A single intensity channel cannot distinguish increasing from decreasing phase at an intensity extremum. Two calibrated quadrature outputs ideally read $X_s = V\cos\phi$, $Y_s = V\sin\phi$ after removal of offsets and gain normalisation. Recover wrapped phase with the two-argument arctangent. Unwrap successive phase differences only when the sampling interval and noise allow the branch to be identified.

Open the live experiment

Try the calculation

Mirror speed, positive receding (mm/s)	2
Vacuum wavelength (nm)	633
Fringe visibility	0.8



The signed beat is 6319.12 Hz. In 1 ms the mirror travels 2.00 µm and the unwrapped phase changes by 39.70 rad.

The signed velocity control reverses the direction traced by the quadratures. Hold its absolute value fixed and change sign. The cosine channel alone remains almost identical at laboratory speeds; the sine channel reverses the progression from its initial value. Reduce the visibility and keep in mind that the graph shows noise-free curves. With fixed electronic amplitude noise a smaller circle makes angular uncertainty larger, even though the exact underlying phase still advances at the same rate.

One full phase turn represents a physical mirror displacement of half the vacuum wavelength at normal incidence. A 20-fringe movement at 633 nm is 6.33 micrometres. If both endpoints retain phase residuals, add their signed difference to the complete turn count before converting to distance. A missed fringe biases displacement by 316.5 nm regardless of how accurately sub-fringe phases are fitted. For the default speed and wavelength the magnitude of frequency is 6.32 kHz. To unwrap a plain uniformly sampled phase with less than half a turn between adjacent samples one needs a sampling frequency above 12.64 kHz, and usually a margin for noise and acceleration.

Quadrature imbalance distorts the ideal circle into an ellipse shifted away from the voltage origin. Taking an arctangent of raw voltages then introduces a periodic position error. Record a slow multi-fringe calibration, fit channel offsets, scales and nonorthogonality, and test the recovered phase on held-out data with reversed motion. Calibration using only a tiny arc of the ellipse makes offset and scale poorly identifiable even if the residuals on that arc are small.

Close the energy and momentum balance at the mirror

One incident photon has energy hf_i and momentum $+hf_i/c$. On reflection it has energy hf_r and momentum $-hf_r/c$. The mirror acquires momentum $h(f_i + f_r)/c$ and energy $h(f_i - f_r)$. Their ratio is exactly v when the prescribed constant-speed reflection formula applies. A recoil-free moving boundary can exchange mechanical work $v\,\Delta p$ while a drive maintains its velocity. For a freely recoiling low-mass mirror illuminated by a small number of photons the fixed-velocity approximation must be replaced by energy and momentum conservation for the joint system.

For an incident beam with power P_i crossing a stationary plane in the lab, the number of photons encountering the receding surface per laboratory time is $P_i(1-\beta)/(hf_i)$. Multiply by transferred momentum per encounter to get the force on that moving surface. The result simplifies to $F = (2P_i/c)(1-\beta)/(1+\beta)$. At rest, a 10 mW perfectly reflecting beam gives 66.7 pN. For a 2.0 mm/s receding mirror at that power, the corresponding mechanical work rate is only 1.33×10^{-13} W to leading order.

A detector fixed upstream sees reflected-wave intensity reduced by the square of the reflected frequency ratio for an ideal steady plane wave. Its received power change compared with a fixed-plane incident flux is not in general equal to the instantaneous work on the mirror. The region of field between the fixed reference plane and the moving surface grows or shrinks and stores energy. Instead compare powers crossing the moving boundary with their proper encounter rates, or account for the change of field energy in a specified control volume. For a finite pulse the integrated photon count is unchanged under perfect reflection and the total energy loss per photon is the Doppler shift already derived.

Estimate realistic errors before pursuing small corrections

At normal incidence in vacuum the first-order speed estimate is $\lambda_0 f_b/2$. For a beam at angle θ to the translation direction, with an appropriately arranged reflection/return geometry interrogating mirror-normal motion, the usual small-speed sensitivity along the normal includes $\cos\theta$. A tilt of two degrees gives a relative cosine factor 0.99939, a 610 parts-per-million reduction. A plane mirror tilted relative to a fixed coaxial receiver can additionally send the reflected beam outside the collection path, so specify how oblique reflected and reference fields are recombined. Blindly interpreting reduced fringe visibility as a velocity correction conflates these two effects.

In a homogeneous stationary transparent medium a quasistatic phase measurement measures optical path nL. If n changes during a displacement measurement, the phase derivative includes both $n\dot{L}$ and $L\dot{n}$ when the simple uniform-medium approximation holds. A refractive-index change of one part in a million over a 0.5 m arm imitates about 0.50 micrometres of path-length change. A short differential arm, a refractive-index reference or a controlled environment can separate it from actual motion. The vacuum relativistic formula cannot simply absorb an arbitrary time-varying medium by replacing c everywhere with c/n.

For a phase-difference velocity estimate over a record of duration T, the displacement noise from two independent endpoint phase errors of standard deviation s_ϕ is $\lambda_0\sqrt{2}s_\phi/(4\pi)$. At 633 nm, $s_\phi = 0.010$ rad and $T = 2$ ms, the resulting velocity uncertainty is about 0.356 micrometres per second. Fitting a

slope over many samples can improve white-noise precision, but laser drift, mechanical acceleration and missed branches require their own models. Report the time interval over which a constant velocity is being claimed.

Recover a small vibration amplitude from optical sidebands

A phase-sensitive receiver is not the only way to recover periodic motion. Let a mirror vibrate at angular frequency Ω about a fixed mean, with displacement $A\cos\Omega t$ and speed sufficiently small for a first-order optical path description. The reflected analytic signal relative to its carrier contains $e^{im\cos\Omega t}$ with modulation index $m = 4\pi A/\lambda_0$. Expand the exponential in its Fourier series. The power of sideband order j relative to the incident unmodulated carrier is $J_j(m)^2$, where J_j is a Bessel function. Energy conservation of the phase factor requires that all the sideband powers sum to one in this phase-only approximation.

For a 10.0 nm displacement amplitude at 633 nm the index is 0.1985. To leading small-index order, each first sideband carries $(m/2)^2 = 0.00985$ of the original carrier power. The central component loses approximately twice this amount. A receiver collecting only one sideband would infer the wrong vibration amplitude if it treated that signal as the sum of both. At larger amplitudes higher Bessel orders become important and a single sideband amplitude is no longer a monotone function of displacement. A multi-sideband fit or an independent coarse amplitude resolves the ambiguity.

With a balanced optical heterodyne reference offset far enough from zero frequency, both sidebands can be separated electronically from the carrier beat. Measuring their power ratio to the central beat cancels a common optical gain, but any electronic response slope between their frequencies needs calibration. Pure phase modulation predicts symmetric sideband powers. Asymmetry can arise from simultaneous amplitude modulation or an unequal frequency response rather than from a change in mirror speed. Measuring their complex phases distinguishes amplitude and phase modulation more directly.

A useful consistency check uses three independent measured quantities. Infer displacement amplitude from the first two sidebands, obtain the mechanical frequency from their separation and predict peak Doppler beat from the product of those two values. Then compare with a separate unwrapped quadrature phase trace. For a rigid sinusoidal mirror these should agree within timing and wavelength uncertainties. An interferometric signal containing two different moving surfaces can fit a few sideband powers yet fail the predicted time-dependent phase; changing the illuminated spot or one surface position tests that possibility. A spectrum and a time trace jointly constrain motion in a way that a single fringe visibility cannot.

Tutorial · Resolve a branch ambiguity in a vibrating mirror

A mirror returns a signed mean beat of 8.0 kHz while moving uniformly over a short time window. The vacuum wavelength is 632.8 nm. The detector samples quadrature at 10.0 kHz and a naive nearest-branch unwrap reports minus 2.0 kHz. Explain the discrepancy, infer both candidate speeds and design a measurement to select the correct one.

▼ **Track the sampled phase and use an independent constraint**

A true phase advance of 0.80 cycle per sample is indistinguishable from minus 0.20 cycle per sample when only consecutive wrapped angles are available. The corresponding physical speeds are plus 2.531 mm/s and minus 0.6328 mm/s. Both give exactly the same ideal complex samples at that sampling rate under the first-order laboratory formula. A smaller least-squares residual on one constant-speed branch cannot resolve the ambiguity without another observation.

Increase the sampling frequency above 16 kHz with margin or use an independently known direction and bounded speed range that excludes alternative aliases. A second wavelength also changes the beat while preserving physical velocity and can resolve the branch if the two ambiguous frequency ladders do not coincide over the admissible range. For accelerated motion verify the condition at the maximum instantaneous beat rather than at its signed average over a complete vibration period.

Tutorial · Can this beat measurement verify a relativistic correction?

A translation standard operates at 1.00 m/s and an interferometer at 500 nm records a nominal 4.00 MHz beat. Estimate the difference between exact and first-order vacuum predictions. A timebase has a fractional uncertainty 10^{-8}, and wavelength is uncertain by 2×10^{-8}. Assess the test and state one way to reject an offset without confusing it with the desired correction.

▼ **Calculate the small difference without subtracting nearly equal optical frequencies**

Use the exact beat formula or expand it directly. The correction is approximately $-2v^2/(\lambda_0 c) = -0.0133$ Hz for the receding mirror. The stated timebase contributes 0.040 Hz and the wavelength scale contributes 0.080 Hz to a 4 MHz prediction, even before including the velocity standard or alignment. This setup does not resolve the correction with those absolute uncertainties. Subtracting two floating-point optical frequencies near hundreds of terahertz is also a poor numerical route to such a small difference.

Reverse the velocity with equal magnitude. The leading signed beat is odd in velocity, while its leading relativistic correction is even. Adding the two signed beats cancels the ideal leading term and leaves about minus 0.0267 Hz. This reversal also preserves a fixed electronic frequency offset, which would add twice to the same sum. Take stationary-mirror reference readings and vary the speed magnitude; the wanted even term scales as speed squared. Different arm alignments or asymmetric velocity calibration during reversal can still imitate part of that effect.

Cambridge Electromagnetism · wave propagation, radiation momentum and Lorentz transformations

Electromechanics, optics and measurement · 13. Weighing a small deposit with a piezoelectric resonator

Two nearby frequencies appear in the electrical response of one mechanical mode. Derive the series and parallel resonances, then use their different sensitivities to recognise added mass and stray capacitance.

Convert mechanical motion into a terminal admittance

A piezoelectric plate converts terminal voltage into force and velocity into current. With a linear reciprocal coupling coefficient n, $F = nV$ and $I_m = nv$. The mechanical velocity impedance is $b + i\omega m + k/(i\omega)$. Dividing it by n^2 maps it to a series branch with $R_m = b/n^2$, $L_m = m/n^2$ and $C_m = n^2/k$. The electrodes also have a static capacitance C_0 in parallel. Thus

$$Y(\omega) = i\omega C_0 + \left[R_m + i\omega L_m + \frac{1}{i\omega C_m} \right]^{-1}.$$

For negligible loss the series branch impedance vanishes at $\omega_s = 1/\sqrt{L_m C_m}$. Just above this frequency its susceptance is inductive and can cancel the parallel capacitance. Setting $Y = 0$ gives

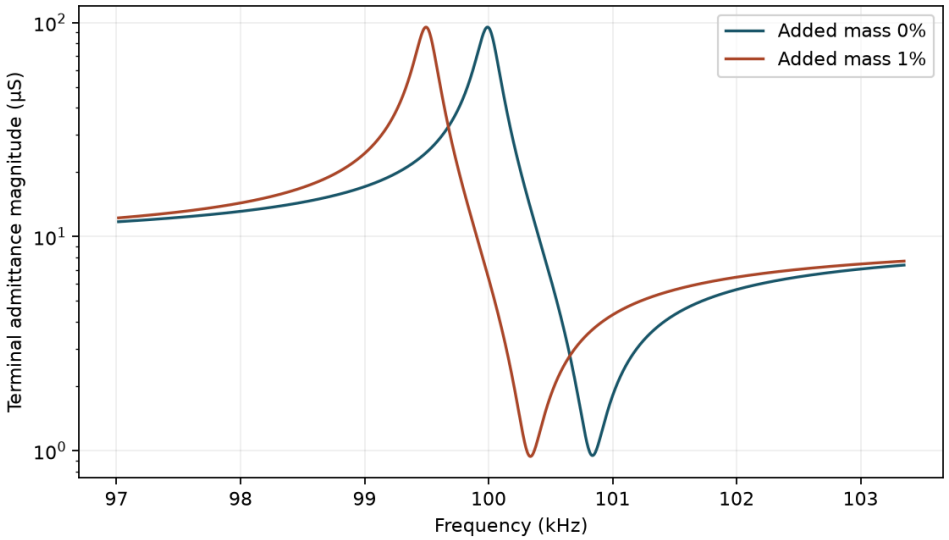
$$\omega_p = \omega_s \sqrt{1 + C_m/C_0}.$$

With finite damping a peak and a dip replace the singular limits. Their extrema need not coincide exactly with the lossless frequencies.

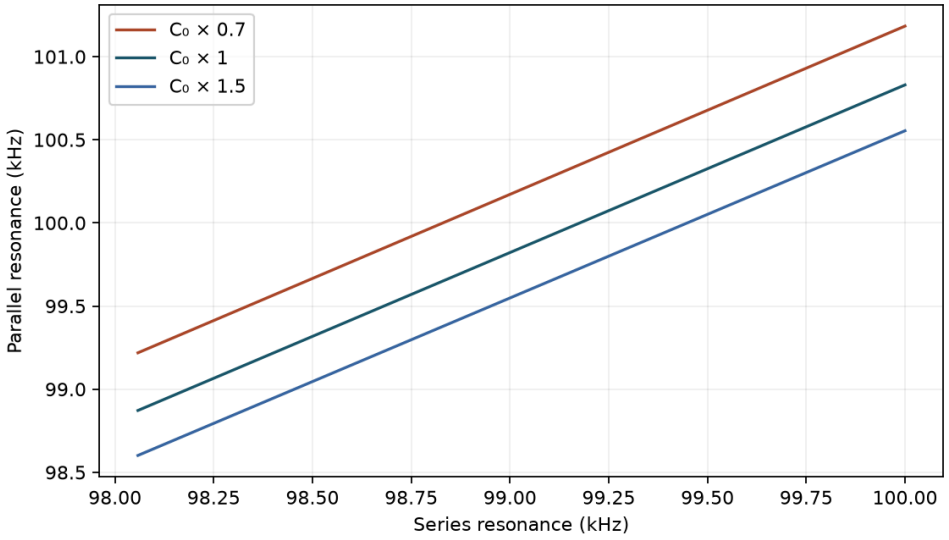
Isolate the perturbation

A thin rigid deposit that changes only the effective mass multiplies L_m by $1 + \eta$. Both ideal frequencies scale as $(1 + \eta)^{-1/2}$; their ratio is unchanged. Additional cable capacitance increases C_0, changing the ratio while leaving the mechanical series frequency fixed. At a load fraction of 0.01 the expected series shift is about minus 0.496 percent. A viscoelastic deposit can also dissipate energy and alter stiffness, so the two-frequency test includes a physical assumption about the coating. For $f_s = 100.000$ kHz, $C_m = 0.25$ pF and $C_0 = 15$ pF, the unloaded parallel frequency is 100.830 kHz. A 1% increase in effective mass puts the series resonance at 99.504 kHz. If the same shift came from extra cable capacitance alone, the series frequency would remain at 100.000 kHz. At quality factor 600 the approximate unloaded resonance linewidth is $f_s/Q = 167$ Hz. The predicted mass shift spans about three linewidths. The height of the peak by itself would confound damping and transduction.

Conversely, fit the two frequencies and infer the capacitance ratio as $(f_p/f_s)^2 - 1$. A small random error in f_p/f_s has a large relative effect on this estimate when the resonances nearly coincide. Zoom the frequency grid and compare the uncertainty from bin spacing with the shift under investigation.



A terminal sweep contains the mechanical resonance and the electrical cancellation. Follow both features before inferring added mass.



Changing cable capacitance displaces the parallel resonance at fixed series frequency. Mass loading moves both frequencies along a diagonal path.

Exercise · recover a capacitance ratio

A nearly lossless device gives $f_p/f_s = 1.01$. What ratio of motional to static capacitance is consistent with it?

▼ **Work through the solution**

Squaring and subtracting one gives $C_m/C_0 = 0.0201$. The difference between the squares matters when the shift is used for accurate capacitance inference.

Exercise · challenge a mass reading

After changing a fixture the dip moves but the series frequency remains within the experimental uncertainty. Does that support a pure mass increase?

▼ **Work through the solution**

A purely inertial change shifts both resonance frequencies. The observed pattern is consistent with an increased shunt capacitance if the dip moved toward the series peak. A sweep of the linewidth and an independent capacitance check would test the model.

Try it · Piezo load

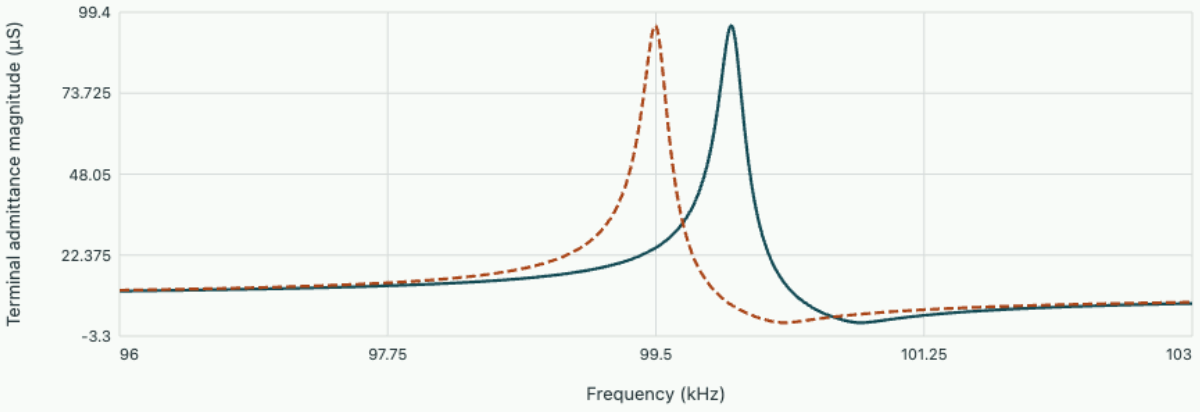
Change the inputs and compare the recalculated curves with the preceding derivation and baseline figure. The axes give the units; the numerical readout states the model assumptions and any limiting cases. Reset the inputs to return to the reference setting.

Open this live calculation

Try the calculation

Added mass fraction **0.01**

Parallel capacitance (pF) **15**



Loaded lossless series/parallel frequencies 99504 / 100330 Hz. Quality factor 600; motional capacitance 0.25 pF.

Download the corresponding editable notebook. The browser recalculates the reduced equations directly; the notebook exposes the full calculation and its checks.

Open editable notebook

Download .ipynb